

**Tire Model Parameterization for NH90 Main Landing Gear
in MSC.ADAMS program.**

**I. Kostas
D&C 2016.010**

Internship's report

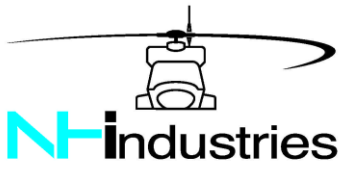
Coach(es): Ruud Louw (Fokker Technologies)

Supervisor : prof.dr. H. Nijmeijer

Committe: dr.ir. I.J.M. Besselink

Eindhoven University of Technology
Master Automotive Technology
Department of Mechanical Engineering
Dynamics & Control

Eindhoven, January, 2016



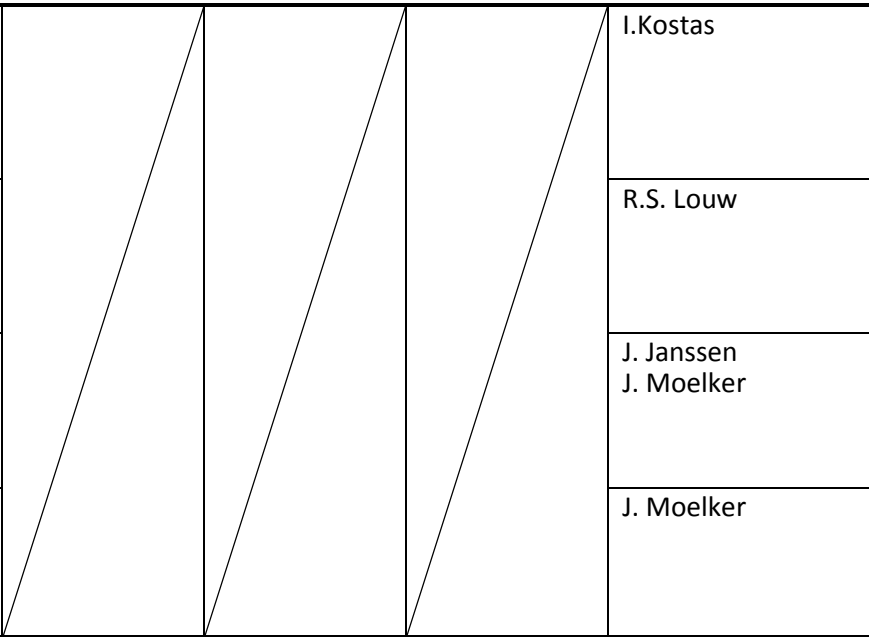
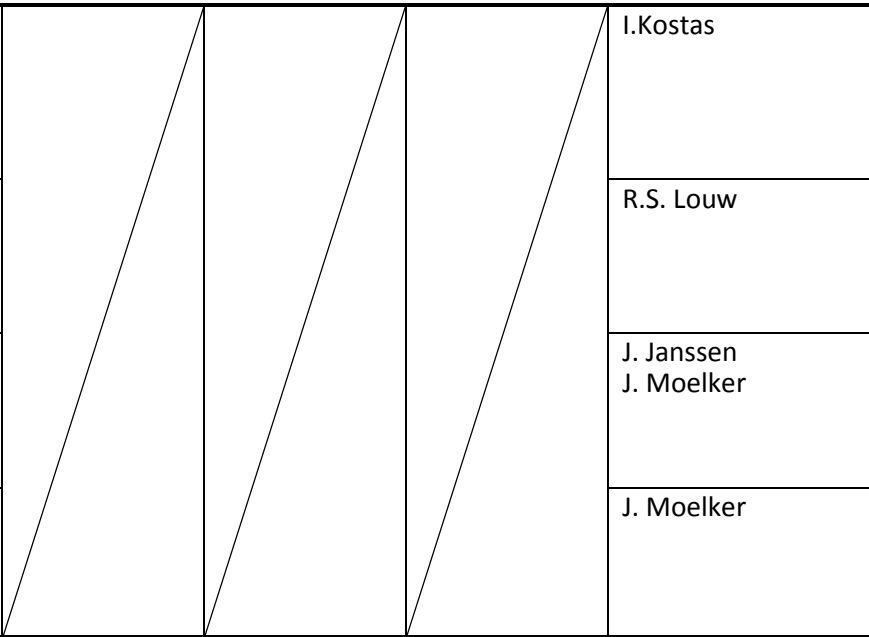
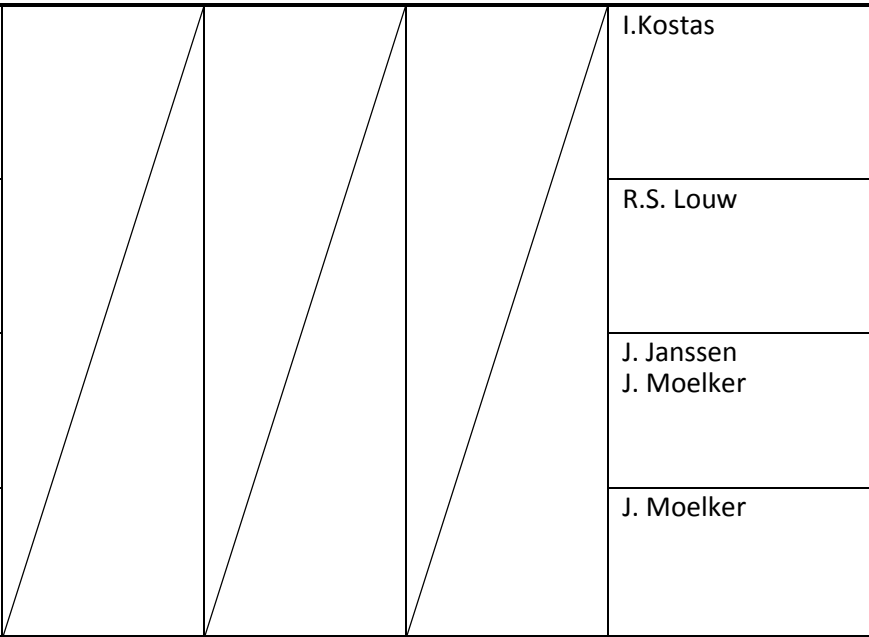
CLASSIFICATION
NATO UNCLASSIFIED
INDUSTRY UNCLASSIFIED

AGUSTA WESTLAND

AIRBUS HELICOPTERS

AIRBUS HELICOPTERS DEUTSCHLAND

FOKKER

DOC No: TN S324F0518E01		Issue: A		WBS No: 2015-004-JV1											
TITLE: Tire Model Parameterization for NH90's Main Landing Gear in MSC.ADAMS program.					<u>Distribution List</u> FK: J. van der Linde Henk Vasmel										
Summary: In this report aircraft tire models available in MSC.ADAMS/2013.2 are described and used for modelling the Main Landing Gear. These tire models have been parameterized and tested by using a test rig model in the MSC.ADAMS multibody program. Herewith these models have been validated showing that they are accurate, realistic and comply with the tire characteristics as supplied by the DUNLOP tire manufacturer. Further the most suitable aircraft tire model has been implemented in the modelling of the MLG model and some preliminary drop test simulations have been performed. The tire model evaluations and experiences gained as reported herein will be used for the correct transition of the present Landing Gear Model in the Pro/MECHANICA MOTION Multi-Body Software to the new MSC.ADAMS Multi-Body Software program.					<table border="1"> <tr> <th colspan="5">Program Archives</th> </tr> <tr> <td>AW</td> <td>AH</td> <td>AHD</td> <td style="background-color: #ADD8E6;">FK</td> <td>NHI</td> </tr> </table>	Program Archives					AW	AH	AHD	FK	NHI
Program Archives															
AW	AH	AHD	FK	NHI											
Applicable Variants: ALL															
Prepared by:				I.Kostas											
Signature:															
Date:															
Checked by:				R.S. Louw											
Signature:															
Date:															
Approved by:				J. Janssen											
Signature:				J. Moelker											
Date:															
Authorized by:				J. Moelker											
Signature:															
Date:															
	AW	AH	AHD	FK	NHI										
This document contains proprietary information and may not be reproduced in any form whatsoever, nor may be used by or its contents divulged to third parties without written permission from the owner. All rights reserved. Printed copy is not controlled.															

AMENDMENT RECORD SHEET

Issue	Issue date	Change reasons/ change proposal	Affected pages	Prepared by	Checked by	Approved by	Authorized by
A	15-01-2016	Initial release	All	I. Kostas	R.S. Louw	J. Janssen J. Moelker	J. Moelker

TABLE OF CONTENTS

1	Introduction.....	9
2	NH90 Tire Properties	10
2.1	NH90 Tire Construction.....	10
2.2	Tire Mechanical Properties.....	11
2.2.1	Deflection and Height.....	11
2.2.2	Tire Vertical Stiffness.....	12
2.2.3	Footprint.....	13
2.2.3.1	Footprint length.....	13
2.2.3.2	Footprint Width.....	14
2.2.3.3	Footprint Area	15
2.2.4	Lateral Stiffness	16
2.2.5	Torsional Stiffness	17
2.2.6	Fore-Aft Stiffness.....	18
2.2.7	Rolling Relaxation Length	19
2.2.7.1	Un-yawed relaxation length	19
2.2.7.2	Yawed relaxation length.....	20
2.2.8	Effective Rolling Radius	21
2.2.9	Cornering Power.....	21
2.2.10	Normal and Cornering Force	23
2.2.11	Aligning Torque	26
2.2.12	Pneumatic Trail.....	27
2.2.13	Tire parameters for shimmy stability analysis.....	28
3	Tire Model Parameterization for NH90 in MSC.ADAMS	30
3.1	Introduction.....	30
3.2	Tire Models.....	30
3.2.1	Empirical Models.....	30
3.2.2	Physical Models.....	30
3.2.3	Combined Models	30
3.3	Tire Models in MSC.ADAMS	31
3.3.1	TR-R-64 Aircraft Tire Model.....	34
3.3.2	Basic Aircraft Tire Model	35
3.3.3	Enhanced Aircraft Tire Model	35
3.4	Tire Model Comparisons	36
3.4.1	Introduction.....	36
3.4.2	Test Rig Model.....	36

3.4.3	Tire Measurements by the Tire Manufacturer.....	38
3.4.4	Simulations with tire’s inflation pressure 130.5 psi.....	38
3.4.4.1	Discussion of the simulation results.....	45
3.4.5	Simulations with tire’s inflation pressure 143.6 psi.....	46
3.4.5.1	Discussion of the simulation results.....	52
4	Conclusions.....	53
5	Reference Documents.....	54
APPENDIX A	Tire Models.....	56
APPENDIX B	Axis System in MSC.ADAMS/tire.....	59
APPENDIX C	Tire Property Files in MSC.ADAMS/tire.....	61
APPENDIX D	PAC2002 Tire Data and Fitting Tool in MSC.ADAMS.....	68
APPENDIX E	Preliminary landing gear simulations.....	75
E.1	Introduction.....	75
E.2	Landing Gear Simulations.....	76
APPENDIX F	Student Assignment Schedule.....	83
APPENDIX G	Folder Location for the ADAMS Files.....	85

LIST OF ABBREVIATIONS

ADAMS	Automated Dynamic Analysis of Mechanical Systems
AHD	Airbus Helicopters Deutschland
AH	Airbus Helicopters
AW	Agusta Westland
CAD	Computed Aided Design
CATIA	Computer Aided Three-dimensional Interactive Application
FEM	Finite Element Method
FK	Fokker Technologies
FTire	Flexible Ring Tire model
MBD	Multi-Body Dynamics
MF-SWIFT	Magic Formula – Short Wavelength Intermediate Frequency Tire
MF-Tyre	Magic Formula Tyre
MLG	Main Landing Gear
MSC	MacNeal - Schwendler Corporation
NASA	National Aeronautics and Space Administration
NASTRAN	NAsa STRucture ANalysis
NFH	NATO Frigate Helicopter
NH90	Nato Helicopter 90
NLG	Nose Landing Gear
TDFT	Tire Data and Fitting Tool
TTH	Tactical Transport Helicopter

LIST OF SYMBOLS

a	Ratio of the Footprint Net Area to Gross Footprint Area [-]
A_g	Gross Footprint Area [sq. ins]
A_n	Footprint Net Area [sq. ins]
b	Width of Tire – Ground Contact Area (Footprint) [ins]
C	Tire Yaw Coefficient [rad/lbs.]
C_1	Tire Time Constant [s]
C_c	Cornering – Power Coefficient [lbs./deg]
d	Outside Diameter of Free Tire [ins]
F	Vertical Tire Load [lbs.]
F_d	Flange Diameter [ins]
F_h	Free Height of the Tire [ins]
F_t	Lateral Force for Moreland Hypothesis [lbs.]
$F_{\psi,r,e}$	Steady – State Normal or Lateral Force on the Tire [lbs.]
F_z	Vertical Force acting on Tire from Ground [lbs.]
$F_{y,r,e}$	Cornering Force on the Tire [lbs.]
h	Half of the Footprint [ins]
I	Inertia about pivot [lbs.sec ² .ins]
k_D	Effective Lateral Damping [lbs.sec/in]
k_1	Effective Lateral Stiffness [lbs./in]
K_a	Tire Torsional Stiffness [lbs./in]
k	Vertical Tire Stiffness [lbs./in]
K_x	Tire Fore-Aft Stiffness [lbs./in]
K_λ	Tire Lateral Stiffness [lbs./in]
L	Trail Length [ins]
LF_h	Loaded Free Height [ins]
L_f	Un-yawed Rolling Relaxation Length [ins]
L_y	Yawed Rolling Relaxation Length [ins]
M_A	Moment applied to Test Rig [lb.in]
$M_{z,r,e}$	Self-Aligning Torque [lb.in]
$M_{z,r,e,max}$	Maximum Self-Aligning Torque [lb.in]

M_B	Moment due to Bearing friction [lb.in]
M_t	Moment on Wheel due to Tire Deformation [lb.in]
N	Cornering power or Cornering Stiffness of the Tire [lbs./deg]
p	Tire Inflation Pressure [psi]
p_r	Tire Rated Inflation Pressure [psi]
q	Pneumatic trail or pneumatic caster [ins]
r_e	Rolling Radius of the Tire [ins]
SL_r	Static Loaded Radius [ins]
V_H	Horizontal Rolling Velocity [ins/sec]
w	Maximum Width of Undeformed Tire [ins]
δ	Vertical Tire Deflection [ins]
δ_o	Vertical Tire Deflection for pure vertical conditions ($F_x = F_y = 0$) [ins]
Δ	Lateral Deflection of Footprint Center [ins]
$\dot{\Delta}$	Derivative of Lateral Deflection [ins/sec]
μ_{D1}	Coefficient of Moreland's Series [ins. lbs./deg]
μ_1	Static Torsional Spring Coefficient [ins. lbs./deg]
μ_ψ	Yawed Rolling Coefficient of Friction [ins. lbs./deg]
μ_s	Coefficient of Moreland's Series [ins. lbs./deg]
ψ	Yaw angle of the Tire [deg]
ψ_t	Torsional Twist Angle of the Footprint relative to the Wheel plane [deg]
$\dot{\psi}_t$	Derivative of Torsional Twist Angle [deg/sec]
τ_λ	Lateral – Spring Constant Coefficient [lbs./in]
ω	Wheel Angular Velocity [deg/sec]

1 INTRODUCTION

The landing gear supports the body of the helicopter during ground operations, take-off and landing. The tires are the only components of the helicopter that touch the ground and as a result have to resist a considerable forces and torques. Therefore the tires with its specific characteristics, as part of the landing gear, determine the NH90 landing and ground operation behavior and influence special phenomena like ground resonance and shimmy. For that reason a tire model, as part of a multi-body simulation model, is significant for the understanding of the dynamic behavior of the helicopter's structure. Several tire models are available in the industry and academic world, but in many cases they are applied for different purposes. No general tire model, for the time being, can cover every application with the same accuracy [1],[2],[3].

The tire model within Fokker Aero-structures runs on an obsolete and unsupported multi-body simulation program, which makes the simulations of the NH90 cumbersome. This program will be replaced by the state of the art MSC.ADAMS Multi-Body Dynamics (MBD) program for the simulation of the landing gear dynamic behavior. This program possesses a library of tire models that comes with ADAMS/tire module [5]. These tire models are investigated to evaluate the suitability for the NH90 landing simulations, the most promising tire model could be used in the future. Apart hereof, a custom tire model shall be developed and implemented in the program for comparison and certification purposes. The tire model has to be validated in order to show that the model is accurate, realistic and complies with the parameters as supplied by the tire manufacturer. Accordingly the simulations with the tire model stand alone and implemented in the total landing gear model, shall perform such that the load and deflection responses are in accordance with former tests and simulations within the design envelope. All these steps of parameterizing NH90 tire models will be discussed in the following chapters.

2 NH90 TIRE PROPERTIES

2.1 NH90 Tire Construction

Tires are divided into two main groups, 'Radial' and 'Bias' tires. The main feature that separates the radial tires from the bias ply tires is the tire's belt construction. The cord material (typically nylon or steel) also often differs between the two. The differences affect many functional aspects of the tire behavior. A radial tire is constructed with steel belts of the tire running at a 90 degree angle of the tread center line. A bias ply trailer tire is constructed with nylon belts of the tire running at a 30-45 degree angle of the tread center line.

Radial tires are common in the automotive industry because of the lower fuel consumption. However bias tires are currently the most popular to the world's aviation fleet because they can withstand higher load in the vertical direction. The NH-90 helicopter uses bias tire type and the internal construction of this tire type is illustrated in the [Figure 2.1](#). The following two paragraphs are dedicated to describing all the parts of the bias tire type.



Figure 2.1: Cross-section of the Bias tire type [32].

First of all, the *tread* is the area of the tire that makes contact with the ground. This is made of rubber, compounded for toughness, durability and wear resistance. The tread pattern is designed in accordance with aircraft operational requirements. The tread of most tires contain longitudinal *grooves* that are designed to remove water between the tire and the runway surface, and therefore by doing so improving ground traction on wet runways. The *sidewall* is a protective layer of flexible, weather-resistant rubber covering the outer casing ply, extending from tread edge to bead area. The *under-tread* is a layer of rubber that is designed to improve the adhesion between the tread of the tire and the casing plies. Casing plies are layers of rubber coated fabric which run radially from bead to bead. The casing plies provide the strength of the tire. Casing plies are anchored by wrapping them around the wire beads, thus forming the *casing ply turn-ups* [10].

The *bead* is made of several bead wires and holds the tire to the wheel. The bead wires are made from steel wires that are layered together and embedded in rubber to form a bundle. This bundle is then

wrapped with rubber coated fabric for reinforcement. Generally, bias tires are made with 2–6 bead bundles (1–3 per side). The *bead toe* is the inner bead edge closest to the tire center line and the *bead heel* is the outer bead edge that fits against the wheel flange. The *apex strip* is a wedge of rubber affixed to the top of the bead bundle. Finally, the *inner liner* is made of low permeability rubber and acts as a built-in tube and restricts gas from diffusing into the casing plies. Important thing to be mentioned here is that the tire is usually filled with Nitrogen (N₂) gas [10].

2.2 Tire Mechanical Properties

The properties of the helicopter's tires are of crucial importance for the safety and stability during take-off, landing and ground maneuvering. The NH90 MLG is equipped with two types of Dunlop tires. In this report the heavy duty tire for austere operations (DR18429T) has been used [32]. Most of the properties along with the tire dimensional properties will be used for modelling the NH90 tire in the multi-body dynamics program. However not all mechanical properties are measured by the tire manufacturer because the test equipment available at Dunlop only enables vertical load and deflection to be measured. The other mechanical properties can be calculated in accordance with tire models, test data and empirical equations, and showing equivalence with former tires. In the past, Dunlop performed validation testing and achieved to a certain degree reasonable agreement between the models and test data. The empirical equations are obtained from Smiley and Horne (1958) [8], which employs data from several aircraft tires and tire measurements and is considered an accepted industry standard source for aircraft tire calculations.

The empirical tire equations need several types of input data to provide the mechanical properties. The dimensional tire properties that shall be used as an input to the equations are:

- tire size
- nominal and maximum diameter of the tire
- nominal and maximum width of the tire
- tire bead diameter
- flange height

Furthermore some physical properties are used:

- the maximum rated pressure and
- operating pressure

Usually only the load which is exerted to the tire and the deflection of it, are measured by and obtained from the tire manufacturer. Using these data along with the empirical equations one can arrive at an approximation of the tire's mechanical properties. This procedure reduces cost and time and provides a first estimate of the tire characteristics in the expected conditions, within the design envelope. The following paragraphs are dedicated to describing in detail the input data and the particular empirical equations in order to obtain these tire mechanical properties, and are primarily attributed to [8].

2.2.1 Deflection and Height

A common term used when talking about aircraft tires is the amount of deflection when rolling under load. The term *Deflection* is calculated using the following formula:

$$\delta = \frac{F_h - LF_h}{F_h} \quad (2-1)$$

where,

δ : *Vertical Tire Deflection (ins)*

F_h : *Free Height (ins)*

LF_h : *Loaded Free Height (ins)*

The Free Height is given by:

$$F_h = \frac{d - F_d}{2} \quad (2-2)$$

where,

d : *Outside Diameter of the Free Tire (ins)*

F_d : *Flange Diameter (ins)*

And the Loaded Free Height,

$$LF_h = SL_r - \frac{F_d}{2} \quad (2-3)$$

where,

LF_h : *Loaded Free Height (ins)*

SL_r : *Static Loaded Radius (ins)*

Aircraft bias tires are designed to operate at 32% deflection, with some at 35%. As a comparison the aforementioned radial tires of cars and trucks operate in the 17% range [\[10\]](#).

2.2.2 Tire Vertical Stiffness

The load and the deflection of the tire are measured and provided by the manufacturer. Consequently the *vertical stiffness* is obtained by using a linear law as follows:

$$F = k * \delta \quad (2-4)$$

where,

F : *Vertical Load (lbs.)*

k : *Vertical Stiffness $\left(\frac{\text{lbs.}}{\text{in}}\right)$*

δ : *Vertical Tire Deflection (ins)*

2.2.3 Footprint

Tires under pure vertical load show deformation and deflections as sketched in [Figure 2.2](#). The footprint is the contact area of the tire with the ground.

2.2.3.1 Footprint length

Experiments for tire types I and VII tires [8] led to [Figure 2.3](#) and the experimental data can be represented by the empirical [equation 2.5](#) for the footprint length. More information how to determine the empirical equations from measurements data can be found on Appendix A in [8]. However the general idea is that a simple equation can represent the measurements.

$$2 * h = 0.85 * 2d \sqrt{\left(\frac{\delta}{d}\right) - \left(\frac{\delta}{d}\right)^2} \quad (2-5)$$

where,

h: Half of the Footprint (ins)

d: Outside Diameter of Free Tire (ins)

δ : Vertical Tire Deflection (ins)

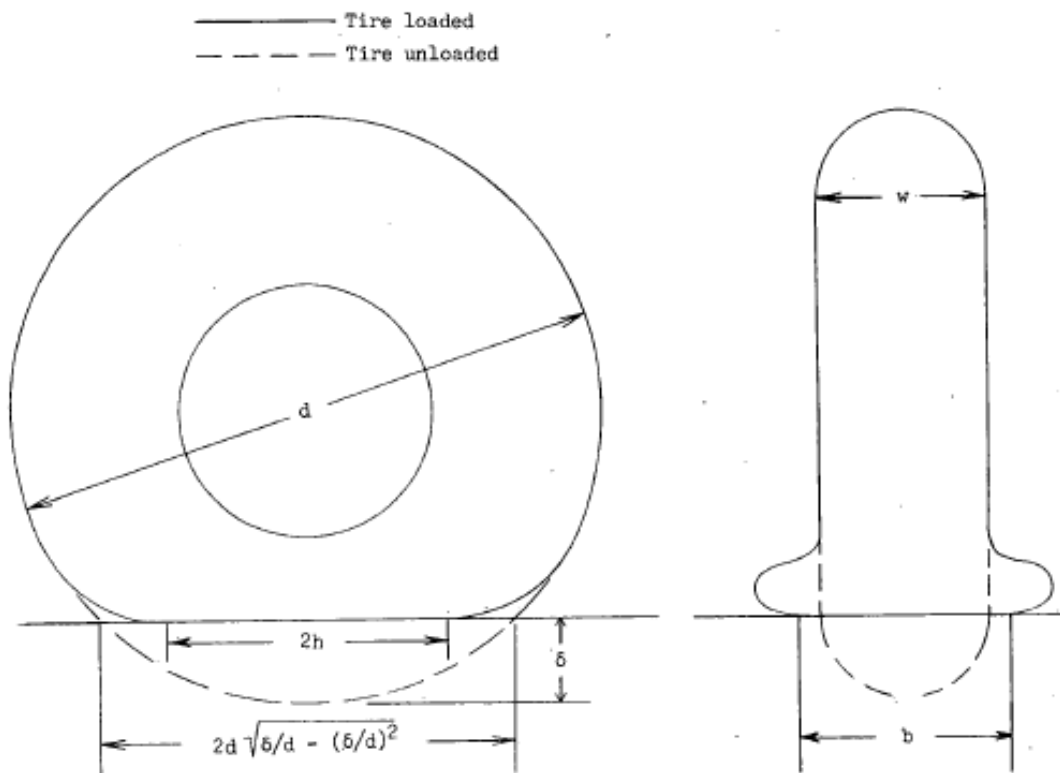


Figure 2.2: Sketch of tire under pure vertical loading.

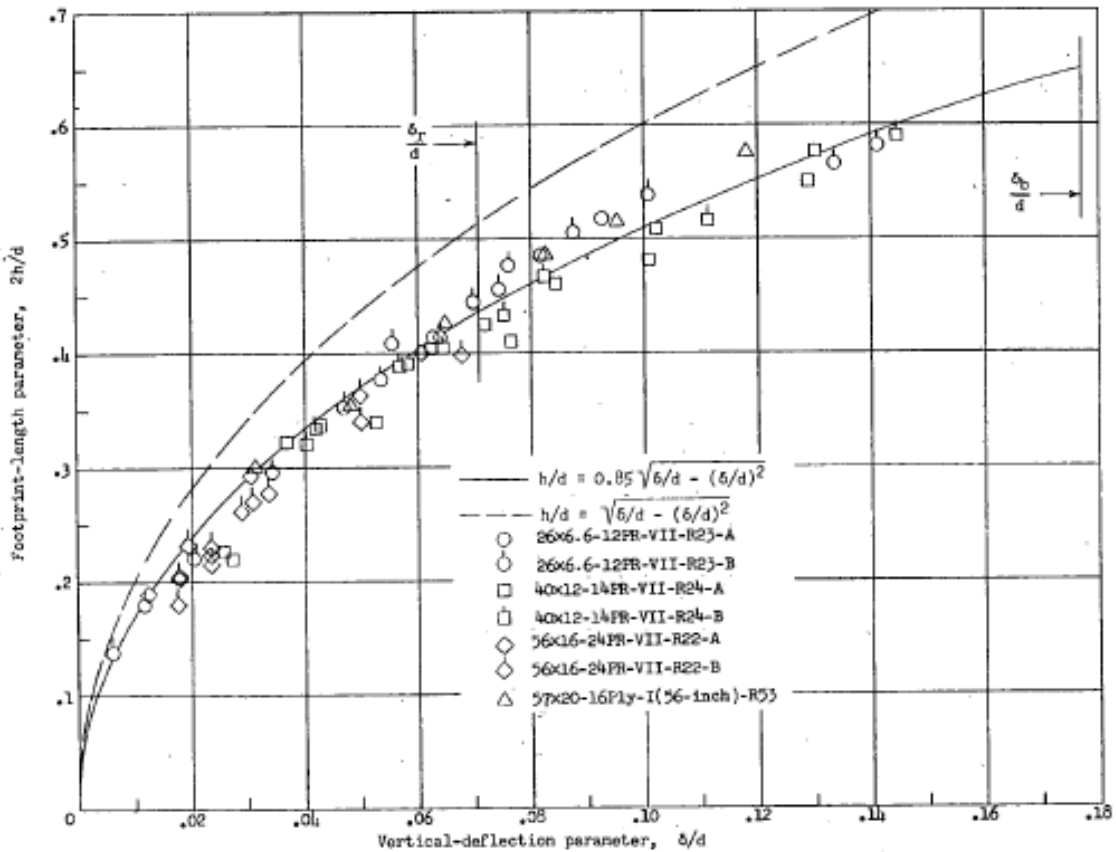


Figure 2.3: Variation of footprint-length parameter with vertical-deflection parameter for several types I and VII tires.

2.2.3.2 Footprint Width

A similar procedure was followed for the Footprint Width. Experimental data [8] showing the variation of footprint width with tire vertical deflection in the [Figure 2.4](#), led to the empirical equation for the footprint width as follows:

$$\frac{b}{w} = 1.7 \sqrt{\left(\frac{\delta}{w}\right) - 2.5 \left(\frac{\delta}{w}\right)^4 + 1.5 \left(\frac{\delta}{w}\right)^6} \tag{2-6}$$

where,

b: Width of tire – ground contact area (footprint) (ins)

w: Maximum width of undeflected tire (ins)

The equation (2.6) can be simplified and approximated as follows:

$$\frac{b}{w} = 2 \sqrt{\left(\frac{\delta}{w}\right) - \left(\frac{\delta}{w}\right)^2} \quad (2-7)$$

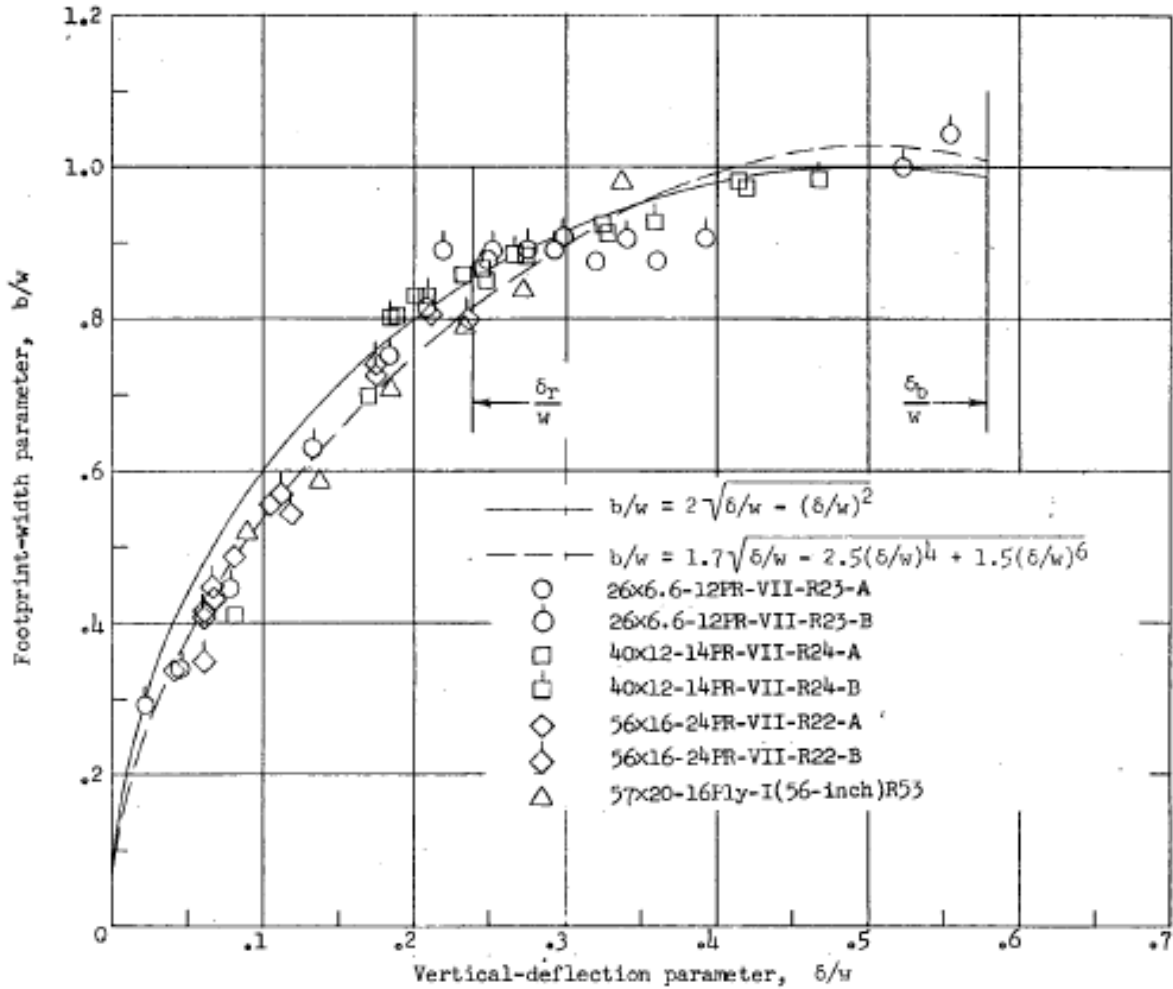


Figure 2.4: Variation of footprint-width parameter with vertical-deflection parameter.

2.2.3.3 Footprint Area

The gross footprint area is defined as the area of contact between the tire and ground, including the spaces between the tire's treads. The empirical equation for the footprint gross area is given as follows [8]:

$$A_g = 2.3\delta\sqrt{wd} \quad (2-8)$$

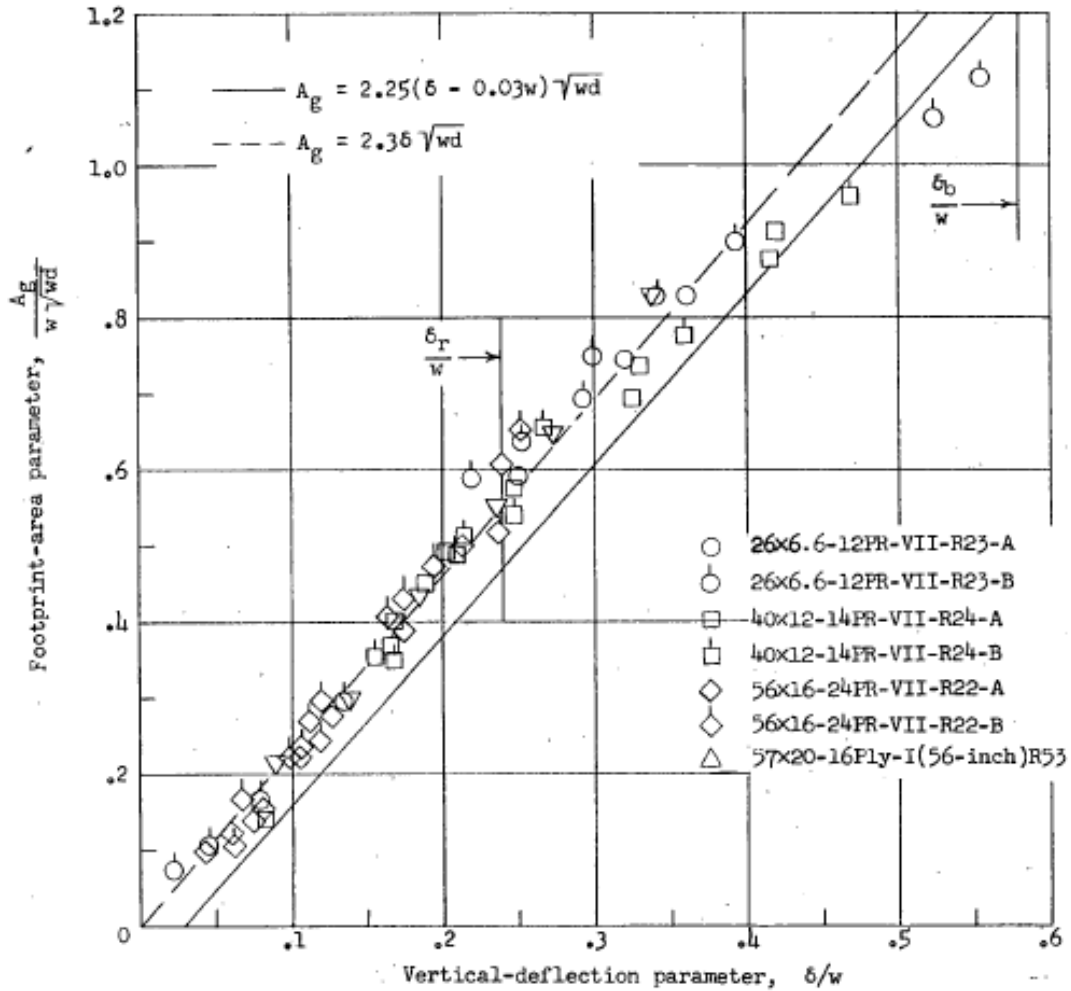


Figure 2.5: Variation of gross-footprint-area parameter with vertical-deflection parameter for types I and VII tires.

The footprint net area is defined by the following formula [8]:

$$A_n = aA_g \tag{2-9}$$

where,

a: Ratio of net footprint area to gross footprint area [-]

2.2.4 Lateral Stiffness

Dimensional considerations and observation of plots like in the [Figure 2.6](#) [8] provides the empirical equation for the lateral stiffness as follows:

$$K_{\lambda} = \tau_{\lambda} w (p + 0.24 p_r) \left[1 - \left(\frac{0.7 \delta_o}{w} \right) \right] \quad (2-10)$$

where,

τ_{λ} : Lateral – spring constant coefficient ($\frac{\text{lbs.}}{\text{in}}$)

w : Maximum width of undeflected tire (ins)

p : Tire inflation pressure (psi)

p_r : Tire rated inflation pressure (psi)

δ_o : Vertical tire deflection for pure vertical loading conditions (ins)

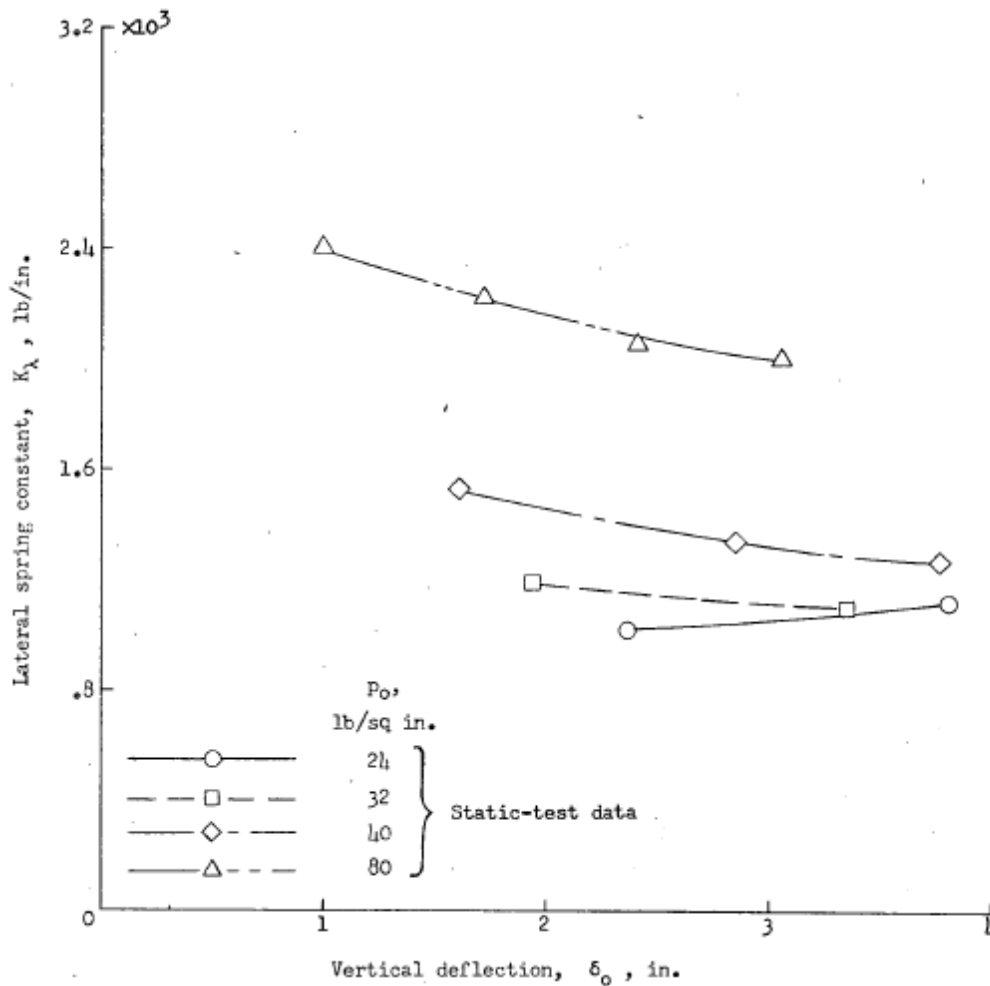


Figure 2.6: Variation of lateral spring constant with vertical deflection and inflation pressure for a 28x9x19PR-10PR-I (27-inch)-R21-E2 tire.

2.2.5 Torsional Stiffness

Sample experimental data [8] illustrating the effects of vertical deflection and inflation pressure are illustrated in Figure 2.7 and give the empirical equation for the torsional stiffness:

$$\frac{K_a}{(p+0.8p_r)w^3} = 475 \left(\frac{\delta_o}{d}\right)^2 \quad \left(\frac{\delta_o}{d} \leq 0.02\right) \quad (2-11)$$

$$\frac{K_a}{(p+0.8p_r)w^3} = 19 \left(\frac{\delta_o}{d}\right) - 0.01 \quad \left(\frac{\delta_o}{d} \geq 0.02\right) \quad (2-12)$$

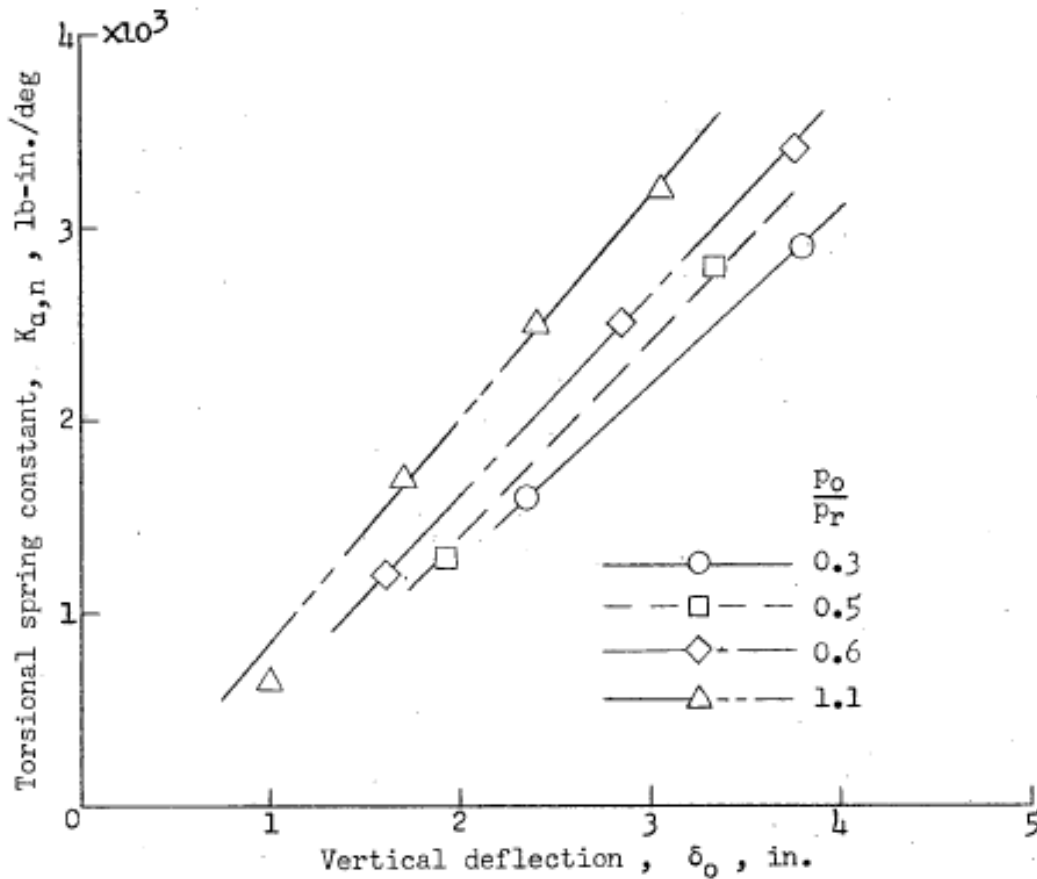


Figure 2.7: Experimental variation of static torsional spring constant with vertical deflection and inflation pressure for a 28x9-10PR-I(27-inch)R21-E2 tire.

2.2.6 Fore-Aft Stiffness

Experimental data [8] for the fore-and-aft spring constant show that it increases with increasing tire vertical deflection and increases slightly with increasing inflation pressure. The aforementioned information along with Figure 2.8 led to the empirical equation for the fore-aft stiffness as follows:

$$K_x = k_1 d (p + k_2 p_r) f\left(\frac{\delta_o}{d}\right) \quad (2-13)$$

where,

k_1 and k_2 are numerical constants

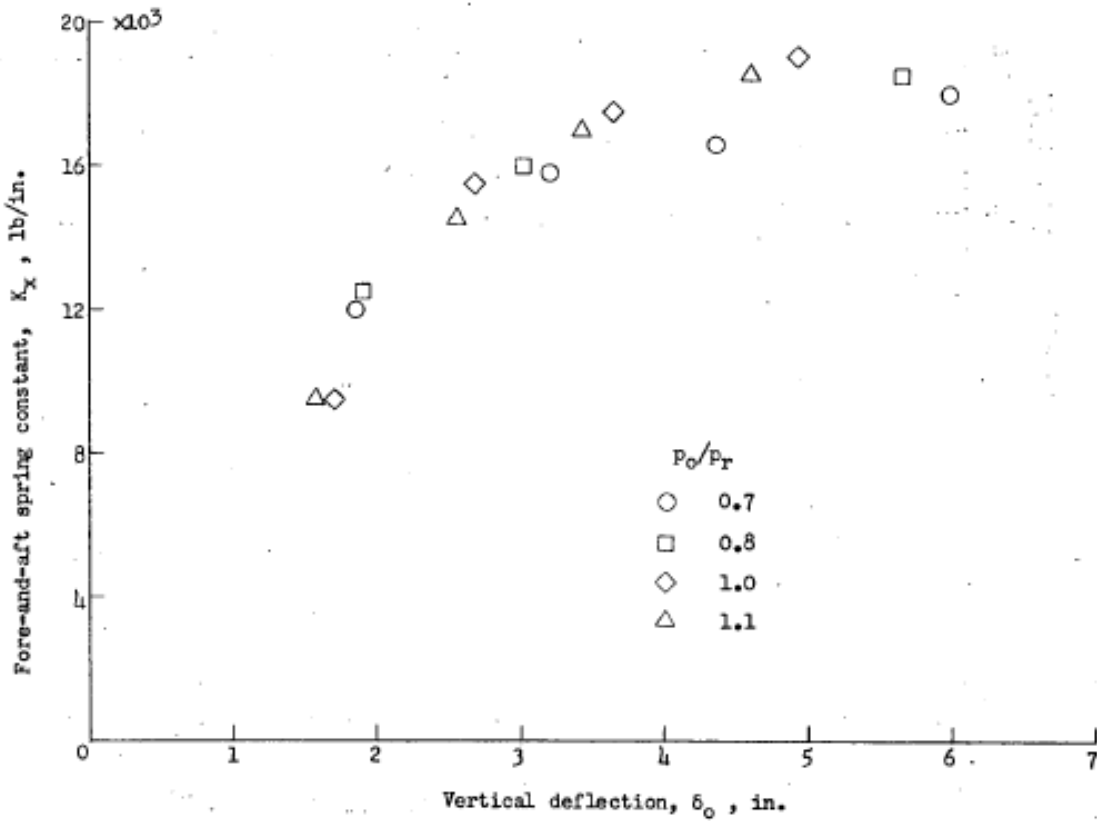


Figure 2.8: Experimental variation of fore-and-aft spring constant with vertical deflection and inflation pressure for a 56x16-32PR-VII tire.

2.2.7 Rolling Relaxation Length

2.2.7.1 Un-yawed relaxation length

Experimental measurements [8] as shown in [Figure 2.9](#) have to lead to the empirical equation for the un-yawed rolling relaxation length:

$$L_f = \left(2.8 - \frac{0.8p}{p_r}\right) \left(1 - \frac{4.5\delta_o}{d}\right) w \quad (2-14)$$

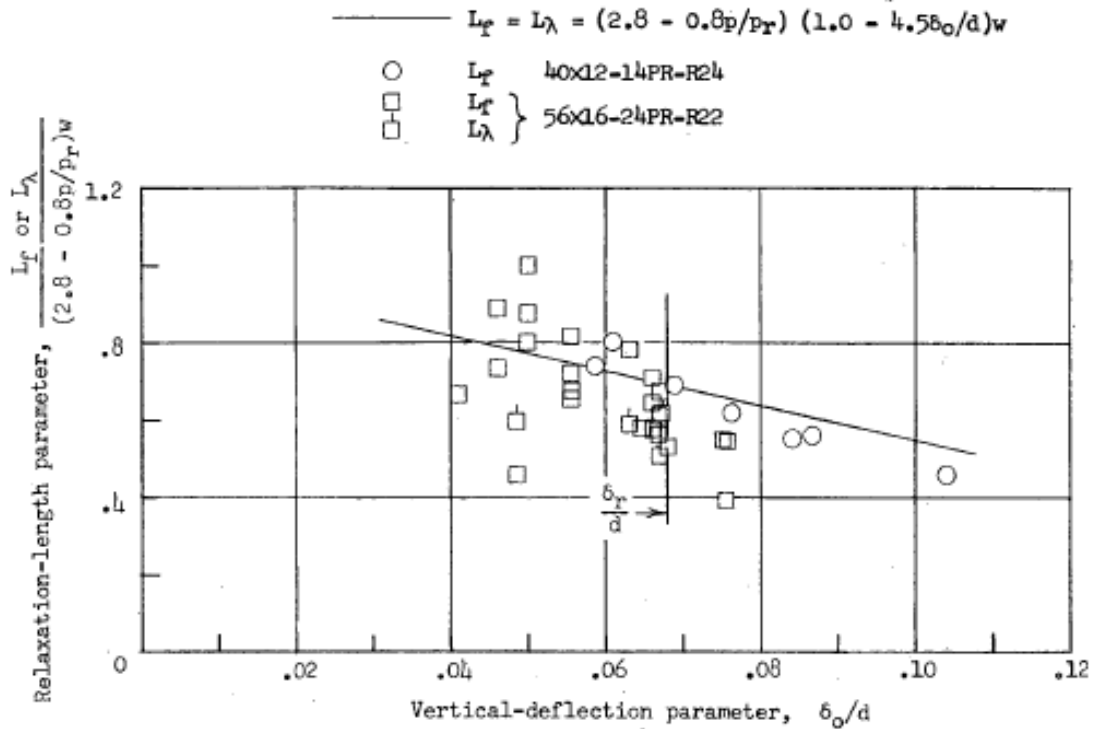


Figure 2.9: Variation of unyawed-rolling relaxation-length parameters with vertical-deflection parameter for two pairs of type VII tires.

2.2.7.2 Yawed relaxation length

Experimental data [8] gives the variation of yawed-rolling relaxation-length parameter with vertical-deflection parameter. The empirical equation for the yawed rolling relaxation length is as follows:

$$\frac{L_y}{\left(2.8 - \frac{0.8p}{p_r}\right)} = \frac{11\delta_o}{w} \quad \left(\frac{\delta_o}{d} \leq 0.053\right) \quad (2-15)$$

$$\frac{L_y}{\left(2.8 - \frac{0.8p}{p_r}\right)} = \left(\frac{64\delta_o}{w}\right) - 500\left(\frac{\delta_o}{d}\right)^2 - 1.4045 \quad \left(0.053 \leq \frac{\delta_o}{d} \leq 0.068\right) \quad (2-16)$$

$$\frac{L_y}{\left(2.8 - \frac{0.8p}{p_r}\right)} = 0.9075 - \left(\frac{4\delta_o}{d}\right) \quad \left(0.068 \leq \frac{\delta_o}{d}\right) \quad (2-17)$$

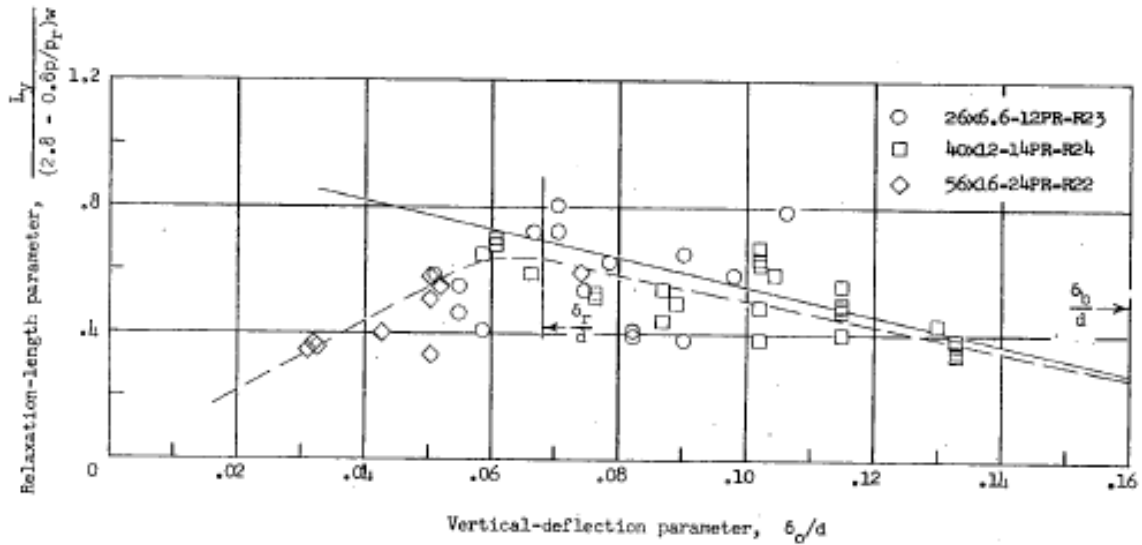


Figure 2.10: Variation of yawed-rolling relaxation-length parameter with vertical-deflection parameter for three type VII tires.

2.2.8 Effective Rolling Radius

The effective rolling radius is defined as the ratio of the horizontal displacement of the wheel axle to the rotation angle of the wheel and is given by the following equation [8]:

$$r_e = \frac{V_H}{\omega} \quad (2-18)$$

where,

V_H : Horizontal rolling velocity ($\frac{ins}{sec}$)

ω : Wheel angular velocity (radians/sec)

2.2.9 Cornering Power

The Cornering Power or Cornering Stiffness of a tire is defined as the rate of change of cornering force with yaw angle ψ for $\psi \rightarrow 0$. Analysis of the available experimental data of the [Figure 2.11](#) [8] led to the empirical equation for the empirical cornering power as follows:

$$\frac{N}{c_c(p+0.44p_r)w^2} = 1.2 \left(\frac{\delta}{d}\right) - 8.8 \left(\frac{\delta}{d}\right)^2 \quad (\delta/d \leq 0.0875) \quad (2-19)$$

$$\frac{N}{c_c(p+0.44p_r)w^2} = 0.0674 - 0.34 \left(\frac{\delta}{d}\right) \quad (\delta/d \geq 0.0875) \quad (2-20)$$

where,

N : Cornering power (lbs./deg)

C_c : Cornering – Power coefficient

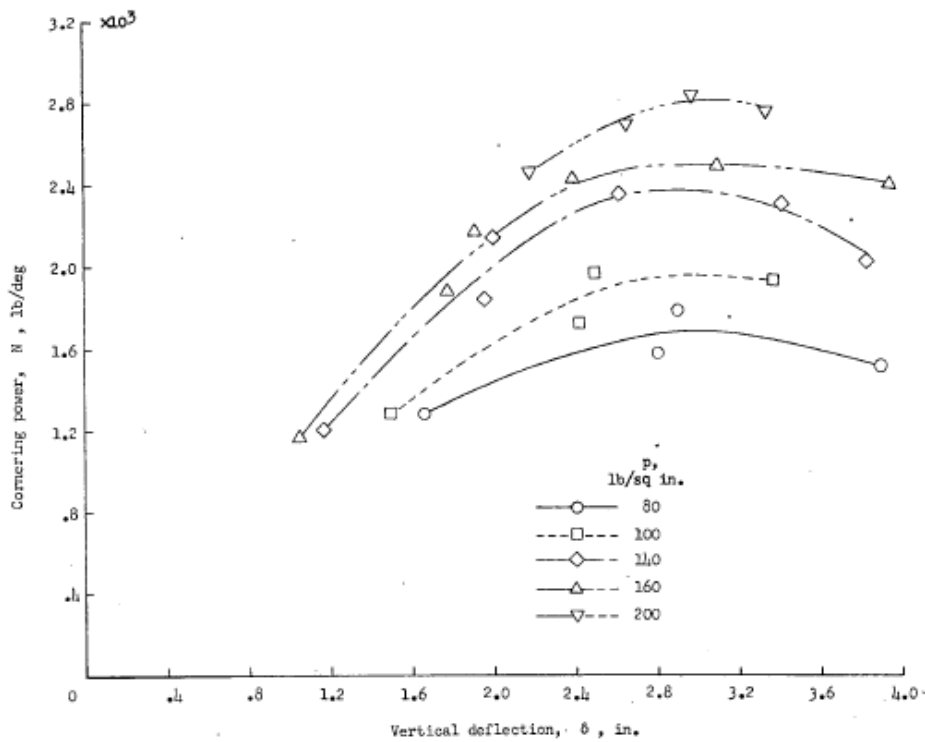


Figure 2.11: Variation of cornering power with vertical deflection for several inflation pressures for a pair of 56x16-24PR-VII-R22 tires.

The theoretical cornering power is given as follows [8]:

$$N = (L_y + h)K_\lambda \quad \text{per radian} \quad (2-21)$$

$$N = \frac{\pi}{180} (L_y + h) K_\lambda \quad \text{per degree} \quad (2-22)$$

where,

L_y : Yawed – rolling relaxation length (ins)

2.2.10 Normal and Cornering Force

The Normal Force is exerted perpendicular to the wheel plane and it is slightly bigger than the Cornering Force which is exerted perpendicular to the direction of motion. For vertical deflections up to approximately the rated deflection, the steady-state normal force can be calculated by the following empirical equation [8]:

$$\frac{F_{\psi,r,e}}{\mu_\psi F_z} = \emptyset - \frac{4}{27} \emptyset^3 \quad (\emptyset \leq 1.5) \quad (2-23)$$

$$\frac{F_{\psi,r,e}}{\mu_\psi F_z} = 1 \quad (\emptyset \geq 1.5) \quad (2-24)$$

where the yaw-angle parameter is given by,

$$\emptyset = \frac{N}{\mu_\psi F_z} \psi \quad (2-25)$$

And the other parameters,

$F_{\psi,r,e}$: Steady – state normal force (lbs.)

μ_ψ : Yawed rolling coefficient of friction (ins. lbs./deg)

F_z : Vertical force acting on tire from ground (lbs.)

ψ : Yaw angle (deg)

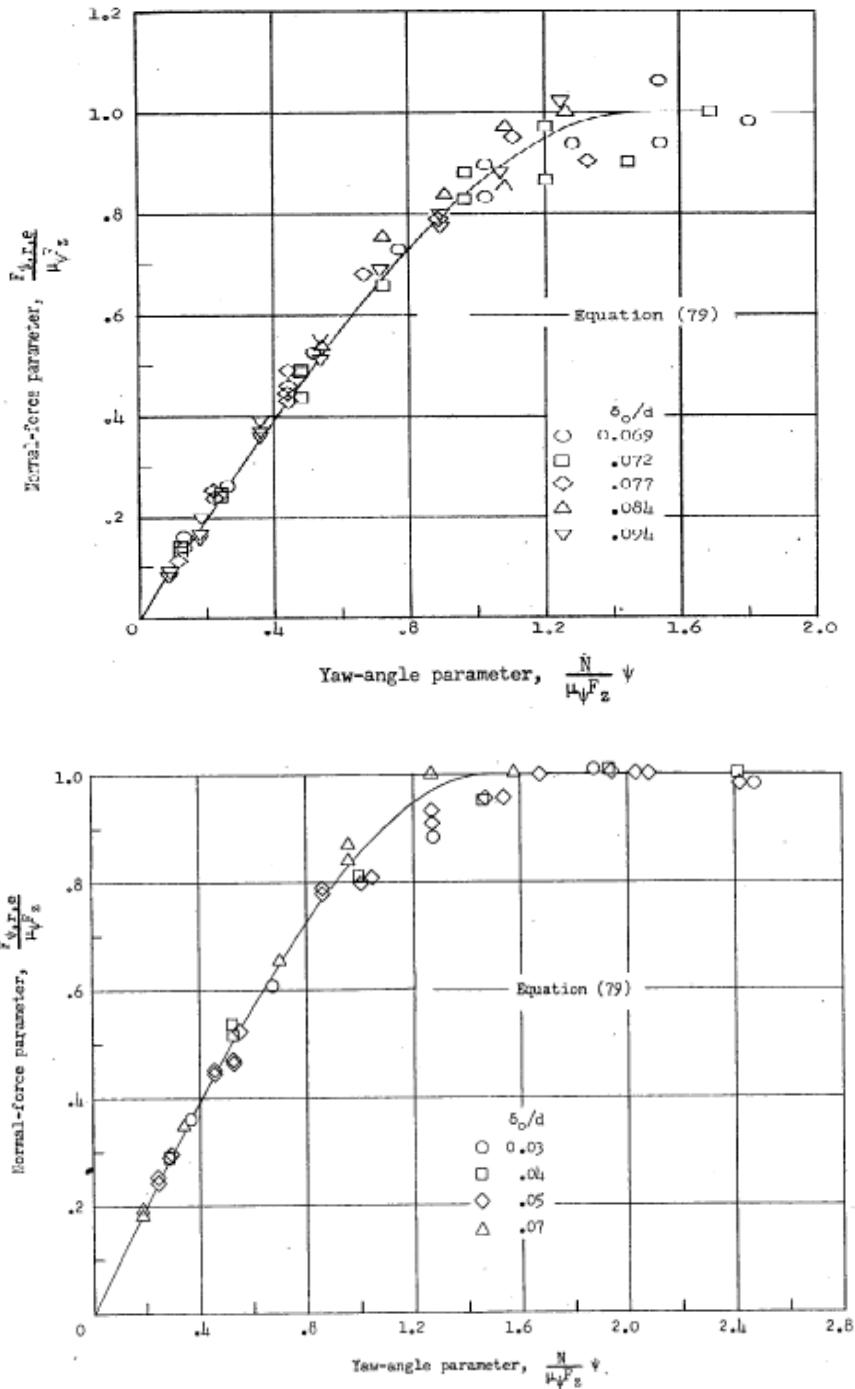


Figure 2.12: Variations of normal-force parameter with yaw-angle parameter for steady-state yawed rolling of type VII tires.

The relation between the normal force and the cornering force can be obtained by the equation [8]:

$$F_{y,r,e} = F_{\psi,r,e} \cos \psi \tag{2-26}$$

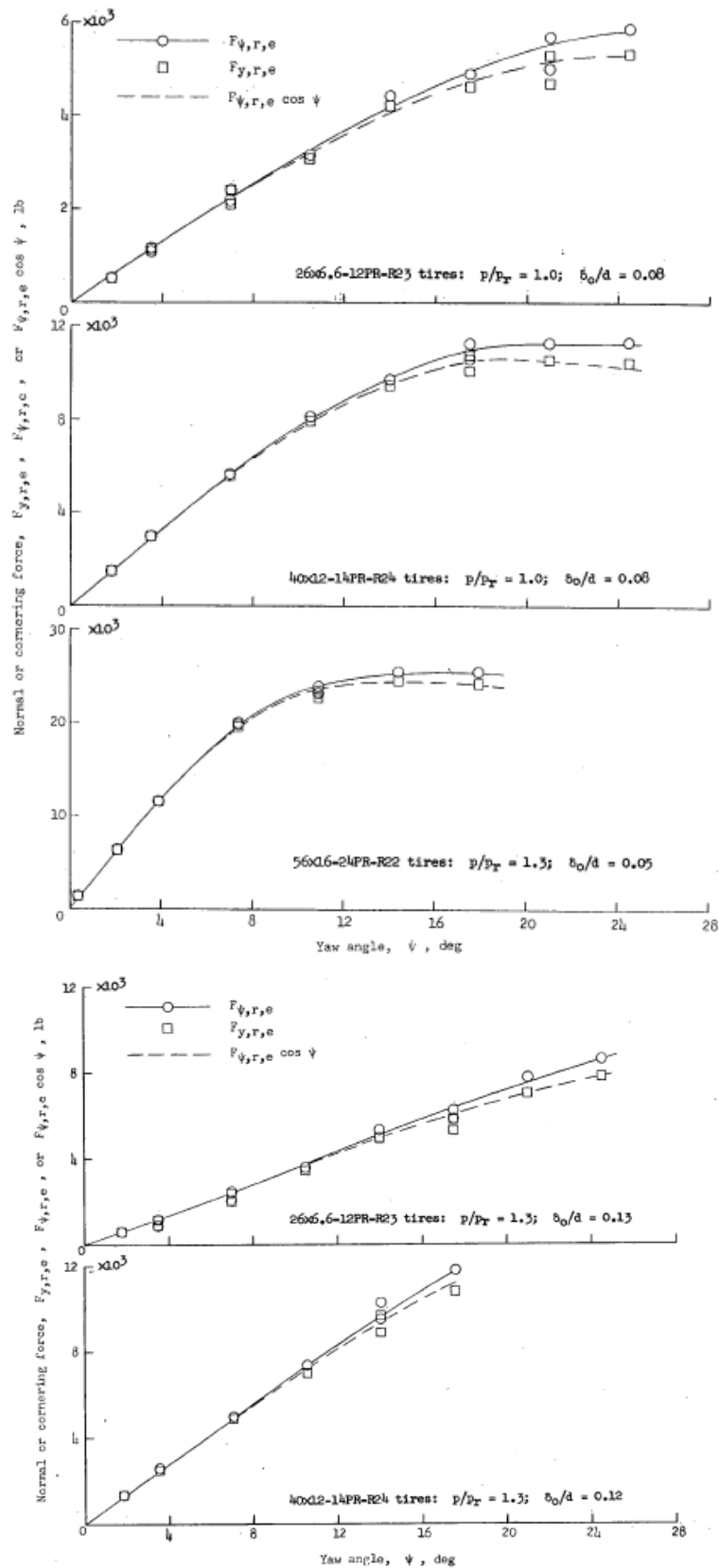


Figure 2.13: Comparison of normal and cornering forces for yawed rolling of several type VII tires.

2.2.11 Aligning Torque

Figure 2.14 shows that the self-aligning torque can be described by the following set of empirical equations[8]:

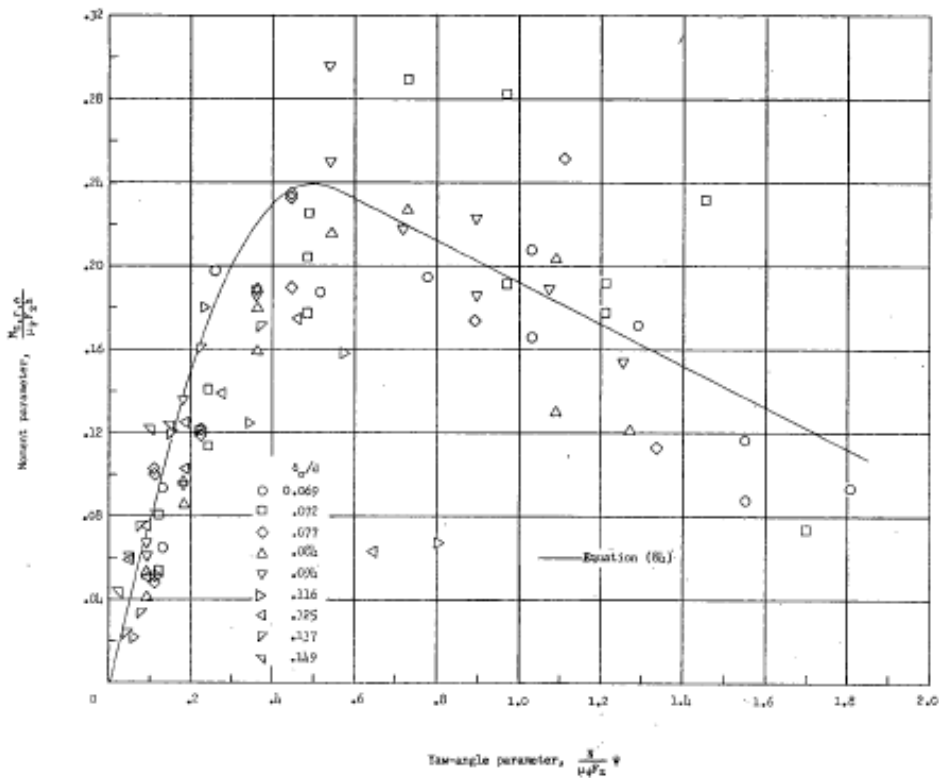
$$\frac{M_{z,r,e}}{\mu_{\psi}F_z h} = 0.8\varnothing \quad \varnothing \leq 0.1 \quad (2-27)$$

$$\frac{M_{z,r,e}}{\mu_{\psi}F_z h} = \varnothing - \varnothing^2 - 0.01 \quad (0.1 \leq \varnothing \leq 0.55) \quad (2-28)$$

$$\frac{M_{z,r,e}}{\mu_{\psi}F_z h} = 0.2925 - 0.1\varnothing \quad \varnothing \geq 0.55 \quad (2-29)$$

where,

$$\varnothing = \frac{N}{\mu_{\psi}F_z} \psi \quad (2-30)$$



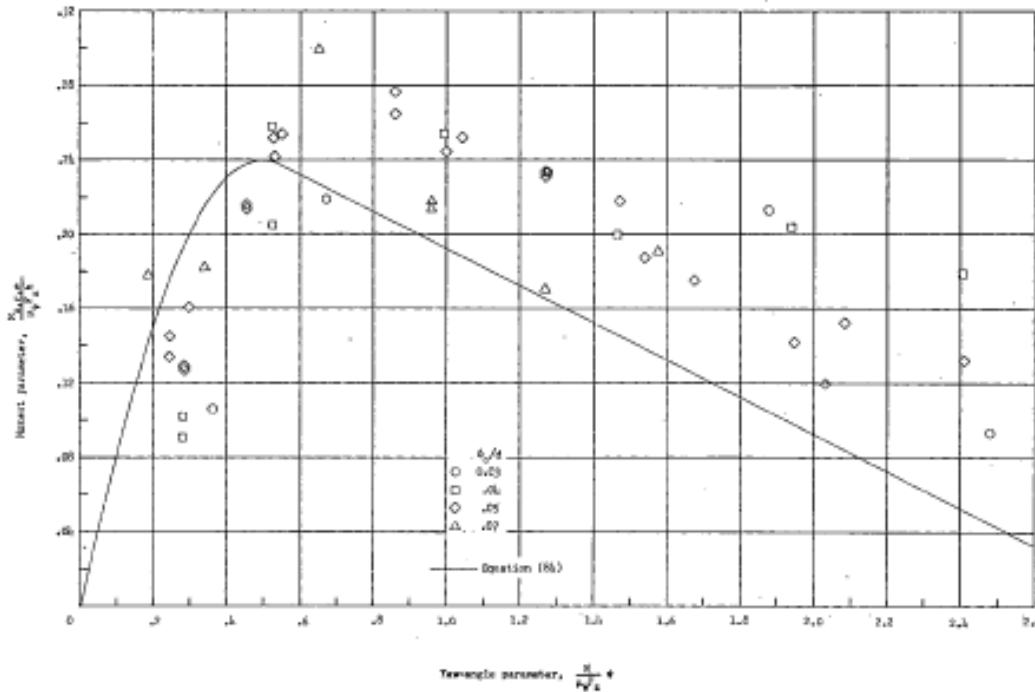


Figure 2.14: Variation of self-aligning-torque parameter with yaw-angle parameter for steady-state yawed rolling of several type VII tires.

The maximum self-aligning torque, according to the equations (2.27)–(2.30) is given by [8]:

$$M_{z,r,e,max} = 0.24\mu_{\psi}hF_z \tag{2-31}$$

2.2.12 Pneumatic Trail

The pneumatic trail, which is also called pneumatic caster in [8], is based on measurements as shown in Figure 2.15. By definition the pneumatic trail equals:

$$q = \frac{M_{z,r,e}}{F_{\psi,r,e}} \tag{2-32}$$

where,

q : Pneumatic trail or pneumatic caster (ins)

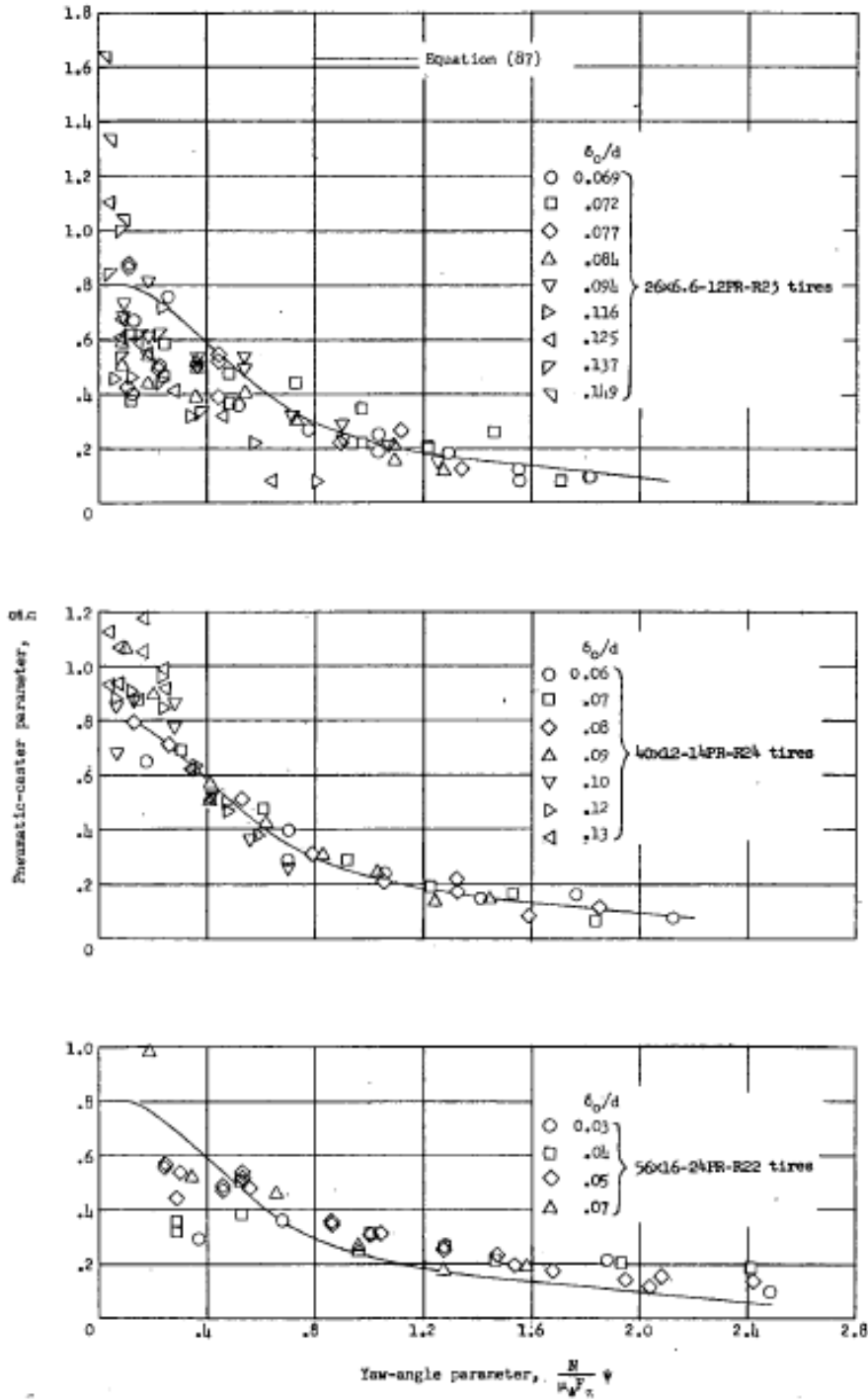


Figure 2.15: Variation of pneumatic-caster parameter with yaw- angle parameter for several pairs of type VII tires.

2.2.13 Tire parameters for shimmy stability analysis.

All the information and equations presented so far can be found on the work of Smiley and Horne [8]. On the following page the work of Collins and Black [31] will be discussed to obtain some tire parameters

which can be used for shimmy analyses of the landing gear. In this paper the suggestion by Moreland is considered which relates the force acting on the wheel to the tire distortion angle ψ_t and its derivative $\dot{\psi}_t$. Analytical predictions of the parameters, using the tire mechanics equations, show good correlation with experimental results [8].

A landing gear system may be analyzed as a lumped mass frame which has a shimmy damper. The general form of equations for the landing gear is given as follows:

$$\sum_{j=1}^N m_{ij} q_j'' + \sum_{j=1}^N C_{ij} q_j' + \sum_{j=1}^N k_{ij} q_j = Q_i \quad i = 1, 2, 3 \dots N \quad (2-33)$$

where m_{ij} is the generalized inertia matrix, C_{ij} the equivalent viscous damping matrix for the structure, k_{ij} the stiffness matrix of the structure and q_i the N generalized coordinates of the structure.

The Moreland hypothesis describes the lateral tire Force with the following equations:

$$F_t = k_1 \Delta + k_D \dot{\Delta} \quad (2-34)$$

where k_1 is the effective lateral stiffness and k_D is the effective lateral damping of the tire.

$$CF_t = \psi_t + C_1 \dot{\psi}_t \quad (2-35)$$

where C is referred to as the tire yaw coefficient and C_1 as the tire time constant.

The tire moment was proposed by Moreland to be given with the following expression:

$$M_t = \mu_1 \psi_t \quad (2-36)$$

where $\mu_1 = \mu_s + \mu_{D1}$

The summation of moments about the pivot shows that,

$$M_A + LF_t + Mt + M_B = I \ddot{\psi} \quad (2-37)$$

where M_A is the applied moment about the pivot and M_B denotes the frictional losses in the bearings.

By using the above equation and the kinematic rolling constraint, one can obtain the coefficient of yaw, the rolling tire torsional stiffness, the lateral stiffness, the lateral damping coefficient, the drag force slip coefficient and the yaw time constant. These parameters can be used for shimmy and stability analyses of the landing gear of the helicopter. More information and analytical explanations can be found on the paper of Collins and Black [31]. The analytical description of the procedure is out of the scope of this report.

3 TIRE MODEL PARAMETERIZATION FOR NH90 IN MSC.ADAMS

3.1 Introduction

The main objective of this report is to provide all the information needed in order to parameterize a new aircraft tire in MSC.ADAMS (2013.2 version). Before starting a review of the current tire models, that are available in industry and universities, will be performed.

3.2 Tire Models

There are various approaches to build a tire model that describes the tire's behavior. The complexity of the tire structure and its non-linear behavior are such that no complete theory has yet been proposed. However thanks to new experimental and advanced computing techniques, more accurate tire models have been developed the last decades. Two main tire model approaches can be distinguished: the *empirical tire models* and the *physical tire models* as will be discussed.

3.2.1 Empirical Models

The empirical tire models represent the measurements by using an empirical mathematical model. In this category, the following models can be found: the Magic Formula model, MF-Tyre/MF-SWIFT model, the Burckhardt model, Fiala model, the Kience and Daiss model, the similarity method model, TMeasy tire model and UniTire model see references [1],[11], and ,[12].

3.2.2 Physical Models

The physical tire models are created with detailed modelling of the tire structure in steady-state conditions. In this category, the following models can be found: RMOD-K model, the stretched string model, the brush model, Dynamic tire friction model, the beam tire model, FTire model, TreadSim model, Soft-Soil model and CDtire model, see references [1],[3],and, [30]. The aforementioned models are suited for steady-state conditions. There are also physical tire models suited for the time-varying or transient conditions like the, Bliman model, Kinematic model, Dahl model and LuGre model, see references [11] and, [12].

3.2.3 Combined Models

Besides the aforementioned empirical and physical models, also combinations are possible giving semi-empirical models like the Hankook tire model, see references [28]and, [30].

More information about each tire model can be found in [Appendix A](#).A comparison of the different type of models and their ability to predict the tire performance is shown in [Figure 3.1](#).

comparison of different approaches:

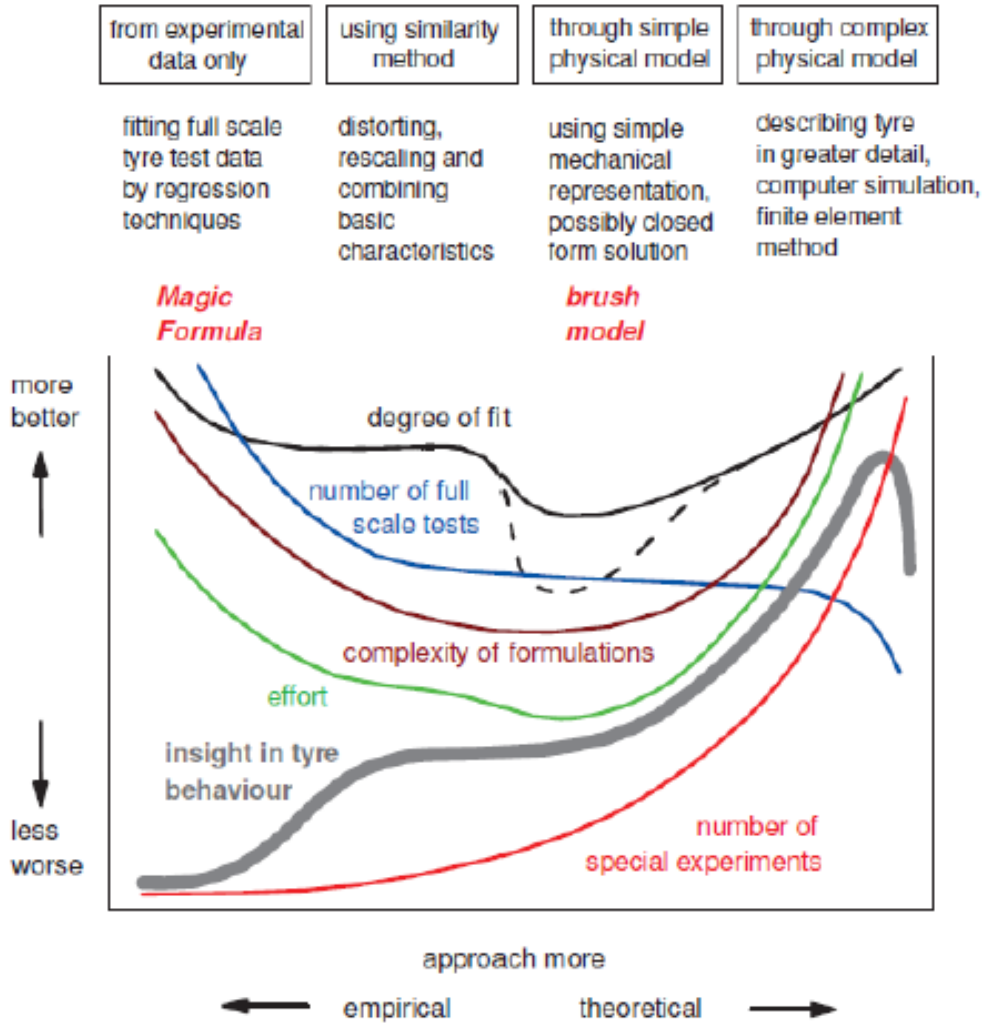


Figure 3.1: Comparison of different tire models [1].

3.3 Tire Models in MSC.ADAMS

The program MSC.ADAMS includes a considerable number of tire models for a variety of applications. Further, the open tire interface of the program allows the users to develop and include custom tire models of their own design. An overview of the features of the included tire models in MSC.ADAMS can be seen in [Figures 3.2](#) and [3.3](#).

ADAMS v2006 r1	Event / Maneuver	ADAMS/ Handling Tire							Specific Models	
		PAC2002 [‡]	PAC-TIME [‡]	PAC89 [‡]	PAC94 [‡]	FIALA [‡]	5.2.1. [†]	UA Tire [†]	PAC-MC [†]	FTire
Handling	Stand still and start	+	o/+	o/+	o/+	o/+	o/+	o/+	o/+	+
	Parking (standing steering effort)	+	-	-	-	-	-	-	-	+
	Standing on tilt table	+	+	+	+	+	+	+	+	+
	Steady state cornering	+	+	o/+	+	o	o	o/+	+	o/+
	Lane change	+	+	o/+	+	o	o	o/+	+	o/+
	ABS braking distance	+	o/+	o/+	o/+	o	o	o/+	o/+	+
	Braking/power-off in a turn	+	+	o	o	o	o	o	+	o/+
	Vehicle Roll-over	+	o	o	o	o	o	o	o	+
Ride	On-line scaling tire properties	+	-	-	-	-	-	-	-	o
	Cornering over uneven roads [‡]	o/+	o	o	o	o	o	o	o	o/+
	Braking on uneven road [‡]	o/+	o	o	o	o	o	o	o	+
	Crossing cleats / obstacles	-	-	-	-	-	-	-	-	+
	Driving over uneven road	-	-	-	-	-	-	-	-	+
	4 post rig (A/Ride)	+	o/+	o/+	o/+	o/+	o/+	o/+	o/+	o/+
	ABS braking control	o/+	o	o	o	o	o	o	o	+
	Shimmy [§]	o/+	o	o	o	o	o	o	o	+
Chassis Control	Steering system vibrations	o/+	o	o	o	o	o	o	o	+
	Real-time	+	-	-	-	-	-	-	-	-
	Chassis control systems > 8 Hz	o/+	-	-	-	-	-	-	-	+
	Chassis control with ride	-	-	-	-	-	-	-	-	+
Dura-bility	Driving over curb	-	-	-	-	-	o	o	-	o/+
	Driving over curb with rim impact	o	-	-	-	-	o	o	-	o/+
	Passing pothole	-	-	-	-	-	o	o	-	o/+
	Load cases	-	-	-	-	-	o	o	-	o/+

-	not possible/not realistic;	‡ wavelength road obstacles > tire diameter
o	possible;	† use_mode on transient and combined slip
o/+	better;	§ wheel yawing vibration due to suspension flexibility and tire dynamic response
+	best to use.	

Figure 3.2: Application examples of ADAMS/Tire module (version 2006) [5].

The ADAMS/Tire module offers the following models:

- PAC2002, an updated Pacejka tire model in accordance with [1].
- PAC-TIME, a Pacejka tire model that uses the TIME measurement procedure [21].
- PAC89, the original Pacejka tire model based on the first papers on the ‘Magic Formula’ [5].
- PAC94, based on PAC89 with improvements in camber effects of the tire [23].
- Fiala, a tire model which uses a simple physical approach [24].
- 5.2.1-Tire, a simple model that requires a small set of parameters or experimental data to simulate the behavior of tires. The 521-Tire is the first tire model incorporated in Adams. The name “5.2.1” refers to the version number of Adams/Tire when it was first released. [30]
- UA-Tire, the University of Arizona Tire model is a more sophisticated approach than Fiala and 5.2.1-Tire models and can handle camber effects [25].

- PAC-MC, a Pacejka tire model for motorcycle tires, which can handle a large inclination angle with respect to the road plane [1].
- FTire, a sophisticated coarse FEM tire model which uses a physical approach to model the tire's structure [26].
- Soft Soil, a tire model that offers a basic model to describe the tire-soil interaction forces for any tire on elastic/plastic grounds, such as sand, clay, loam and snow [30].

MD	Event / Maneuver	Specific Models			Aircraft		
		PAC-MC	FTire	SoftSoil	Basic	Enhanced	TRR64
Adams	Stand still and start	o/+	+	-	o/+	o/+	o/+
	Parking (standing steering effort)	-	+	-	-	-	-
	Standing on tilt table	+	+	-	+	+	+
	Steady state cornering	+	o/+	+	o	+	o/+
	Lane change	+	o/+	+	o	+	o/+
	ABS braking distance	o/+	+	o/+	o	o/+	o/+
	Braking/power-off in a turn	+	o/+	+	o	o	o
	Vehicle Roll-over	o	+	o/+	o	o	o
	On-line scaling tire properties	-	o	-	-	-	-
Ride	Cornering on uneven roads ¹	o	o/+	o	o	o	o
	Braking on uneven roads ¹	o	+	o	o	o	o
	Crossing cleats / obstacles	-	+	o	-	-	-
	Driving over uneven road	-	+	o	-	-	-
	4 post rig (A/Ride)	o/+	o/+	-	o/+	o/+	o/+
Chassis Control	ABS braking control	o	+	-	o	o	o
	Shimmy ²	o	+	-	o	o	o
	Steering system vibrations	o	+	-	o	o	o
	Real-time	-	-	-	-	-	-
	Chassis control systems > 8 Hz	-	+	o	-	-	-
	Chassis control with ride	-	+	-	-	-	-
Dura-bility	Driving over curb	-	o/+	o	-	o	o
	Driving over curb with rim impact	-	o/+	-	-	o	o
	Passing pothole	-	o/+	o	-	o	o
	Load cases	-	o/+	o	-	o	o
Misc	Design of Experiments	-	+	-	-	-	-
	SMP parallel	+	+	+	+	+	+

-	Not possible/Not realistic
o	Possible
o/+	Better
+	Best to use

¹ wavelength road obstacles > tire diameter
² wheel yawing vibration due to suspension flexibility and tire dynamic response
 tire models assumed to be used in transient and combined slip mode

Figure 3.3: Application examples of ADAMS/Tire module (version 2011) [30].

Besides the aforementioned models which are suitable for vehicle handling and comfort simulations, specific tire models have been developed for the simulation of the aircraft tires:

- Aircraft Basic Tire, which is based on the Fiala method [30].

- Aircraft Enhanced Tire, which uses the UA-Tire model approach [30].
- Aircraft TR-R-64 Tire Model, which employs the empirical expressions of [8] for aircraft tire [27].

Most of the tire models in MSC.ADAMS are used for handling and ride comfort simulations. However in this project the main scope is to represent the drop test of a landing gear as realistic as possible. For this kind of simulations the last three aircraft tire models are suitable. More information about each aircraft tire model parameters can be found in the next 3 sections.

3.3.1 TR-R-64 Aircraft Tire Model

The Aircraft TRR64 Tire Model's Basic Handling Force model is a basic version of the NASA TR-R-64 tire model which is based on [8]. This model is very popular for aircraft studies and modelling in the aerospace field. The model used in ADAMS is a simple version of the original tire model and includes some modifications to make it appropriate for modelling in ADAMS. The TRR64 Tire Model is comprised of a basic version of the NASA TR-R-64 tire model, with options to use additional handling force computations, such as those similar to the Adams/Tire Fiala and UA (University of Arizona) tire models. The following paragraphs are dedicated to describing the procedure of getting the NH90 tire parameters included in MSC.ADAMS program.

The basic parameters of the tire were provided by the tire manufacturer [32]. More specifically these parameters are:

- unloaded radius
- width
- aspect ratio
- rated pressure
- inflation pressure

The values of the mechanical properties of the tires were calculated with the help of the work of Smiley and Horne [8]. To that end, the tire manufacturer measured the vertical load and the deflection of the tire in a tire testing machine and the result is illustrated in Figure 3.7. Consequently, it is straight forward to take the tire vertical stiffness coefficient by applying the equation (2.4). For each load case the stiffness coefficient is different due to the tire's non-linear behavior. The manufacturer didn't give any information about vertical damping coefficient but as a rule of thumb, it is 1000 times less than stiffness coefficient. This information was given in the tire files provided by MSC.ADAMS/2013.2.

The rolling resistance coefficient was taken from the report [33] to be 0.08. The rolling radius deflection factor was given 0.33 in the ADAMS/tire manual [14]. The longitudinal lateral deflection factors were taken to be 0.15 and 0.70 by using the equations (38) and (41), from reference [8], for VII tire types which are similar to the current NH90 tire type. The footprint factor which is defined as the experimental footprint length divided by the geometric length for aircraft tires is approximately 0.85 and was taken from equation (2.5) or (5) from [8]. This value was found after experiments and measurements of the real and geometric footprint.

The gross and the net footprint area can be found in equations (2.8) and (2.9). The footprint area ratio is defined as the ratio between net and gross footprint area. The footprint area ratio is almost constant for all

the loads and was found to be 0.85 for NH90 case [8]. The bottoming radius and the bottoming curve was measured by the tire manufacturer [32]. There are still two parameters with no information from the tire manufacturer, the reference velocity for friction coefficient determination and factor used in the calculation of slip stiffness. However the TR-R-64 tire default file has already a similar tire with the NH90 tire, therefore the factor used in the calculation of slip stiffness was not changed. The reference velocity for friction coefficient determination is used only if FRICTION_MODE = 2 or 3, but in TRR64 model the FRICTION_MODE was set to 1.

3.3.2 Basic Aircraft Tire Model

The Aircraft Basic Tire Model is comprised of the ADAMS/Tire Fiala tire model, with modifications that are necessary for aircraft landing analysis. The following paragraphs are dedicated to describing the procedure of obtaining the parameters to be used in MSC.ADAMS program with the Basic Aircraft Tire Model chosen.

Besides the parameters that are similar between the BASIC and the TRR64 tire model, still the following parameters need to be specified for this particular model.

- relaxation length
- fore-aft stiffness
- cornering stiffness
- load-tire deflection curve

The yawed relaxation length is given by the equations (2.15)-(2.17). The fore-aft stiffness is given by (2.13) and the cornering stiffness by (2.19)-(2.20), The load-tire deflection curve measurements can be taken from [32] since they were measured by the tire manufacturer and can be seen in Figure 3.7. There is again no information for the reference velocity for friction coefficient determination. However the BASIC tire model uses FRICTION_MODE=1 and therefore this parameter is not needed for the calculations.

3.3.3 Enhanced Aircraft Tire Model

The Aircraft Enhanced Tire Model is comprised of the ADAMS/Tire Fiala and UA (University of Arizona) tire models, with modifications that are necessary for aircraft landing gear analysis in Adams.

Besides the parameters that are the same between the BASIC, the TRR64 and the ENHANCED tire model, still the following parameters need to be specified for this particular model.

- camber stiffness
- lateral stiffness

Tire's camber stiffness is defined as the partial derivative of lateral force with respect to inclination (camber) angle (γ) at zero camber angle. There is no information for that parameter in the tire's manufacturers report. However if tire's camber stiffness is put zero, the model makes an estimation of the parameters as explained in ADAMS/tire [30]. The Lateral stiffness is given by the equation (2.10) as it was explained in the second chapter. No information was given for the reference velocity for friction coefficient determination and factor used in the calculation of slip stiffness. For the last two parameters was applied the same with the previous models.

3.4 Tire Model Comparisons

3.4.1 Introduction

In this section, the three aircraft tire models will be compared with the data provided by the tire manufacturer.

3.4.2 Test Rig Model

The tire model parameter sets, described in the previous chapters, have to be compared with the tire manufacturer's data. For that reason a tire test rig model was created in the MSC.ADAMS program. A real test rig machine can be seen in the [Figure 3.4](#). The drum is rolling and the tire touches the rolling drum with a specific vertical force. A side slip angle is applied by the steering wheel.



Figure 3.4: Tire test rig machine.

The test rig model consists of the following components:

- massless test rig body
- rod
- steering rod
- tire
- road
- 2 translational joints
- 2 revolute joints
- motions

The test rig model is illustrated in [Figure 3.5](#). First of all, a massless test rig body was built and a straight motion with a translation joint was implemented with respect to the road plane. A translational joint was selected to connect the test rig body and the road. The road is illustrated with gray color. The red rod, connected to the test rig, allows free motion only in the vertical direction (perpendicular to the road plane) with a translation joint. The steering rod, depicted with green color, is connected with the rod and the wheel center. The connection with the rod is realized with a revolute joint that points to the vertical direction (like the previous joint). The steering rod is connected with the wheel with a revolute joint in the

horizontal direction (parallel to the road plane) which leaves the tire to roll freely with respect to the ground. The steering angle was being changed during the simulation by prescribing motion in the revolute joint between the rod and the steering rod. The forces and the moments between the tire and the road were measured. The ISO axis system is used to represent the forces and the torques. More details on this sign convention can be found in [Appendix B](#).

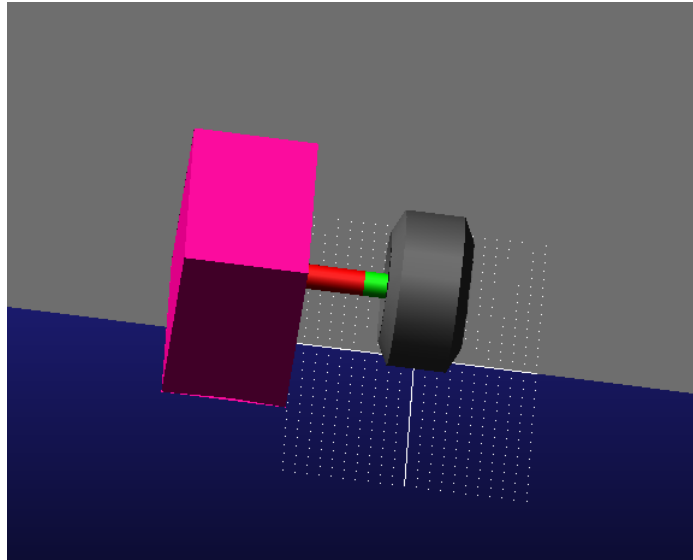


Figure 3.5: Tire test rig for the simulations in MSC.ADAMS.

It is worthwhile to mention that at the start, a test rig model was created with a rolling drum, as can be seen in [Figure 3.6](#). However this approach could not be followed because it was impossible to incorporate road characteristics to the drum. Choosing a horizontally moving rolling tire that touches a fixed road solved this problem.

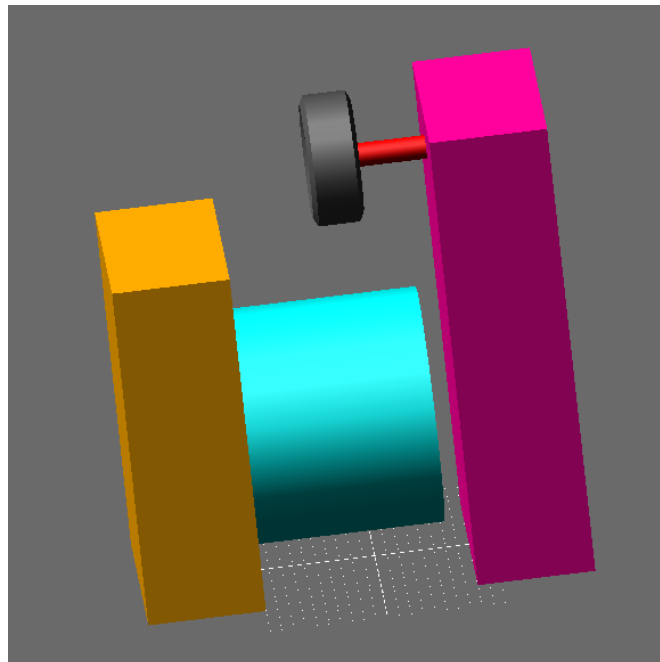


Figure 3.6: The obsolete test rig model.

3.4.3 Tire Measurements by the Tire Manufacturer

Usually only the vertical load which is exerted to the tire and the deflection of it are measured by the tire manufacturer. For the NH90 tire [32], the vertical load and tire deflection can be seen in Figure 3.7, as it was measured by the tire manufacturer for two tire inflation pressures. For these two inflation pressures the other tire characteristics have been calculated and are compared with the manufacturer statements in [32].

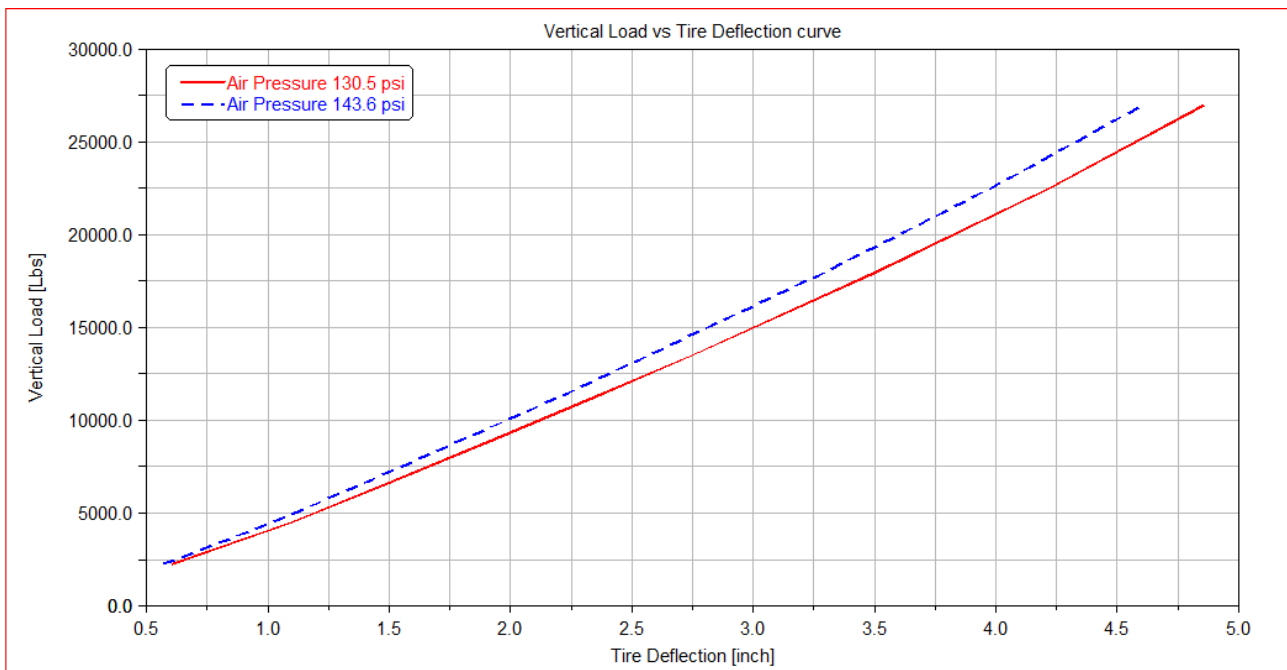


Figure 3.7: Tire Deflection with respect to Tire Vertical Load.

3.4.4 Simulations with tire's inflation pressure 130.5 psi

The following figures illustrate the results from the 3 aircraft tire models in MSC.ADAMS. These results are compared with the calculations provided by the tire manufacturer. The tire inflation pressure, for this case, is 130.5 psi.

It is important to mention that the tire properties cannot change during the simulation, but includes the dependency of the vertical force. Therefore different tire property files have to be used for each load case and different tire parameters need to be chosen. Because the tire manufacturer presents 6 load conditions in ref [32], consequently 6 different tire property files have been used for each load case simulation per tire model. This results in a total of 18 different property files.

This method thus can be used for constant vertical load, i.e. during steady state loading. However the drop test represents an un-steady load condition, therefore for drop test or landing simulations average values for these parameters should be used.

The simulations with the MSC.ADAMS program then result in typical graphs representing the Helicopter's MLG tire during steady-state conditions in the test rig machine.

For each load case and each parameter set the lateral force and the self-aligning torque against the slip angle have been calculated and is presented together with the tire manufacturer's results in the Figure 3.8 through 3.21.

A discussion and comparison between each graph of each model and the manufacturer statements (i.e. calculations) is presented in chapter [3.4.3.1](#).

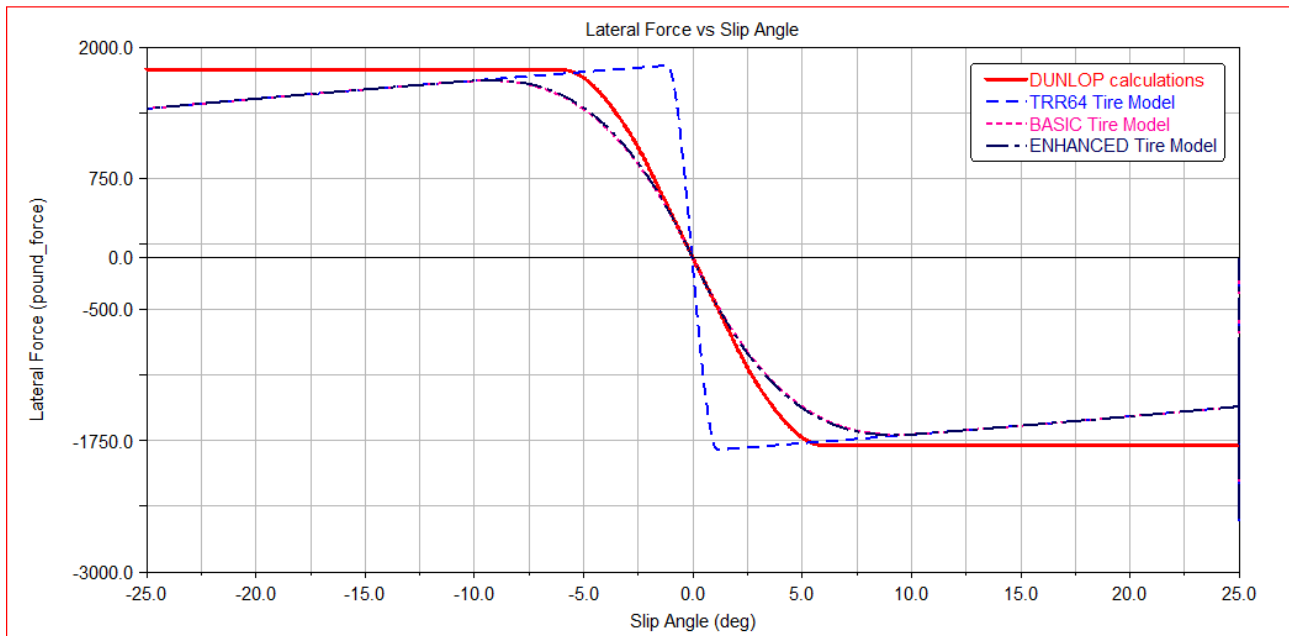


Figure 3.8: Tire Lateral Forces with 2248 lbs. Vertical Load.

It is worthwhile to mention that the negative self-aligning torque above 15 degrees side slip angle and similarly the positive self-aligning torque below -15 degrees are not realistic and do not match with the behavior of the results from MSC. The tire manufacturer should investigate and improve the results for the self-aligning torque.

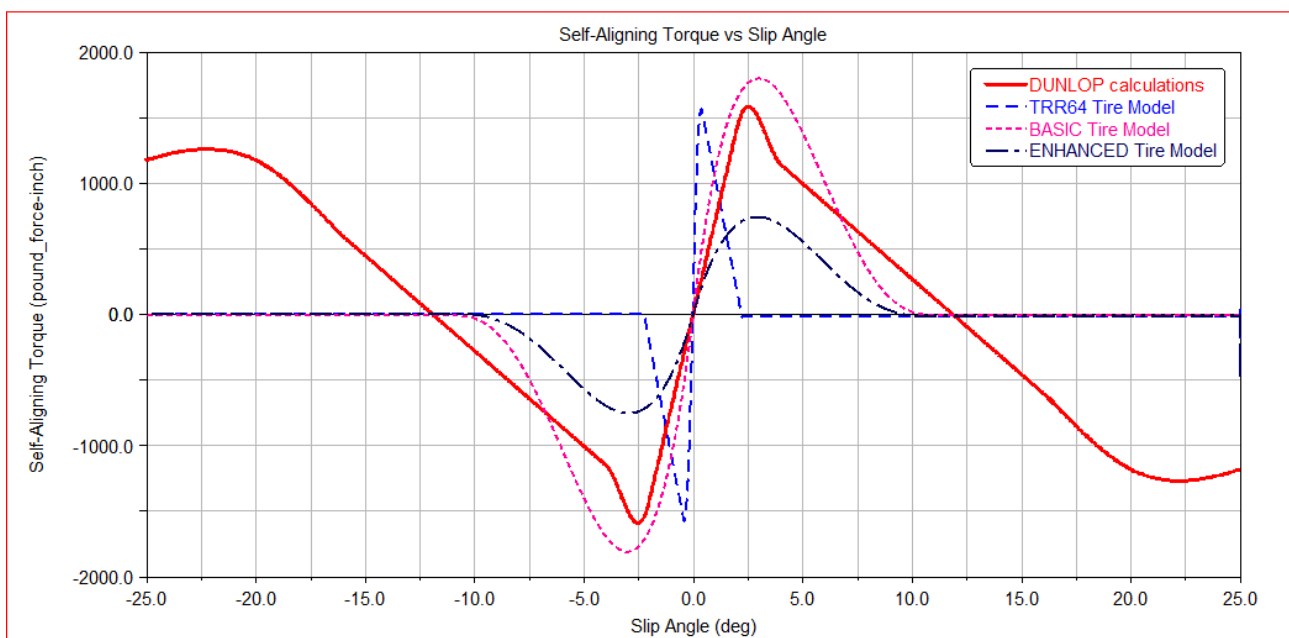


Figure 3.9: Tire Self-Aligning Torque with 2248 lbs. Vertical Load.

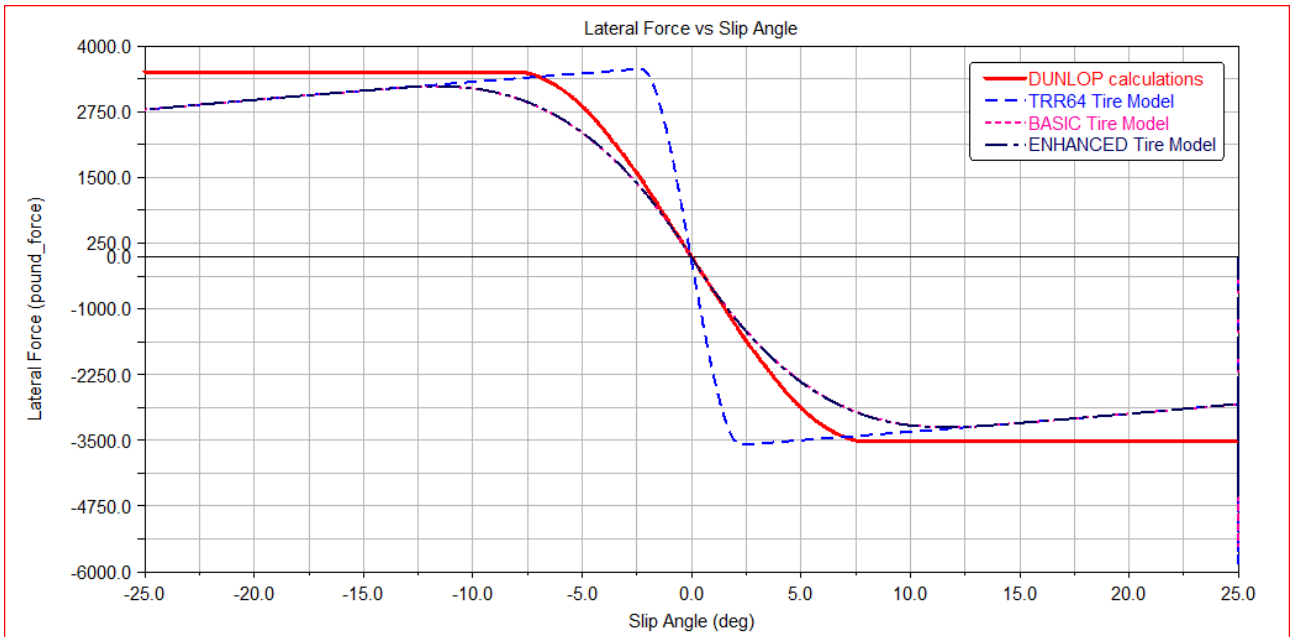


Figure 3.10: Tire Lateral Forces with 4496 lbs. Vertical Load.

Similarly the self-aligning torque is not realistic above and below 15 degrees and thus the tire manufacturer should reinvestigate the results.

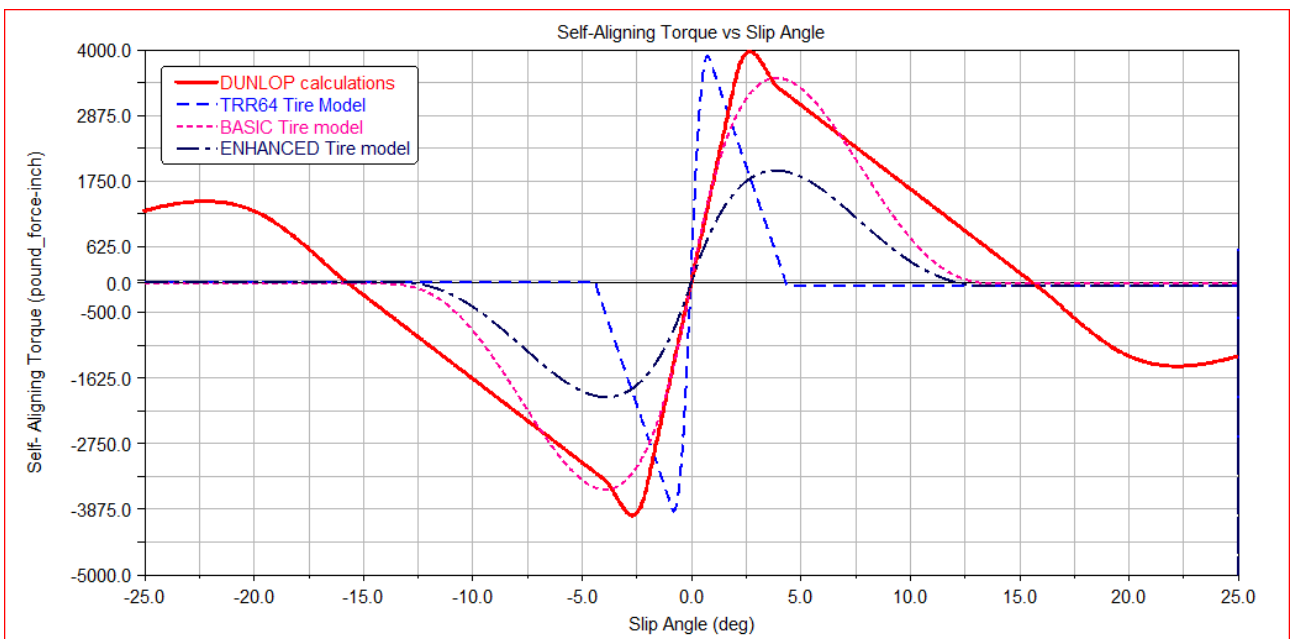


Figure 3.11: Tire Self-Aligning Torque with 4496 lbs. Vertical Load.

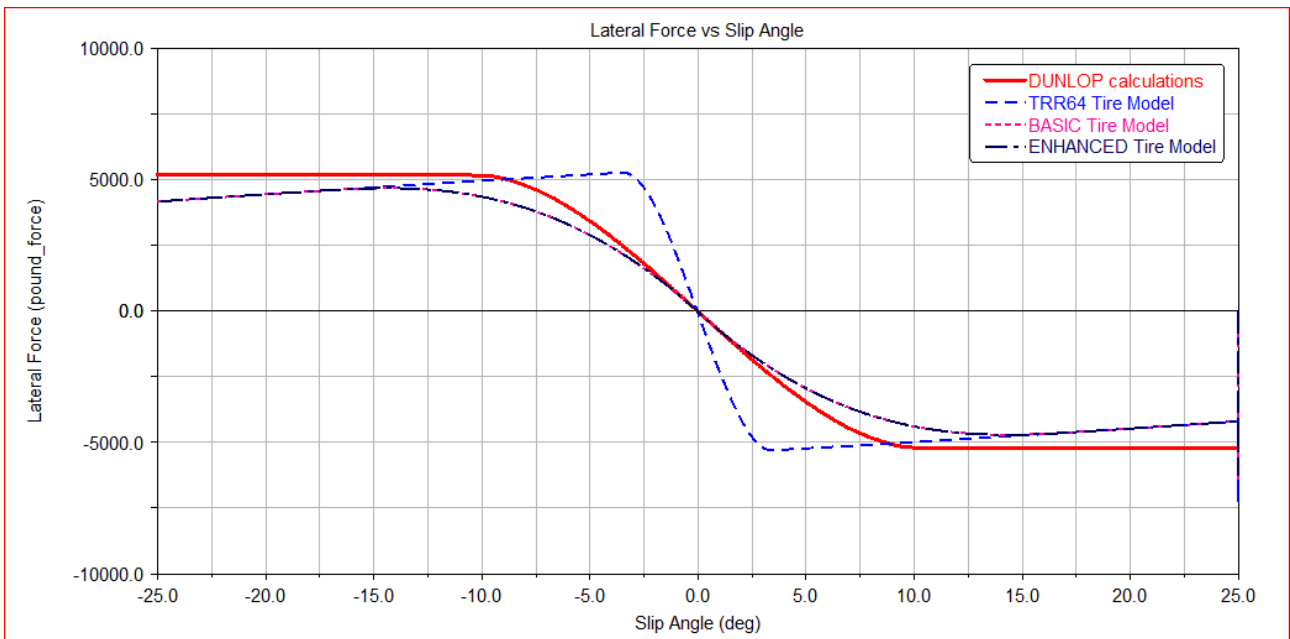


Figure 3.12: Tire Lateral Forces with 6744 lbs. Vertical Load.

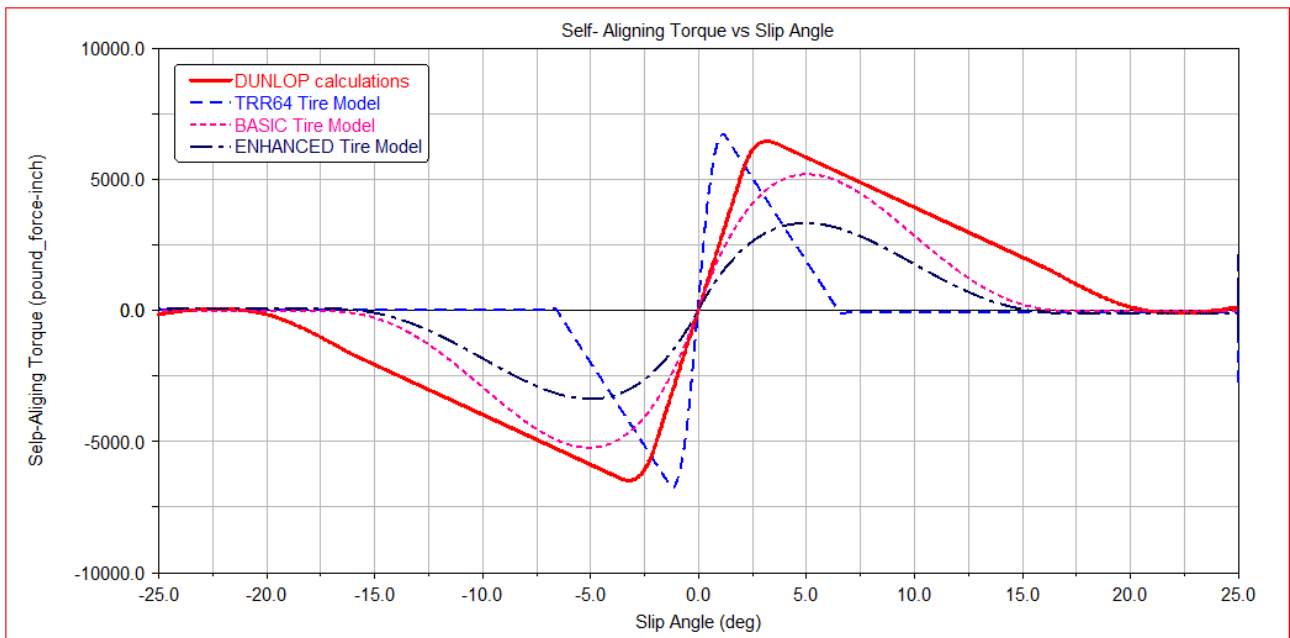


Figure 3.13: Tire Self-Aligning Torque with 6744 lbs. Vertical Load.

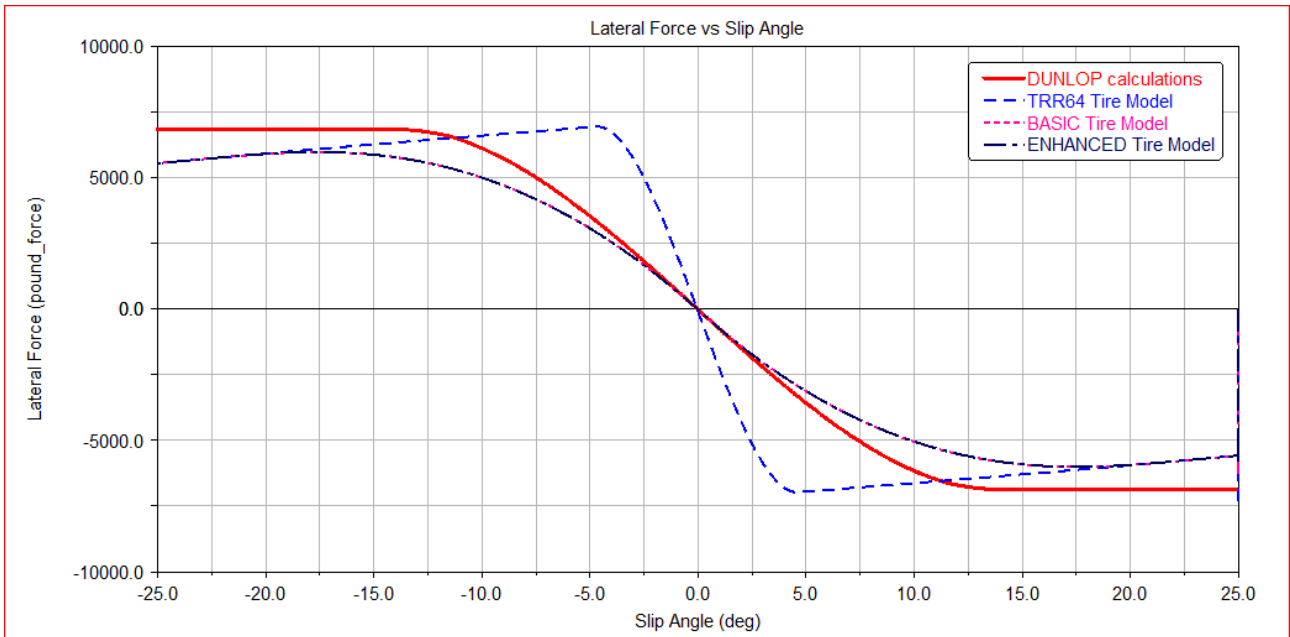


Figure 3.14: Tire Lateral Forces with 8992 lbs. Vertical Load.

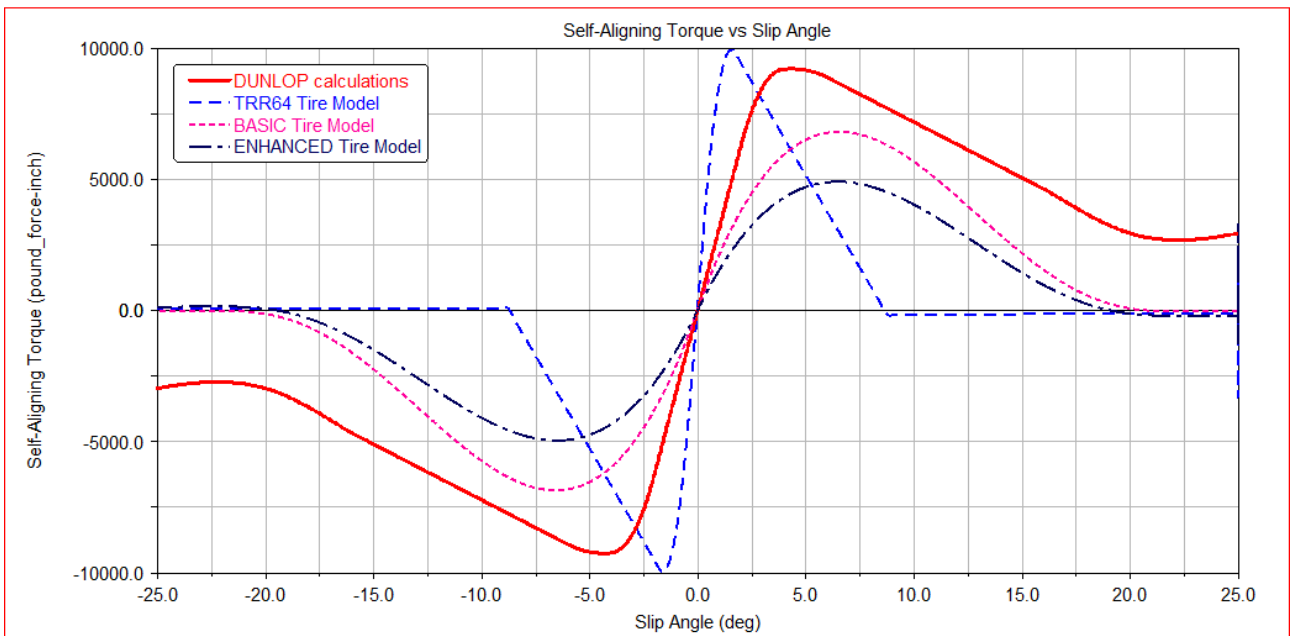


Figure 3.15: Tire Self-Aligning Torque with 8992 lbs. Vertical Load.

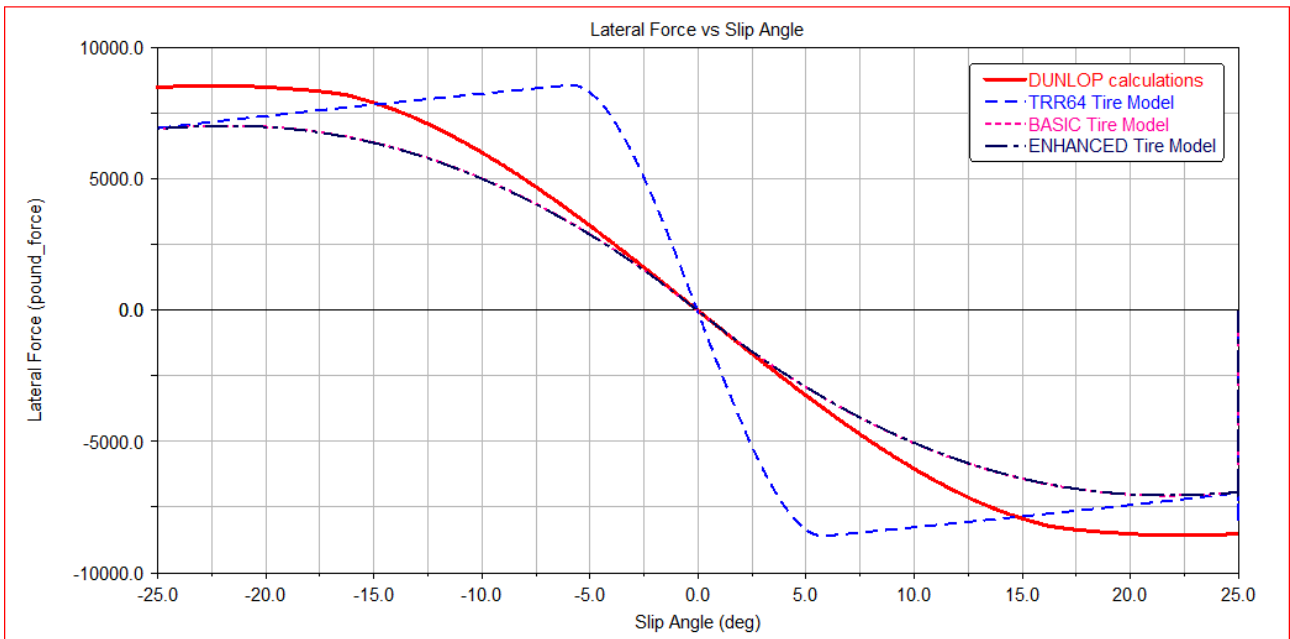


Figure 3.16: Tire Lateral Forces with 11240 lbs. Vertical Load.

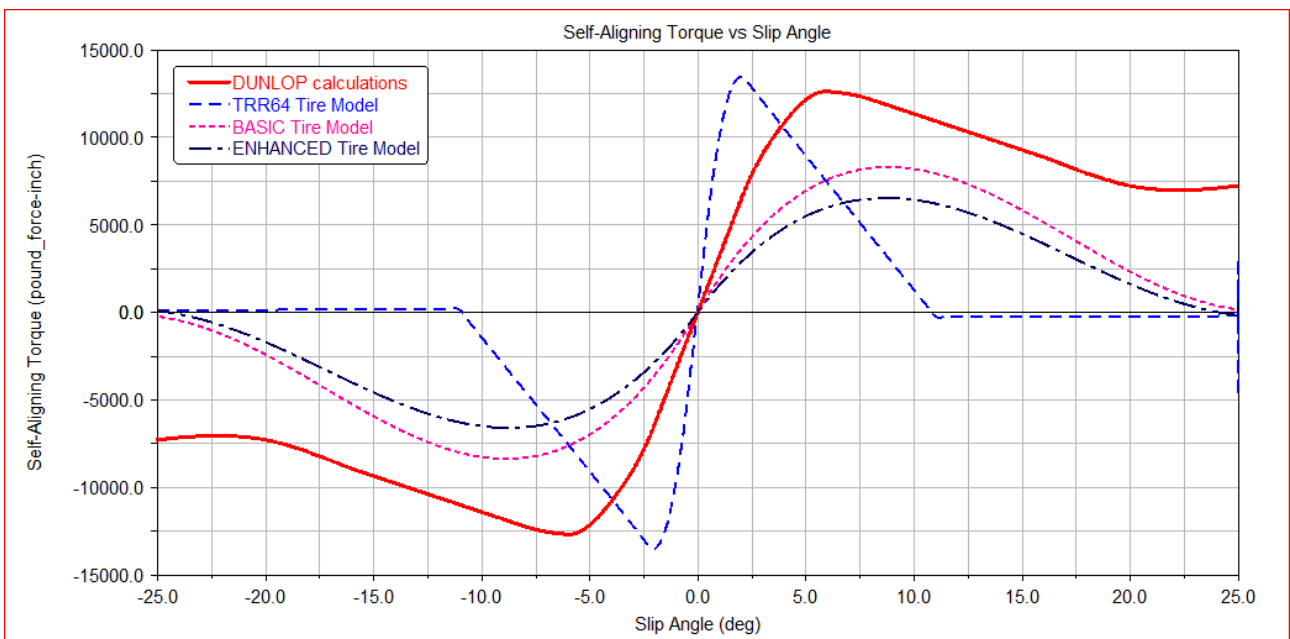


Figure 3.17: Tire Self-Aligning Torque with 11240 lbs. Vertical Load.

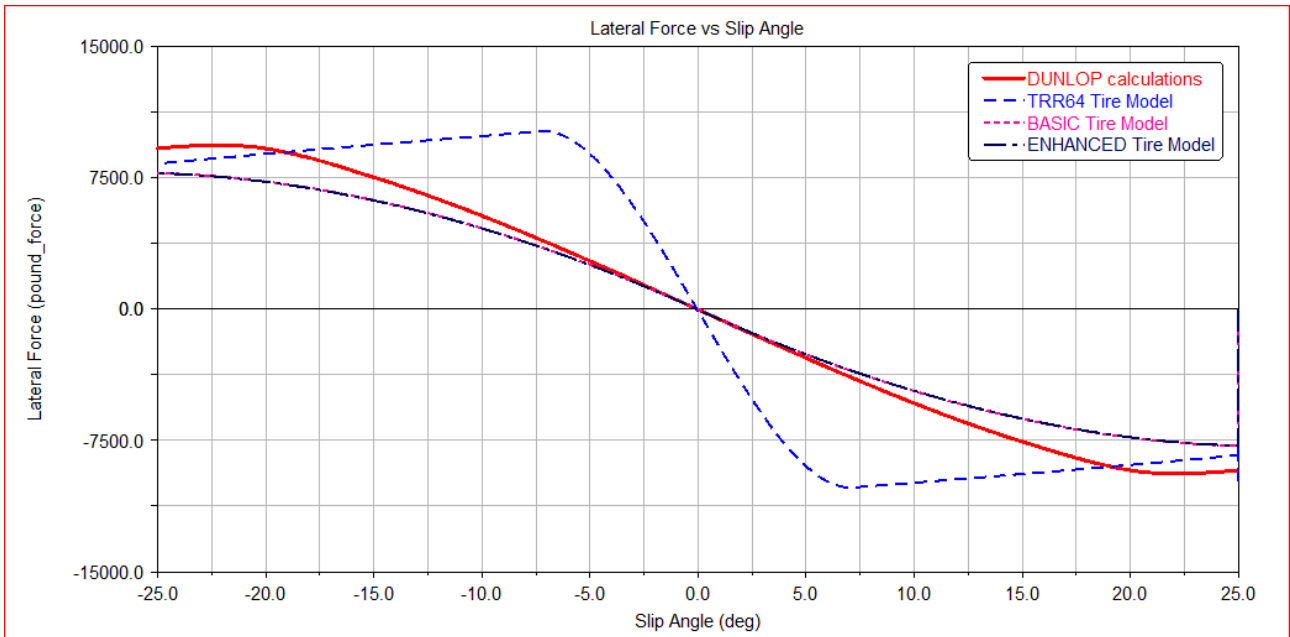


Figure 3.18: Tire Lateral Forces with 13488 lbs. Vertical Load.

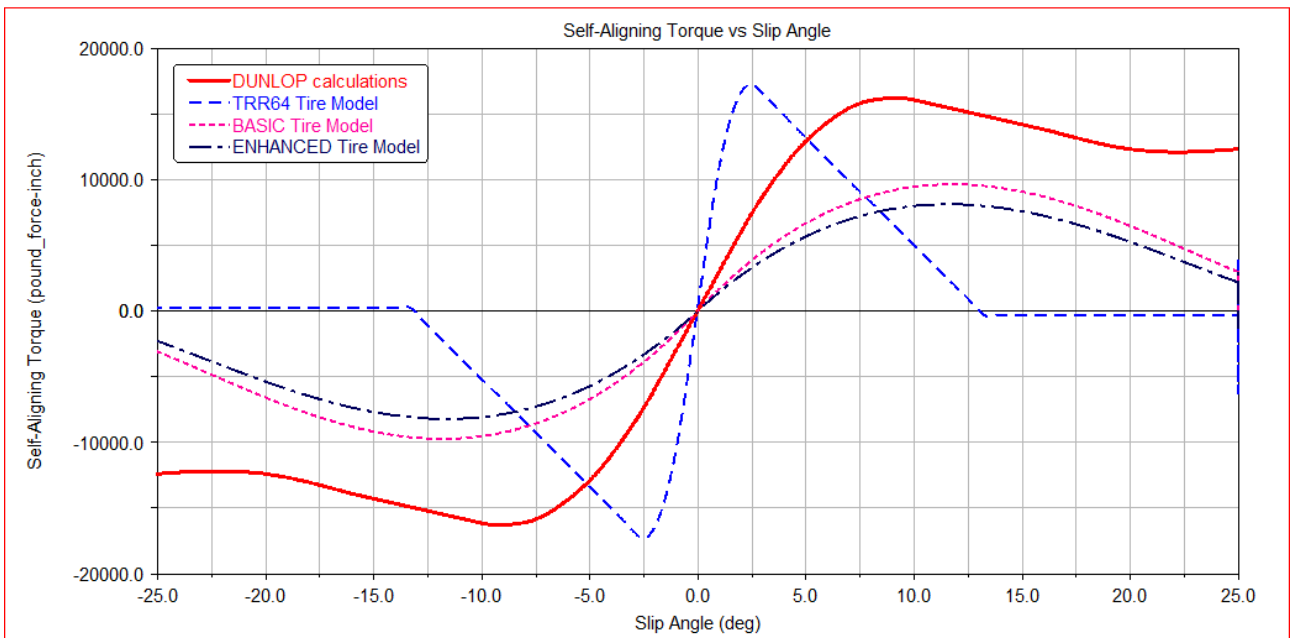


Figure 3.19: Tire Self-Aligning Torque with 13488 lbs. Vertical Load.

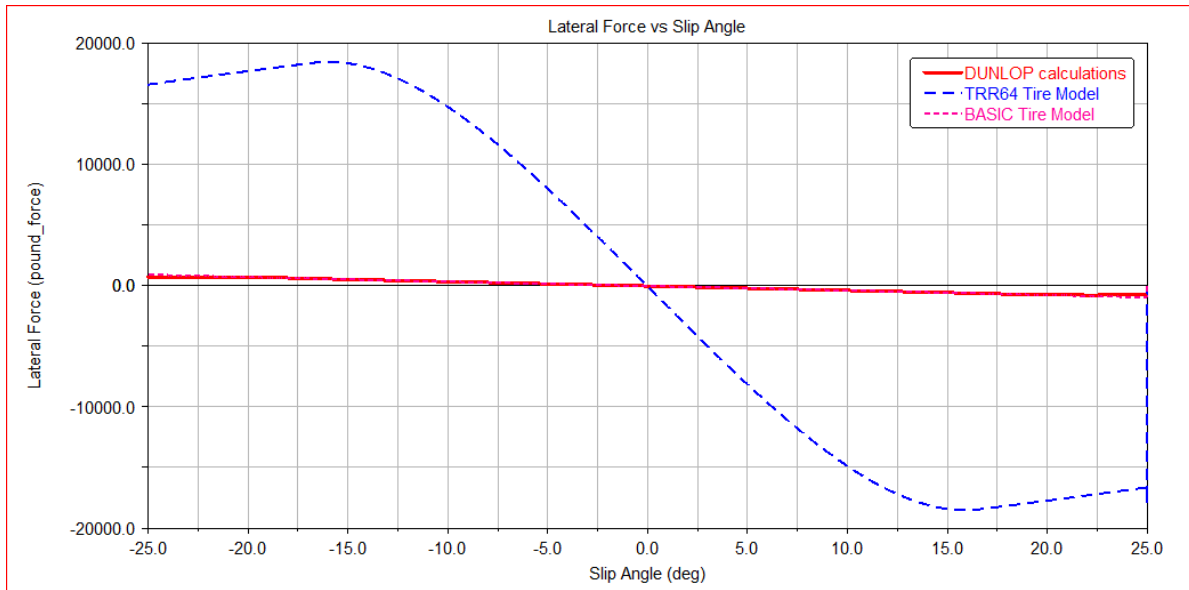


Figure 3.20: Tire Lateral Forces with 26977 lbs. Vertical Load.

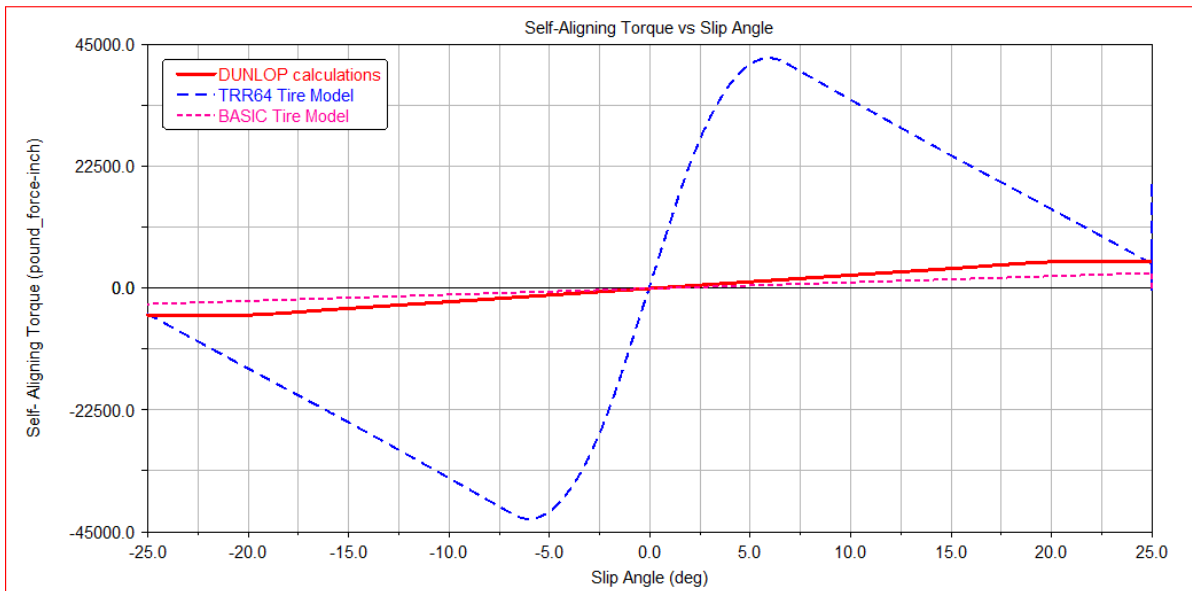


Figure 3.21: Tire Self-Aligning Torque with 26977 lbs. Vertical Load.

3.4.4.1 Discussion of the simulation results.

It can be observed that the simulations of the 3 aircraft tire models conform to the tire’s manufacturer calculations, with the BASIC Tire Model be the most close to the manufacturer data of all. More explicitly the BASIC and ENHANCED tire models show a difference of 10-20% for the lateral force while the TRR64 model is less accurate with 30-40% difference for most of the load cases. All three models are less accurate for the self-aligning torque with the BASIC and ENHANCED models to give better performance with difference of 30-40% while the TRR64 model is more than 50-60% different for most of the load cases. However ENHANCED and TRR64 tire models are not satisfactory above the vertical load of 13488 lbs. due to the high amount of vertical deflection as can be seen in Figures 3.20 and 3.21. The ENHANCED Tire Model cannot even simulate above this load due to high deflection and the TRR64 Tire Model is not accurate. However the BASIC Tire Model seems to follow the trend even for high loads.

As a conclusion the BASIC Tire Model is the most appropriate to represent the tire’s manufacturer calculations.

3.4.5 Simulations with tire’s inflation pressure 143.6 psi

The same simulations were performed with higher inflation pressure since most of the tire characteristics, change slightly with the different tire inflation pressure. For the following simulations the inflation pressure is 143.6 psi.

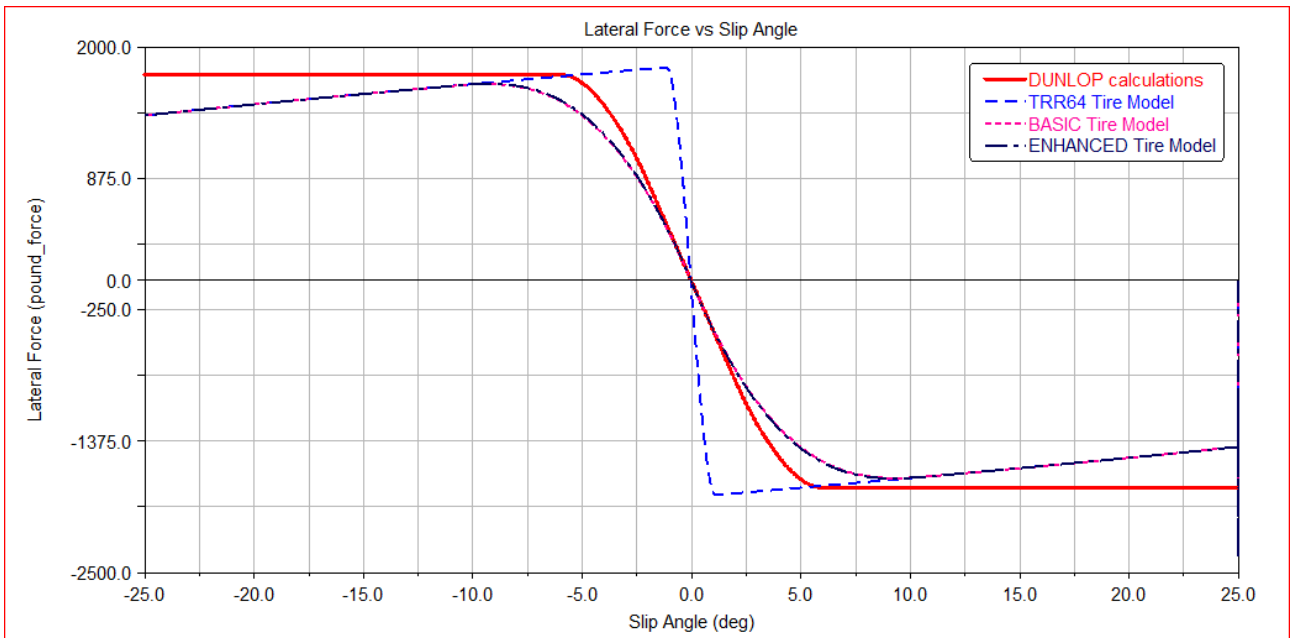


Figure 3.22: Tire Lateral Forces with 2248 lbs. Vertical Load.

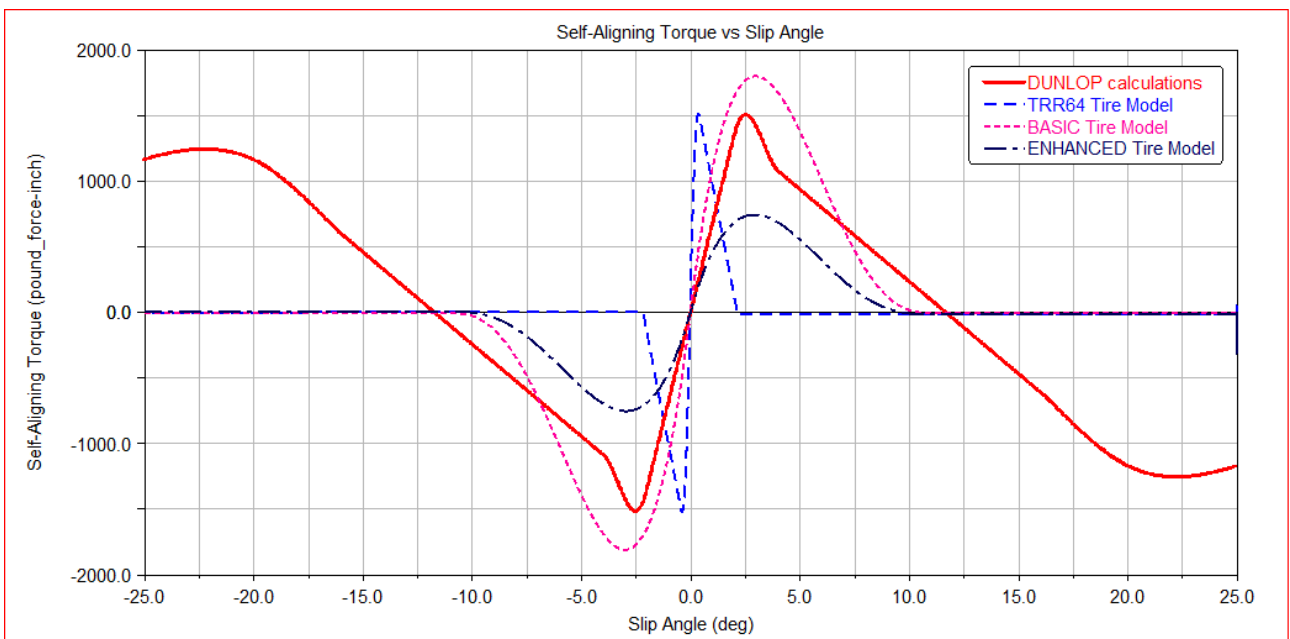


Figure 3.23: Tire Self-Aligning Torque with 2248 lbs. Vertical Load.

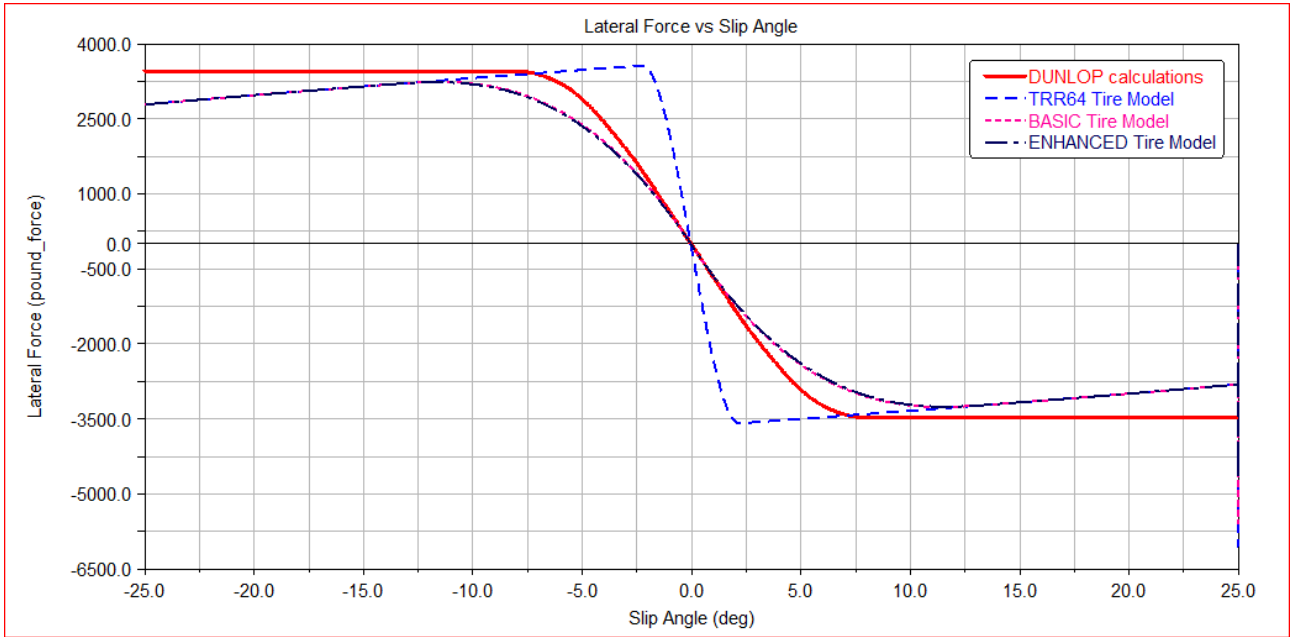


Figure 3.24: Tire Lateral Forces with 4496 lbs. Vertical Load.

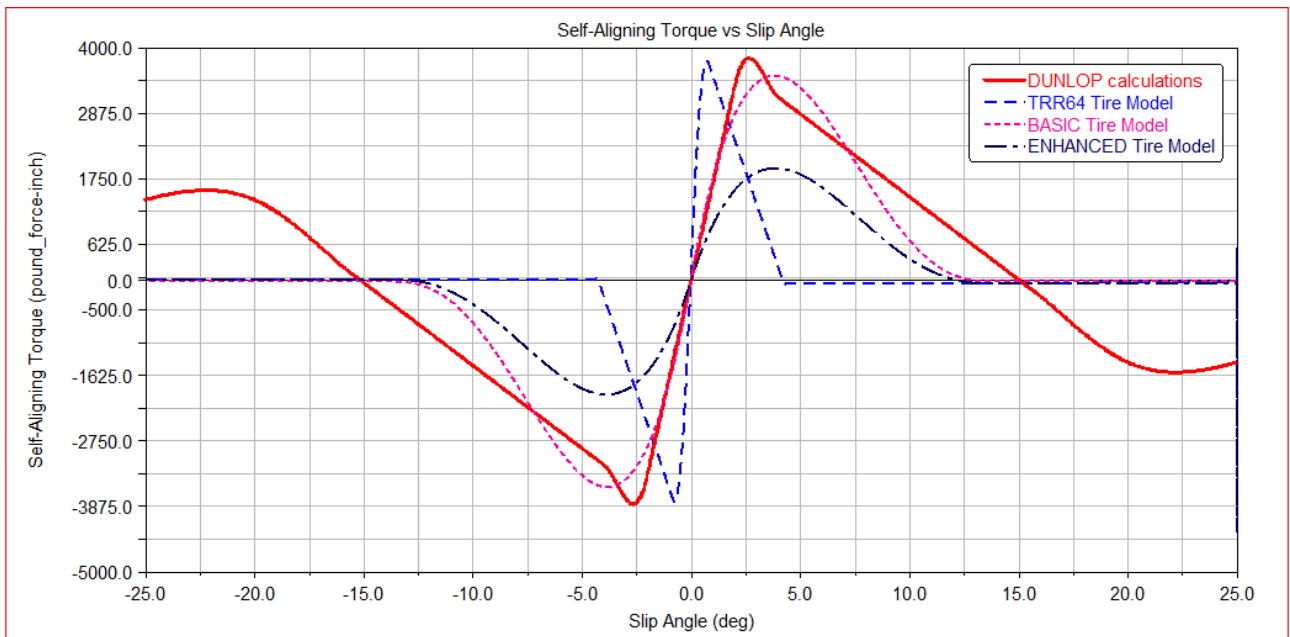


Figure 3.25: Tire Self-Aligning Torque with 4496 lbs. Vertical Load.

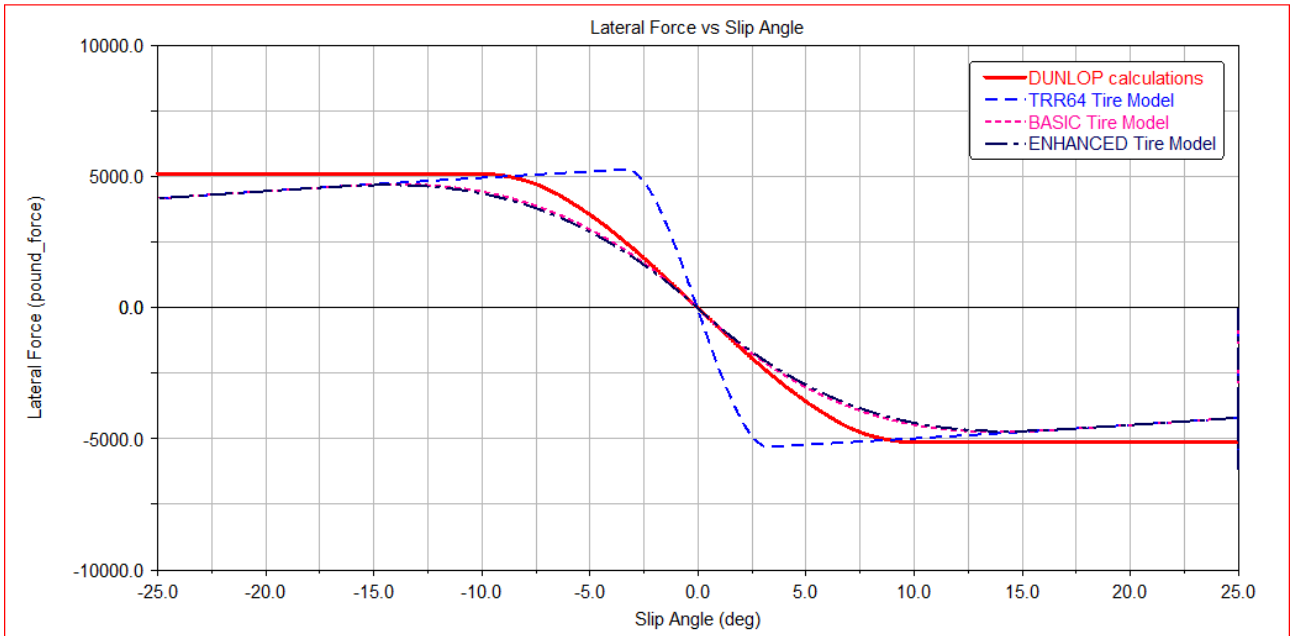


Figure 3.26: Tire Lateral Forces with 6744 lbs. Vertical Load.

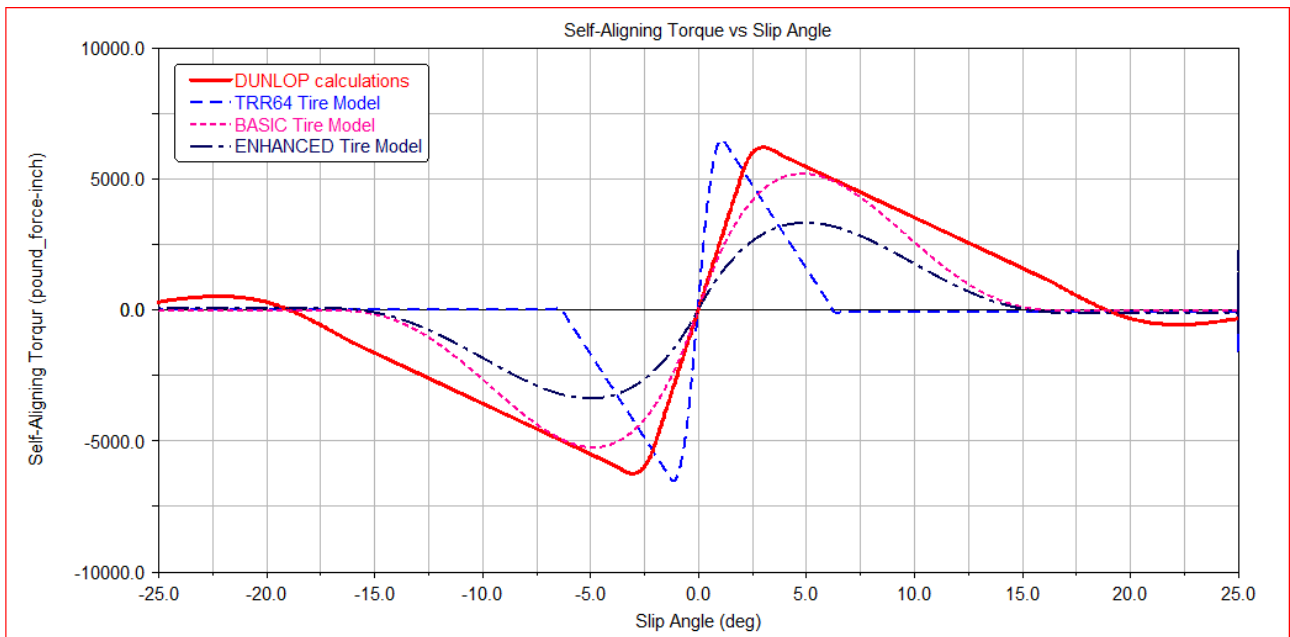


Figure 3.27: Tire Self-Aligning Torque with 6744 lbs. Vertical Load.

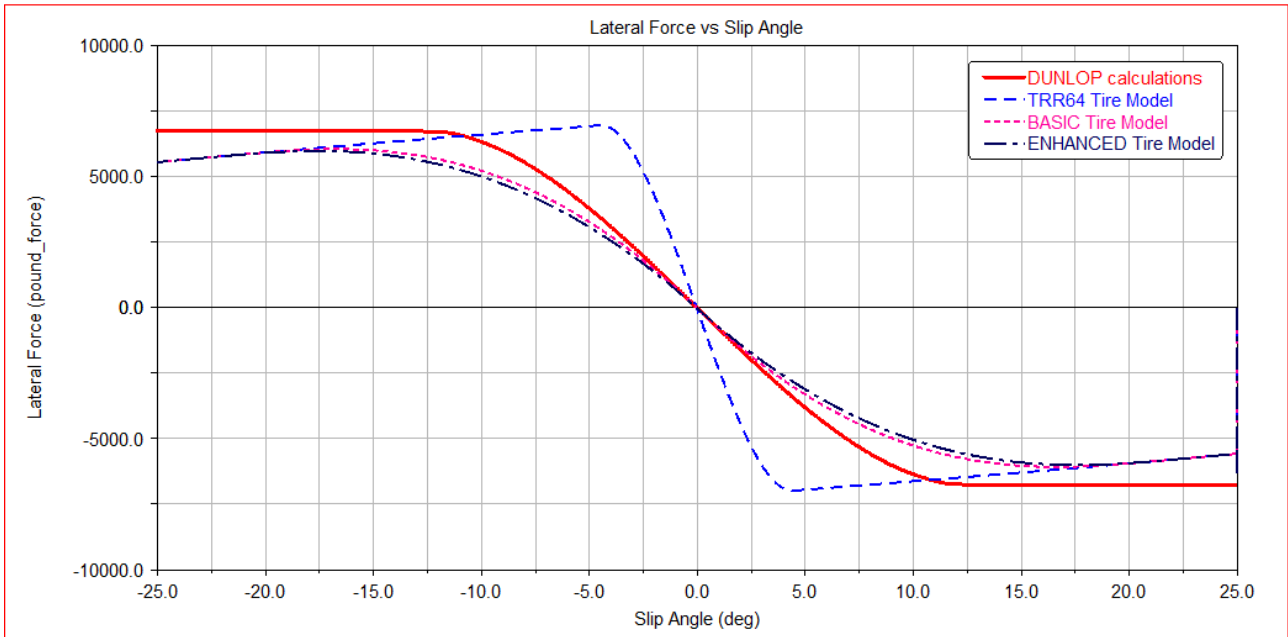


Figure 3.28: Tire Lateral Forces with 8992 lbs. Vertical Load.

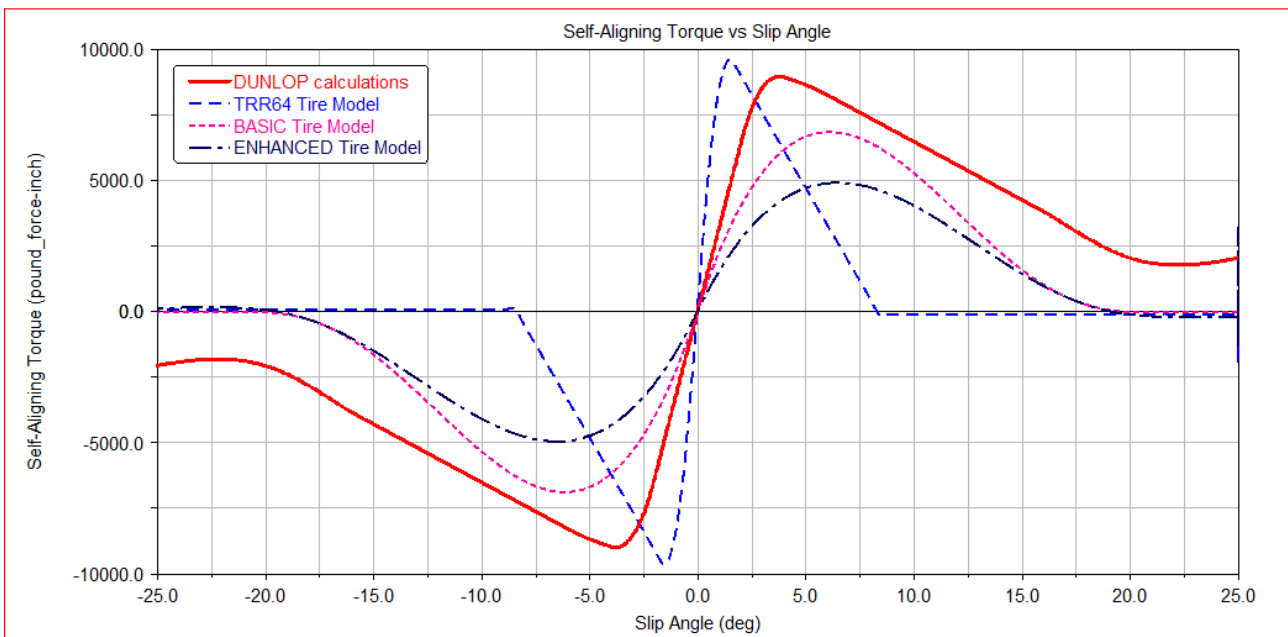


Figure 3.29: Tire Self-Aligning Torque with 8992 lbs. Vertical Load.

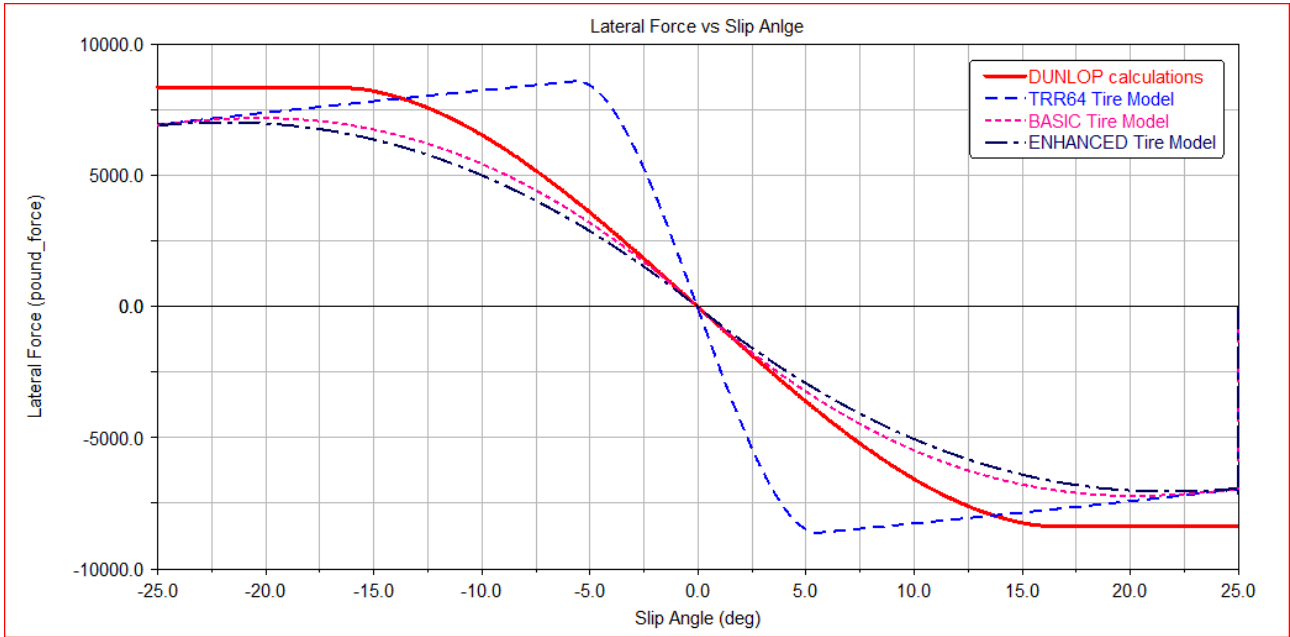


Figure 3.30: Tire Lateral Forces with 11240 lbs. Vertical Load.

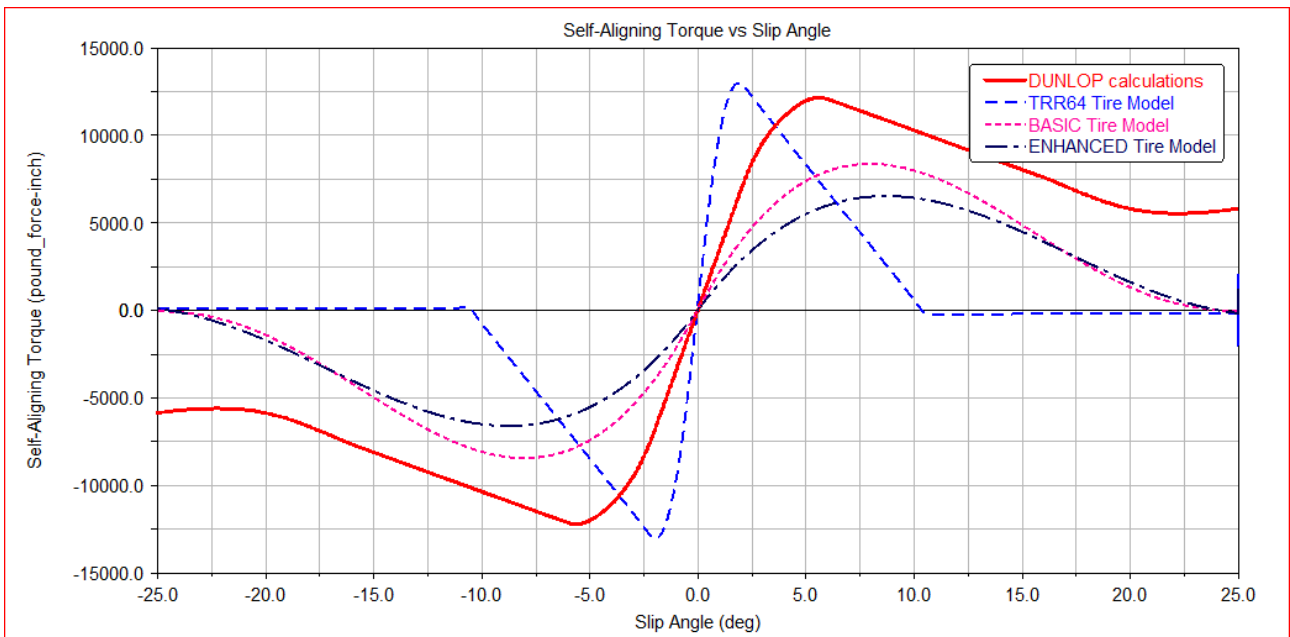


Figure 3.31: Tire Self-Aligning Torque with 11240 lbs. Vertical Load.

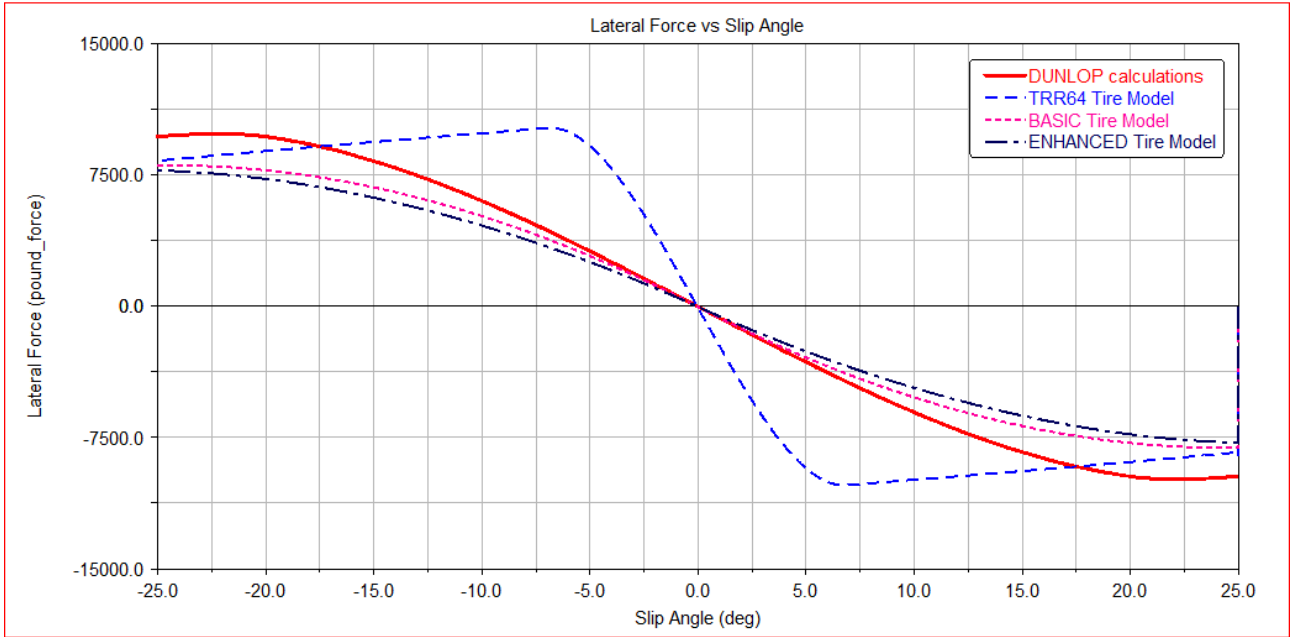


Figure 3.32: Tire Lateral Forces with 13488 lbs. Vertical Load.

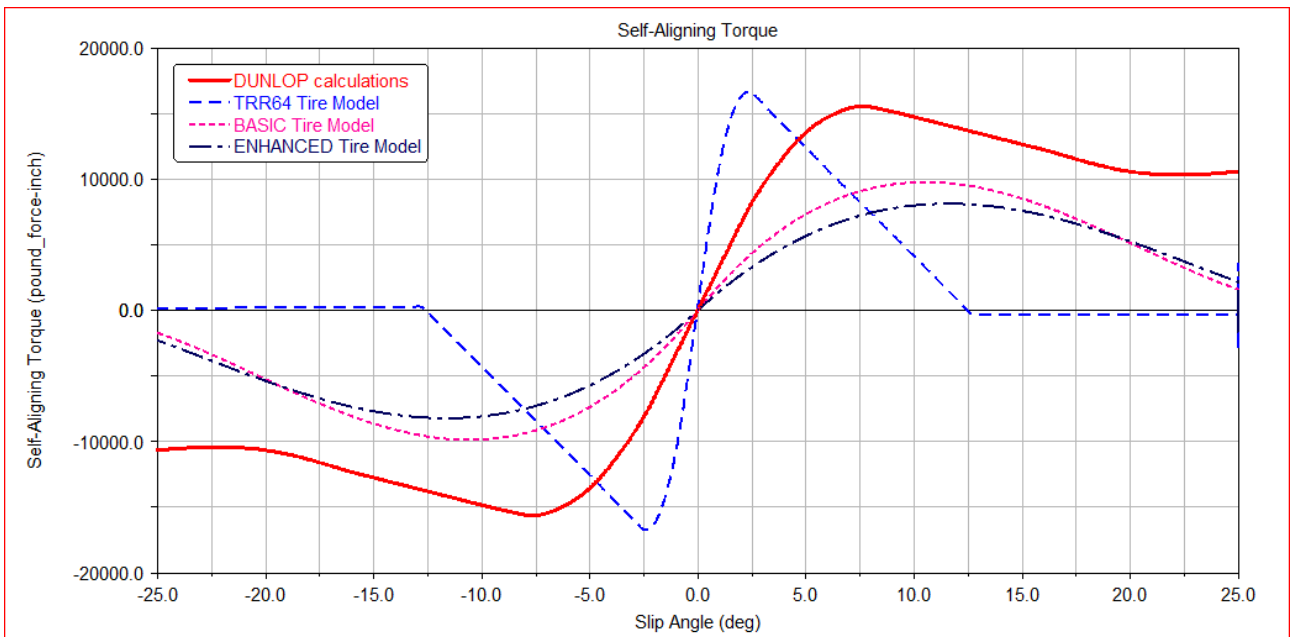


Figure 3.33: Tire Self-Aligning Torque with 13488 lbs. Vertical Load.

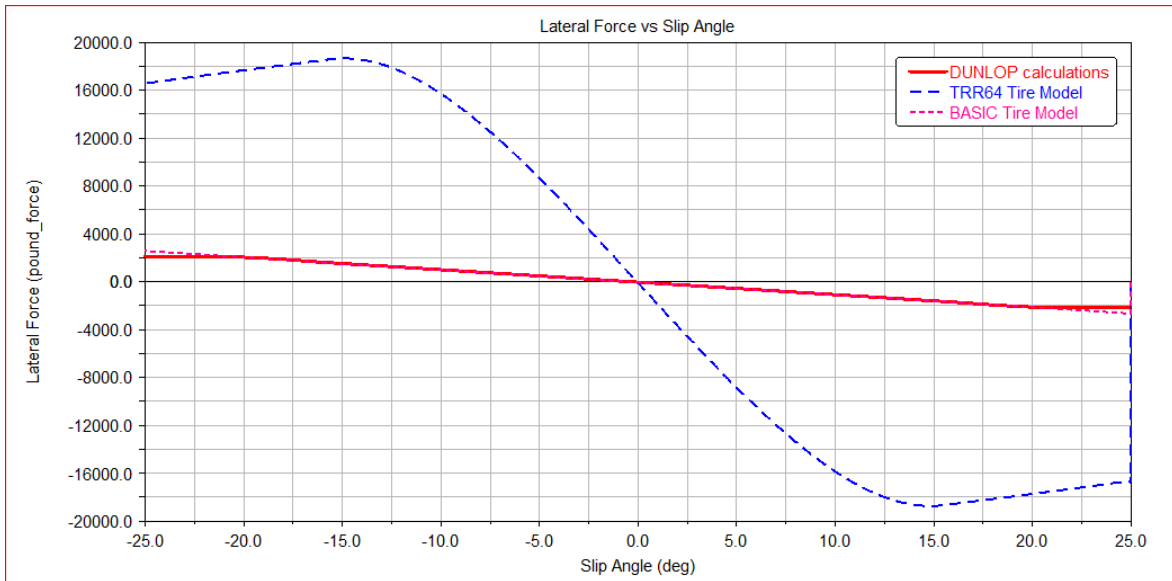


Figure 3.34: Tire Lateral Forces with 26977 lbs. Vertical Load.

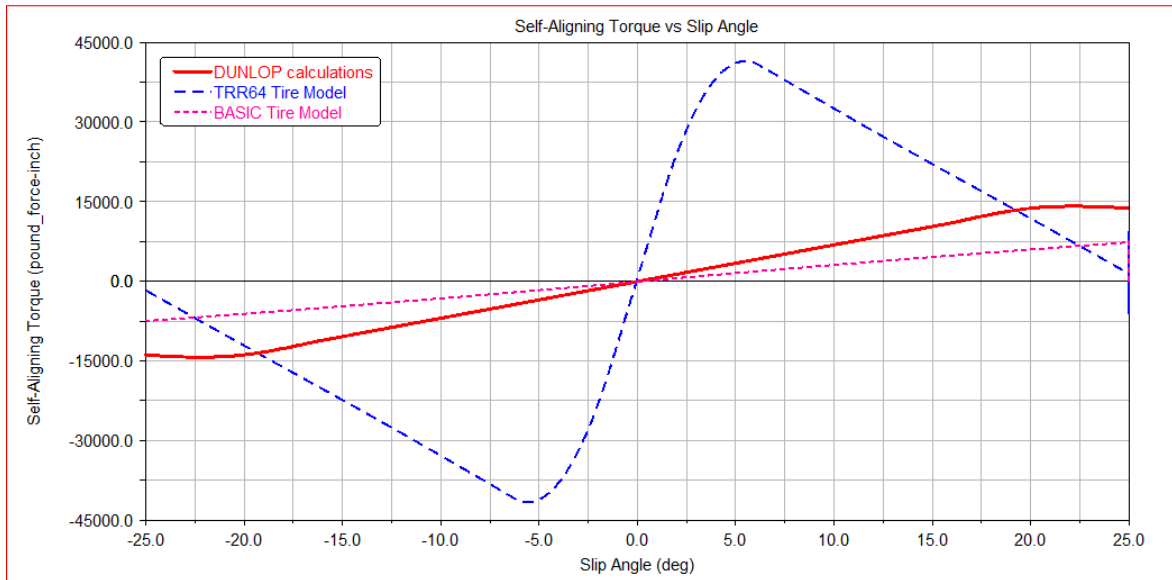


Figure 3.35: Tire Self-Aligning Torque with 26977 lbs. Vertical Load.

3.4.5.1 Discussion of the simulation results.

The conclusions are very much similar to the other inflation pressure case because the parameters have only slightly changed. Again the BASIC Tire Model seems to be the best out of the three aircraft tire models. The same behavior of the models was observed for loads in excess of 13488 lbs. The simulations for the load of 26977 lbs. are illustrated in Figures 3.34 and 3.35. Again the enhanced tire model fails to simulate properly and the TRR64 is not even close with respect to the tire manufacturer data.

4 CONCLUSIONS

Most of the work in this project was performed using the MSC.ADAMS 2013.2 simulation software. MSC.ADAMS is very powerful multi-body program that comprises a variety of tire models in its library but it is also possible to create a user-written tire subroutine in FORTRAN or C++. This functionality gives the designer the freedom to start with a simple MSC tire model or build up a new one as a dedicated subroutine. The built-in tire models can reduce the time needed to develop a new landing gear model and give a first impression of a tire's behavior with no or few information about it.

Furthermore the report introduces the procedure for obtaining the tire property parameters and accordingly how to implement them in MSC.ADAMS such to define a functional aircraft tire model that will generate forces and moments due to slip. The majority of the tire property parameters have been extracted from the Smiley and Horne paper [8]. The MSC.ADAMS aircraft tire models represent tire models where all the parameters are assigned only once and stay unchanged during the simulation. However a new type of tire model has been developed from MSC Software that scales the tire parameters during the simulation. More information about this procedure is given in ref [35] and in the tech article of MSC Software about on-line scaling of tire properties [37].

Having performed the simulations, it became obvious that the BASIC aircraft tire model appears to be the most suitable to represent the manufacturer's tire calculations for all load cases. This choice is based upon the simulation of the 3 aircraft tire models and comparing their outputs for each load case. Even though all three models have similar behavior until 13488 lbs. vertical load, after that load, tire deflection makes the ENHANCED and TRR64 models inaccurate. It appears that the ENHANCED and TRR64 models just can be used if the vertical load does not exceed 13488 lbs. during the simulations. Nevertheless, the BASIC tire model has the desired behavior with respect to that of the manufacturer. For that reason it was selected to be included in the landing gear model for preliminary simulation trials.

To that end, the current work could be taken in consideration for future landing gear developments when trying to find a satisfactory starting point for tire implementations. When developing a dedicated tire subroutine the tire characteristics can be compared with the developed built-in tire models. This can be performed by simulations in the test rig model and substituting the specific tire only. In that way it will become clear which of the approaches leave the best tire behavior with respect to that of the tire manufacturer or that of the drop test. Further it is recommended to pursue the development of a transient tire model capable to simulate transient loading conditions like the helicopter landing using the techniques as referred in ref [35] and [37].

5 REFERENCE DOCUMENTS

- [1] H. B. Pacejka, *Tire and Vehicle Dynamics*, 3rd Edition, 2012.
- [2] Dr. Ir. I.J.M. Besselink, *Vehicle Dynamics - Lecture notes*, Dynamics and Control Group, Department of Mechanical Engineering, Eindhoven University of Technology, 2012.
- [3] Dr. Ir. I.J.M. Besselink, *Advanced Vehicle Dynamics - Lecture notes*, Dynamics and Control Group, Department of Mechanical Engineering, Eindhoven University of Technology, 2015.
- [4] Dr. Ir. I.J.M. Besselink, Dr. Ir. A.J.C. Schmeitz, *Introduction Vertical Dynamics*, January 2013.
- [5] J. J. M. Van Oosten, *TMPT tire modeling in ADAMS*, Manager Development, MSC Software Benelux B.V., 2007.
- [6] Yun Wang, MV Blundell, G Woodand and C Bastien, *Tyre model development using co-simulation technique for helicopter ground operation*, June 2014.
- [7] Wolf R. Kruger, Marco Morandini, *Recent developments at the numerical simulation of landing gear dynamics*, May 2011.
- [8] Robert F.Smiley and Walter B.Horne, *Mechanical properties of pneumatic tires with special reference to modern aircraft tires*, NATIONAL ADVISORY COMMITTEE FOR AERONAUTICS, January 1958.
- [9] Norman S.Currey, *Aircraft Landing Gear Design: Principles and practices*, 1988.
- [10] The Goodyear Tire & Rubber Company, *Aircraft tyre care and maintenance*, October 2004.
- [11] R. Rajamani, *Vehicle Dynamics and Control*, 2005.
- [12] R. N. Jazar, *Vehicle Dynamics: Theory and Application*, 2009.
- [13] TNO Automotive MF-TYRE & MF-SWIFT 6.1, *USER MANUAL*, 2008.
- [14] Adams/Tire User Manual 2010 Version MD Adams 2010 MSC, 2010.
- [15] E. Fiala, "Seitenkraefte am Rollenden Luftreifen", VDI Zeitschrift, vol.96, 1954.
- [16] R.T. Uil, Master Thesis "Tire models for steady-state vehicle handling analysis" in Eindhoven University of Technology, December 2007.
- [17] G. Gim, Y. Choi, and S. Kim, "A semi-physical tire model for a vehicle dynamics analysis of handling and braking". In: Vehicle System Dynamics: International Journal of Vehicle Mechanics and Mobility 45:S1, 2007.
- [18] C. C. deWit et al. "A new model for control of systems with friction". In: IEEE Transactions on Automatic Control 40 (No. 3), 1995
- [19] Canudas deWit C. and Tsiotras P, "Dynamic tire friction models for vehicle traction Control" In *Proceedings of 38th IEEE Conference on Decision and Control*, (Phoenix, Arizona, USA), 1999.
- [20] [K. Guo](#) and [D. Lu](#), UniTire: unified tire model for vehicle dynamic simulation, 2007
- [21] Jan van Oosten, J.J.M., Kuiper, E., Leister, G., Bode, D., Schindler, H., Tischleder, J. and Khne, S., *A new tyre model for TIME measurement data. Tire Technology Expo 2003*, Hannover, 2003.
- [22] Pacejka, H.B., Bakker, E. and Lidner, L., *A new tire model with an application in vehicle dynamics studies. SAE paper 890087*, 1989.

- [23] Pacejka, H.B. and Bakker, E. , *The magic formula tyre model. Proceedings of the 1st International Colloquium on Tyre Models for Vehicle Dynamics Analysis* (Amsterdam/Lisse: Swets & Zeitlinger B.V.), 1993.
- [24] ADAMS/Tire on-line help, v2005r2.
- [25] Gim, G., *Vehicle dynamic simulation with a comprehensive model for pneumatic tires. PhD thesis*, University of Arizona, 1988.
- [26] Gipser, M., *FTire*. Available online at: www.ftire.com, 2004.
- [27] Jan van Oosten, J.J.M., Unrau, H.-J., Riedel, G. and Bakker, E., *TYDEX workshop: standardisation of data exchange in tyre testing and tyre modelling. Proceedings of the 2nd International Colloquium on Tyre Models for Vehicle Dynamics Analysis, Vehicle System Dynamics, Vol. 27* (Amsterdam/Lisse: Swets & Zeitlinger), 1996.
- [28] Foad Mohammadi, *Tire Characteristics Sensitivity Study – Master thesis* Department of Applied Mechanics, CHALMERS UNIVERSITY OF TECHNOLOGY Gothenburg, Sweden 2012.
- [29] Georg Rill, *TMEASY – A HANDLING TIRE MODEL BASED ON A THREE-DIMENSIONAL SLIP APPROACH*, Germany.
- [30] Adams/Tire manual, Msc Software Corporation, USA, July 2014.
- [31] R.LCOLLINS and R.J.BLACK, *Experimental determination of tire parameters for aircraft landing gear shimmy stability studies*, AIAA paper No.68-311, The Bendix Corporation Sound Bend, Indiana, April 1968.
- [32] Dunlop Aircraft Tyres Limited, *Tire parameters for the NH90 helicopter*, UK, August 2015.
- [33] W.Oud, J.Janssen, M.Gram and J. van de Linde, *Description of NH90 simulation models and model data*, Doc. No.: TN S320 F0516 E01, August 2010.
- [34] C. Duque, J Janssen, M Gram and J. van de Linde, *Description of NH90 Landing Gear Concept – TTH*, Doc. No.: TN S320 F0502 E01, March 2012.
- [35] Dr. Ir. I.J.M. Besselink, Dr. Ir. A.J.C. Schmeitz AND H. B. Pacejka, *An improved Magic Formula/Swift tyre model that can handle inflation pressure changes*, March 2010.
- [36] J. van Schaik, J Janssen, R Schut, R Langeveld, J. Berkelaar, *FAR29 Ground Handling Loads for TTH normal cabin – 11 Ton*, Doc. No.: TN S320 F0506 E05, November 2006.
- [37] Tech Article from MSC Software Corporation, *On-Line Scaling of Tire Properties with PAC2002 Tire Model*, Tech Articles ID KB8016467, February 2009.

APPENDIX A TIRE MODELS

MF-Tyre/MF-SWIFT model

MF-Tyre/MF (Short Wavelength Intermediate Frequency Tire) model is constructed using the latest implementation of Pacejka's renowned 'Magic Formula' tire model. MF-Tyre simulates validated steady-state and transient tire behavior making it a very suitable model for vehicle handling, control prototyping and rollover analysis. MF-Swift is an extension of the MF-Tyre that simulates the tire dynamic behavior up to about 100 Hz and is suitable for ride comfort, road load and vibration analysis. The MF-SWIFT includes four main elements: 1) Magic Formula 2) Contact patch slip model 3) Rigid ring 4) Obstacle enveloping model. For some years, different tire models were available, but recently they have been combined into a single tire model under the name TNO MF-Tyre/MF-SWIFT [1],[4],[13].

Fiala Model

The Fiala tire model, introduced by E. Fiala and extended by the developers of MSC Adams, computes expressions for all tire forces and moments except for the overturning moment. Fiala tire model is the standard tire model in all ADAMS/Tire modules [ref.4]. The Fiala tire model approximates the normal pressure distribution on the contact patch with a rectangular shape. The instantaneous value of the tire-road friction coefficient is determined by a linear interpolation in terms of the resultant slip and the static friction coefficient. The influence of a camber angle on lateral force and aligning moment is not considered [14].

Brush Model

The brush model is perhaps the simplest physical tire model, yet it is still significant and interesting. The brush model consists of a row of elastic bristles that touches the road plane and can deflect in a direction parallel to the road surface. It is a simple tool to analyse qualitatively what goes on in the contact patch and to understand the global mechanical behavior of a wheel with tire [1],[3].

TreadSim Model

The TreadSim tyre model was originally developed by Pacejka and later extended by researchers of Eindhoven University of Technology. This model is developed to investigate different aspects of the tire model which were impossible to include in the analytical brush model [16].

RMOD-K FEM and FB Model

RMOD-K is the name of a family of tire models that mostly reside on the “complex physical models” category. This model was created by the German Professor Cristian Oertel, starting in 1997. This model gives a detailed finite element description of the actual tire structure, but uses a number of simplifications in order to reduce the computing effort. Various editions of RMOD-K have been introduced, like RMOD-K FEM and RMOD-K FB in order to obtain more accurate results. RMOD-K is mainly designed for ride, comfort and durability applications and it has been implemented in ADAMS [\[1\]](#).

FTire Model

FTire (Flexible Ring Tire Model) belongs to the category of pure mechanics-based tire models which was developed by the Professor Gipser in Germany (1998). This model is reviewed here since it is implemented in ADAMS/Car and it is an example of complex theoretical tire models. FTire is considered as a discrete element model and is a compromise between the computationally heavy finite element models and the simple pure in-plane models [\[1\]](#),[\[16\]](#).

TMeasy Model

TMeasy was initially developed to be used in simulations of agricultural and heavy duty vehicles. The TMeasy tire model is based on a semi-physical approach. This model was developed to be used in situations of few tire data being available. The main idea behind this model is to interpolate or extrapolate the features from a similar model and give reasonable tire forces from little information about tire’s parameters [\[28\]](#),[\[29\]](#).

Similarity Method Model

The similarity method is based on the Fiala theory (1954) and has been introduced by professor Pacejka from Delft University of Technology (first version back to 1958). There have been a lot of improvements from the original model until 1995 from Milliken [\[1\]](#).

Stretched String Model

The stretched string approach was proposed by Von Schlippe in 1941. The tire is considered as a massless string of infinite length under a constant pre-tension force and it is uniformly supported elastically in the lateral direction. More information can be found of the book of Pacejka “Tire and vehicle dynamics” [\[1\]](#).

Dynamic Tire Friction Model

Dynamic tire friction model is a physical tire model based on brush and LuGre friction modelling. [\[16\]](#),[\[18\]](#).

Hankook Model

This tire model was developed by Hankook tire Co. Ltd R&D center and it is a semi-empirical model. The physical characteristics of the tire provide the necessary information to obtain the steady-state behavior. However for the transient behavior different slip sweep rates are used to obtain the transient tire characteristics [\[17\]](#).

UniTire Model

UniTire is a semi-physical unified non-linear and non-steady-state tire model made by Chinese Professor Konghui Guo in 1973. UniTire is a tire model for vehicle dynamic simulation and control under complex wheel motion inputs, involving large lateral slip, longitudinal slip, turn-slip, and camber. It works based on fitting a mathematical function to the test data in order to obtain the tire resultant force [\[20\]](#).

LuGre Model

The longitudinal LuGre tire friction model, initially introduced in 1999 and is based on a dynamic viscoelastoplastic friction model for point contact. It was developed by Department of Automatic Control at Lund University (Sweden) and Laboratoire d'Automatique de Grenoble (France). More information can be found in [\[19\]](#).

APPENDIX B AXIS SYSTEM IN MSC.ADAMS/TIRE

Tire Axis Systems

The following sections describe the ISO coordinate systems to which ADAMS/Tire conforms. In ADAMS three axis systems can be distinguished [30]:

- ISO-C (TYDEX C) Axis System
- ISO-W (TYDEX W) Contact-Patch Axis System
- Road Reference Marker Axis System

ISO-C (TYDEX C) Axis System

The TYDEX STI specifies the use of the ISO-C axis system for calculating translational and rotational velocities, and for outputting the force and torque at the wheel centre. The properties of the ISO-C axis system are [30]:

- The origin of the ISO-C axis system lies at the wheel center.
- The + x-axis is parallel to the road and lies in the wheel plane.
- The + y-axis is normal to the wheel plane and, therefore, parallel to the wheel's spin axis.
- The + z-axis lies in the wheel plane and is perpendicular to x and y (such as $z = x \times y$).

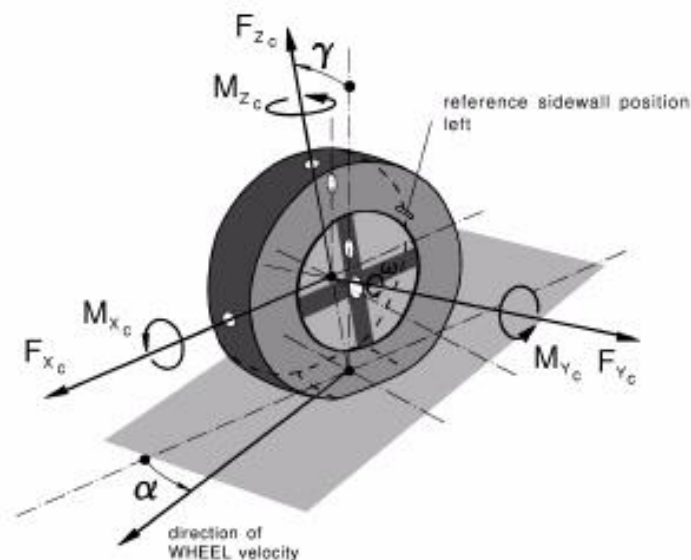


Figure B.1: TYDEX-C Axis System Used in ADAMS/Tire.

ISO-W (TYDEX W) Contact-Patch Axis System

The properties of the ISO-W (TYDEX W) axis system are [30]:

- The origin of the ISO-W contact-patch system lies in the local road plane at the tire contact point.
- The + x-axis lies in the local road plane along the intersection of the wheel plane and the local road plane.
- The + z-axis is perpendicular (normal) to the local road plane and points upward.
- The + y-axis lies in the local road plane and is perpendicular to the + x-axis and + z-axis (such as $y = z \times x$).

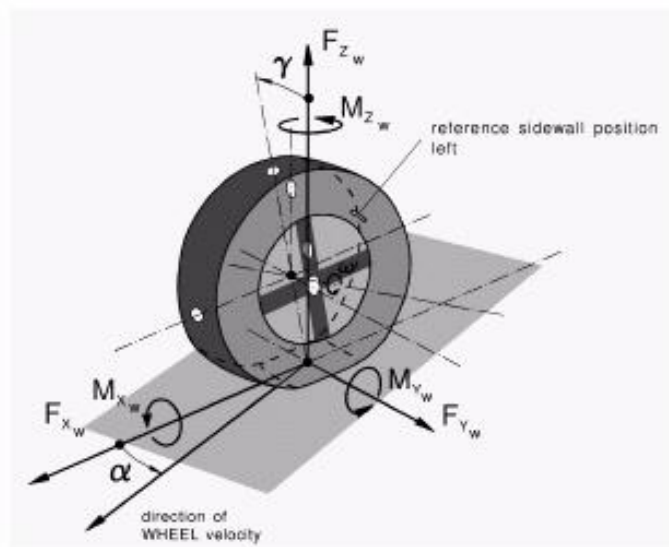


Figure B.2: TYDEX W-Axis System Used in ADAMS/Tire.

Road Reference Marker Axis System

The road reference marker axis system is the underlying coordinate system that ADAMS/Tire uses internally. For example, the tire translational displacement and local road normal for a three-dimensional road are expressed in the axis system of the road reference marker.

The properties of the reference marker axis system are [30]:

- The GFORCE reference marker defines the axis system.
- The + z-axis points upward.

APPENDIX C TIRE PROPERTY FILES IN MSC.ADAMS/TIRE

BASIC AIRCRAFT TIRE MODEL

```

$-----MDI_HEADER
[MDI_HEADER]
FILE_TYPE      = 'tir'
FILE_VERSION   = 3.0
FILE_FORMAT    = 'ASCII'
(COMMENTS)
{comment_string}
'Tire          - DUNLOP DR18429T'
'Pressure      - 130.5'
'Test Date     - 05/08/2015'
'Test tire'
'New File Format v2.1'
$-----UNITS
[UNITS]
LENGTH         = 'inch'
FORCE          = 'pound_force'
ANGLE          = 'degrees'
MASS           = 'pound_mass'
TIME           = 'second'
$-----model
[MODEL]
! Handling Mode for selecting Handling force Model.
! HANDLING MODE          1  2
! -----
! Zero handling forces (only Fz)  x
! Fiala                      x
! -----
! Friction Mode for selecting Friction Model.
! FRICTION MODE          1  2  3  4
! -----
! Slip Ratio based Model          x
! slip velocity based Model A      x
! slip velocity based Model B      x
! User-Input Custom Mu vs. slip Ratio      x
!
PROPERTY_FILE_FORMAT    = 'AIR_BASIC'
FUNCTION_NAME           = 'TYR1500'
HANDLING_MODE           = 2.0
FRICTION_MODE           = 1.0
$-----dimension
[DIMENSION]
UNLOADED_RADIUS        = 12.625
WIDTH                   = 9.5
ASPECT_RATIO           = 0.8
!BOTTOMING_RADIUS      = 7.765
$-----parameter
[PARAMETER]
$ Vertical damping should be roughly 1000 times less than the
$ average vertical stiffness value (if k=lb/in and c=lb/(in/sec)
VERTICAL_DAMPING        = 3.6
RELAXATION_LENGTH       = 5.5
LOW_SPEED_DAMPING       = 3.6
LOW_SPEED_THRESHOLD     = 157
ROLLING_RESISTANCE      = 0.08
  
```

```

CSLIP                = 3516
CALPHA               = 440
UMAX                 = 0.8
UMIN                 = 0.4
V_UREF              = 1000.0
RR_DEFL_FACTOR      = 0.3333
$-----AIR_CURVE
$ Maximum of 25 points
[AIR_CURVE]
{pen                fz}
0.0                 0.0
0.61                2248.0
1.1                 4496.0
1.52                6744.0
1.94                8992.0
2.35                11240.0
2.75                13488.0
3.51                17985.0
4.22                22481.0
4.86                26977.0
!$-----RIMPACT_CURVE
!$ Maximum of 10 points
![RIMPACT_CURVE]
!{pen               fz}
!0.0                0.0
!0.1                100000.0
!0.2                200000.0
!0.3                300000.0
!0.4                400000.0
!0.5                500000.0
!0.6                600000.0
!6.0                6000000.0
$-----contact patch parameters
! 3D contact can be switched on by deleting the comment ! character
! when no further coefficients are specified, default values will be taken
![CONTACT_COEFFICIENTS]
CONTACT_MODEL        = '3D_ENVELOPING'
  
```

ENHANCED AIRCRAFT TIRE MODEL

```

$-----MDI_HEADER
[MDI_HEADER]
FILE_TYPE      = 'tir'
FILE_VERSION   = 3.0
FILE_FORMAT    = 'ASCII'
(COMMENTS)
{comment_string}
'Tire - DUNLOP DR18429T'
'Pressure - 130.5'
'Test Date - 05/08/2015'
'Test tire'
'New File Format v2.1'
$-----UNITS
[UNITS]
LENGTH = 'inch'
FORCE  = 'pound_force'
ANGLE  = 'degrees'
MASS   = 'pound_mass'
TIME   = 'second'
$-----model
[MODEL]
! Handling Mode for selecting Handling force Model.
! HANDLING MODE          1  2  3
! -----
! Zero handling forces (only Fz) X
! Fiala                   X
! UATire                   X
! -----
! Friction Mode for selecting Friction Model.
! FRICTION MODE          1  2  3  4
! -----
! Slip Ratio based Model          X
! Slip velocity based Model A      X
! Slip velocity based Model B      X
! User-Input Custom Mu vs. Slip Ratio X
!
PROPERTY_FILE_FORMAT = 'AIR_ENHANCED'
FUNCTION_NAME        = 'TYR1505'
HANDLING_MODE        = 3.0
FRICTION_MODE         = 1.0
$-----dimension
[DIMENSION]
UNLOADED_RADIUS      = 12.625
WIDTH                 = 9.5
ASPECT_RATIO         = 0.80
!BOTTOMING_RADIUS    = 7.765
$-----parameter
[PARAMETER]
$ vertical damping should be roughly 1000 times less than the
$ average vertical stiffness value (if k=lb/in and c=lb/(in/sec)
VERTICAL_DAMPING      = 3.6
RELAXATION_LENGTH     = 5.5
LOW_SPEED_DAMPING     = 3.6
LOW_SPEED_THRESHOLD   = 157
  
```



```

ROLLING_RESISTANCE      = 0.08
CGAMMA                  = 0
UMAX                    = 0.8
UMIN                    = 0.4
V_UREF                  = 1000.0
RR_DEFL_FACTOR          = 0.3333
SLIP_STIFFNESS_FACTOR   = 1.0
LON_DEFL_FACTOR         = 0.15
LAT_DEFL_FACTOR         = 0.70
FOOTPRINT_LENGTH_FACTOR = 0.85
  
```

\$-----AIR_CURVE

\$ Maximum of 25 points

[AIR_CURVE]

```

{pen      fz}
0.0        0.0
0.61       2248.0
1.1        4496.0
1.52       6744.0
1.94       8992.0
2.35      11240.0
2.75      13488.0
3.51      17985.0
4.22      22481.0
4.86      26977.0
  
```

!\$-----RIMPACT_CURVE

!\$ Maximum of 10 points

![RIMPACT_CURVE]

```

!{pen      fz}
!0.0        0.0
!0.1       100000.0
!0.2       200000.0
!0.3       300000.0
!0.4       400000.0
!0.5       500000.0
!0.6       600000.0
!6.0      6000000.0
  
```

\$-----CORN_STIFFNESS

\$ Maximum of 10 points

[CORN_STIFFNESS]

```

{fz      c_alpha}
2248.0   440.0
4496.0   656.0
6744.0   745.0
8992.0   743.0
11240.0  661.0
13488.0  560.0
17985.0  371.0
22481.0  196.0
26977.0  36.0
  
```

```

$-----LON_STIFFNESS
$ Maximum of 10 points
[LON_STIFFNESS]
{fz      lon_k}
 2248.0    3516.0
 4496.0    4276.0
 6744.0    4769.0
 8992.0    5166.0
11240.0    5507.0
13488.0    5808.0
17985.0    6299.0
22481.0    6696.0
26977.0    7019.0
$-----LAT_STIFFNESS
$ Maximum of 10 points
[LAT_STIFFNESS]
{fz      lat_k}
 2248.0    3100.0
 4496.0    2983.0
 6744.0    2881.0
 8992.0    2782.0
11240.0    2684.0
13488.0    2587.0
17985.0    2406.0
22481.0    2237.0
26977.0    2083.0
$-----contact patch parameters
! 3D contact can be switched on by deleting the comment ! character
! when no further coefficients are specified, default values will be taken
![CONTACT_COEFFICIENTS]
CONTACT_MODEL          = '3D_ENVELOPING'
  
```

TRR64 AIRCRAFT TIRE MODEL

```

$-----MDI_HEADER
[MDI_HEADER]
FILE_TYPE      = 'tir'
FILE_VERSION   = 3.0
FILE_FORMAT    = 'ASCII'
(COMMENTS)
{comment_string}
'Tire - DUNLOP 615x225-10 DR18429T'
'Pressure - 130.5'
'Test Date - 05/08/2015'
'Test tire'
'New File Format v2.1'
$-----UNITS
[UNITS]
LENGTH = 'inch'
FORCE  = 'pound_force'
ANGLE  = 'degrees'
MASS   = 'pound_mass'
TIME   = 'second'
$-----model
[MODEL]
! Handling Mode for selecting Handling force Model.
! HANDLING MODE          1  2  3  4
! -----
! Zero handling forces (only Fz)  X
! Fiala                          X
! UATire                          X
! simple NASA TR-R-64              X
!
! Friction Mode for selecting Friction Model.
! FRICTION MODE          1  2  3  4
! -----
! Slip Ratio based Model          X
! Slip velocity based Model A      X
! Slip velocity based Model B      X
! User-Input Custom Mu vs. Slip Ratio  X
!
PROPERTY_FILE_FORMAT = 'AIR_TRR64'
FUNCTION_NAME        = 'TYR1510'
HANDLING_MODE        = 4.0
FRICTION_MODE        = 1.0
$-----dimension
[DIMENSION]
UNLOADED_RADIUS      = 12.625
WIDTH                 = 9.5
ASPECT_RATIO          = 0.80
!BOTTOMING_RADIUS    = 7.765
$-----parameter
[PARAMETER]
$ Vertical damping should be roughly 1000 times less than the
$ average vertical stiffness value (if k=lb/in and c=lb/(in/sec))
RATED_PRESSURE        = 112
INFLATION_PRESSURE    = 130.5
VERTICAL_DAMPING      = 3.6
  
```

```

LOW_SPEED_DAMPING      = 3.6
LOW_SPEED_THRESHOLD    = 157
ROLLING_RESISTANCE     = 0.08
UMAX                   = 0.8
UMIN                   = 0.4
V_UREF                 = 1000.0
RR_DEFL_FACTOR         = 0.3333
SLIP_STIFFNESS_FACTOR = 1.0
LON_DEFL_FACTOR        = 0.15
LAT_DEFL_FACTOR        = 0.70
FOOTPRINT_LENGTH_FACTOR = 0.85
FOOTPRINT_AREA_RATIO   = 0.85
!$-----RIMPACT_CURVE
!$ Maximum of 10 points
![BOTTOMING_CURVE]
!{pen      fz}
!0.0      0.0
!0.61     2248.0
!1.1      4496.0
!1.52     6744.0
!1.94     8992.0
!2.35    11240.0
!2.75    13488.0
!3.51    17985.0
!4.22    22481.0
!4.86    26977.0
!$-----contact patch parameters
! 3D contact can be switched on by deleting the comment ! character
! when no further coefficients are specified, default values will be taken
![CONTACT_COEFFICIENTS]
CONTACT_MODEL          = '3D_ENVELOPING'

```

APPENDIX D PAC2002 TIRE DATA AND FITTING TOOL IN MSC.ADAMS

PACEJKA 2002 TIRE MODEL

The PAC2002 Tire Data and Fitting Tool (TDFT) calculates the PAC2002 tire model parameters out of tire measurement data for steady-state pure and combined slip conditions. However the tool can also convert existing Adams/Tire property files to a PAC2002 tire property file by fitting on-line generated virtual tire test data. Due to the fact that there were no sufficient measurement data available from the tire manufacturer, the second method was selected to obtain PAC2002 tire model parameters. The conversion takes care of converting the 'steady-state' Force & Moment properties only. More information about the tire data and fitting tool can be found in [30].

The total weight of the helicopter is approximately 11 tones and each main landing gear receives 4110kg of it [36]. However the tire manufacturer provided data for 8992 lbs. (4079kg) load which is almost the same with the aforementioned maximum weight. The ENHANCED Tire Model (8992 lbs. load case) was used to make the conversion to the PAC2002 tire model parameters at 130.5 air pressure. The PAC2002 tire models parameters can be found in the end of this chapter.

The PAC2002 is realistic and accurate for handling and maneuvering simulations. As long as the tire manufacturer provides measurement data, the tire data fitting tool is suitable for calculating the PACEJKA tire parameters and use them for ground maneuvering simulations. However ground maneuvering simulations are out of scope of this report. The available Dunlop calculations [32] are compared with the PAC2002 model arrived at in the hereafter presented figures for the lateral force and self-alignment torque versus the slip angle.

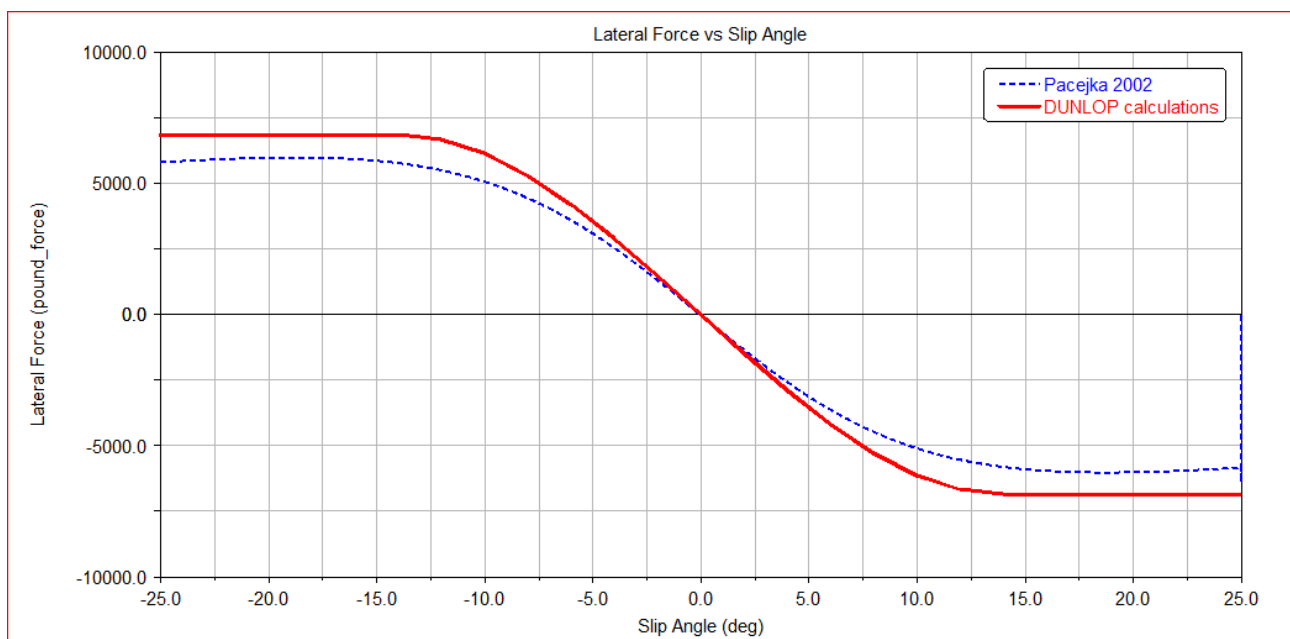


Figure D.1: Lateral Force vs Slip Angle for 4079kg.

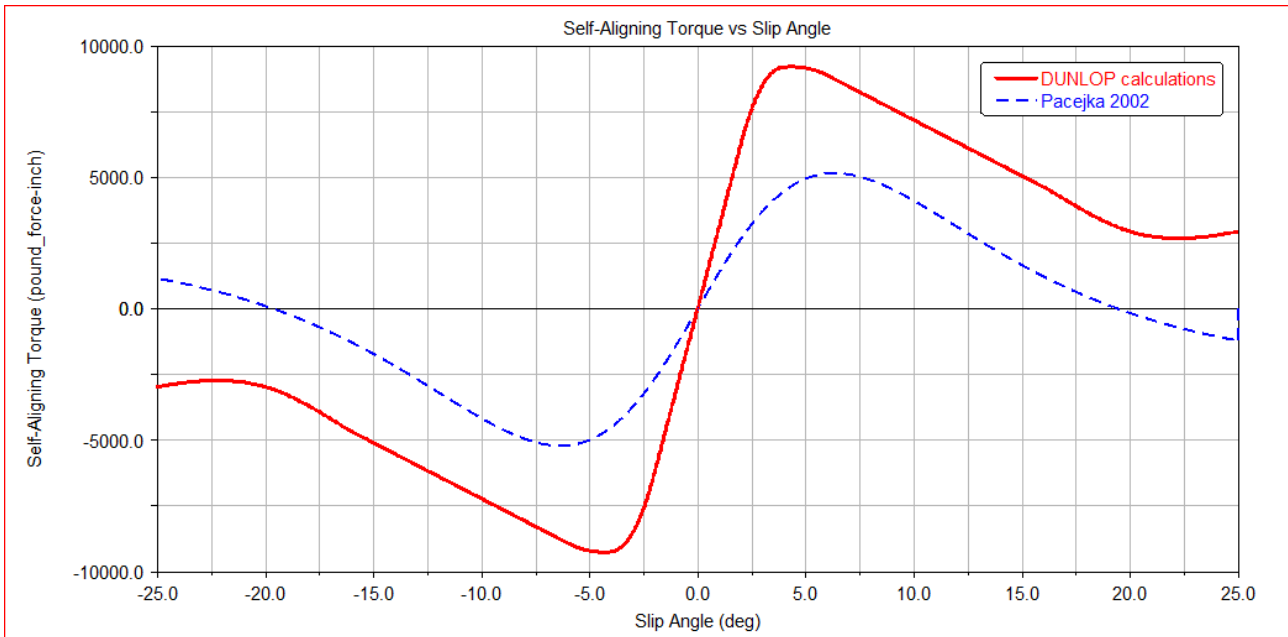


Figure D.2: Self-Aligning Torque vs Slip Angle for 4079kg.

Pacejka 2002 Tire File

```

$-----MDI_HEADER
[MDI_HEADER]
FILE_TYPE           = 'tir'
FILE_VERSION        = 3.0
FILE_FORMAT         = 'ASCII'
! : TIRE_VERSION :   PAC2002
! : COMMENT :       Tire                205/55 R16 90H
! : COMMENT :       Manufacturer
! : COMMENT :       Nom. section width (m)  0
! : COMMENT :       Nom. aspect ratio (-)   0
! : COMMENT :       Infl. pressure (Pa)     0
! : COMMENT :       Rim radius (m)         0
! : COMMENT :       Measurement ID
! : COMMENT :       Test speed (m/s)       0
! : COMMENT :       Road surface
! : COMMENT :       Road condition
! : FILE_FORMAT :   'ASCII'
! : Copyright (c) 2004-2011 MSC software corporation

USE_MODE specifies the type of calculation performed:
0: Fz only, no Magic Formula evaluation
1: Fx,My only
2: Fy,Mx,Mz only
3: Fx,Fy,Mx,My,Mz uncombined force/moment calculation
4: Fx,Fy,Mx,My,Mz combined force/moment calculation
+10: including relaxation behaviour
15: Fx,Fy,Mx,My,Mz combined force/moment calculation, relaxation behaviour, including turn-slip torque
+20: including advanced transient (contact mass approach)
25: Fx,Fy,Mx,My,Mz combined force/moment calculation, advanced transient including turn-slip torque & parking torque
*-1: mirroring of tyre characteristics

example: USE_MODE = -12 implies:
-calculation of Fy,Mx,Mz only
-including relaxation effects
-mirrored tyre characteristics

! Description:
! - This template file is used for the PAC2002 Tire Data and Fitting Tool (PAC2002 TDFT)
! - This template includes the PAC2002 tire model parameters
!   to model the influence of inflation pressure (ip) changes on the
!   steady-state tire behavior.
! - Non-zero parameters are taken from the 205/55 R16 example tire property file

$-----units
[UNITS]
LENGTH           = 'meter'
FORCE             = 'newton'
ANGLE            = 'radians'
MASS             = 'kg'
TIME             = 'second'
PRESSURE         = 'pascal'

```

```

PRESSURE = 'pascal'
$-----model
[MODEL]
PROPERTY_FILE_FORMAT = 'PAC2002'
USE_MODE = 4.0 $Tyre use switch (IUSED)
VXLOW = 2.0 $Threshold speed for scaling down forces and moments
LONGVL = 30.0 $Measurement speed
$-----dimension
[DIMENSION]
UNLOADED_RADIUS = 0.320675 $Free tyre radius
WIDTH = 0.2413 $Nominal section width of the tyre
ASPECT_RATIO = 0.8 $Nominal aspect ratio
RIM_RADIUS = 0.203 $Nominal rim radius
RIM_WIDTH = 0.165 $Rim width
BOTTOMING_RADIUS = 0.0 $Radius for bottoming of the tyre
$-----deflection_load_curve
$ For a non-linear tyre vertical stiffness
$ Maximum of 100 points
[DEFLECTION_LOAD_CURVE]
{PEN_VERTICAL FZ_VERTICAL}
0.000000 0.000000
0.015494 9999.602191
0.027940 19999.204382
0.038608 29998.806573
0.049276 39998.408764
0.059690 49998.010956
0.069850 59997.613147
0.089154 80001.265750
0.107188 100000.470133
0.123444 119999.674515
$-----tire_conditions
[TIRE_CONDITIONS]
IP = 200000.0 $Inflation Pressure
IP_NOM = 200000.0 $Nominal Inflation Pressure
$-----vertical
[VERTICAL]
VERTICAL_STIFFNESS = 960207.623498 $Tyre vertical stiffness
VERTICAL_DAMPING = 805.583442134 $Tyre vertical damping
BREFF = 0.0 $Low load stiffness effective rolling radius
DREFF = 0.0 $Peak value of effective rolling radius
FREFF = 1.0 $High load stiffness effective rolling radius
FNOMIN = 40000.0 $Nominal wheel load
QFZ3 = 1.0 $Variation of vertical stiffness with tire pressure
$-----long_slip_range
[LONG_SLIP_RANGE]
KPUMIN = -1.5 $Minimum valid wheel slip
KPUMAX = 1.5 $Maximum valid wheel slip
$-----slip_angle_range
[SLIP_ANGLE_RANGE]
ALPMIN = -1.5708 $Minimum valid slip angle
ALPMAX = 1.5708 $Maximum valid slip angle

```

```

$-----inclination_angle_range
[INCLINATION_ANGLE_RANGE]
CAMMIN = 0.0 $Minimum valid camber angle
CAMMAX = 0.0 $Maximum valid camber angle
$-----vertical_force_range
[VERTICAL_FORCE_RANGE]
FZMIN = 40.0 $Minimum allowed wheel load
FZMAX = 80000.0 $Maximum allowed wheel load
$-----scaling_coefficients
[SCALING_COEFFICIENTS]
LFZO = 1.0 $Scale factor of nominal (rated) load
LCX = 1.0 $Scale factor of Fx shape factor
LMUX = 1.0 $Scale factor of Fx peak friction coefficient
LEX = 1.0 $Scale factor of Fx curvature factor
LKX = 1.0 $Scale factor of Fx slip stiffness
LHX = 1.0 $Scale factor of Fx horizontal shift
LVX = 1.0 $Scale factor of Fx vertical shift
LGAX = 1.0 $Scale factor of camber for Fx
LCY = 1.0 $Scale factor of Fy shape factor
LMUY = 1.0 $Scale factor of Fy peak friction coefficient
LEY = 1.0 $Scale factor of Fy curvature factor
LKY = 1.0 $Scale factor of Fy cornering stiffness
LHY = 1.0 $Scale factor of Fy horizontal shift
LVY = 1.0 $Scale factor of Fy vertical shift
LGAY = 1.0 $Scale factor of camber for Fy
LTR = 1.0 $Scale factor of Peak of pneumatic trail
LRES = 1.0 $Scale factor for offset of residual torque
LGAZ = 1.0 $Scale factor of camber for Mz
LXAL = 1.0 $Scale factor of alpha influence on Fx
LYKA = 1.0 $Scale factor of alpha influence on Fx
LVYKA = 1.0 $Scale factor of kappa induced Fy
LS = 1.0 $Scale factor of Moment arm of Fx
LSGKP = 1.0 $Scale factor of Relaxation length of Fx
LSGAL = 1.0 $Scale factor of Relaxation length of Fy
LGYR = 1.0 $Scale factor of gyroscopic torque
LMX = 1.0 $Scale factor of overturning couple
LVMX = 1.0 $Scale factor of Mx vertical shift
LMY = 1.0 $Scale factor of rolling resistance torque
LIP = 1.0 $Scale factor of inflation pressure
$-----longitudinal_coefficients
[LONGITUDINAL_COEFFICIENTS]
PCX1 = 2.14864677781 $Shape factor cfx for longitudinal force
PDX1 = 0.695107241679 $Longitudinal friction Mux at Fznom
PDX2 = -0.1 $Variation of friction Mux with load
PDX3 = 0.0 $Variation of friction Mux with camber
PEX1 = 0.672133637921 $Longitudinal curvature Efx at Fznom
PEX2 = 0.0 $Variation of curvature Efx with load
PEX3 = 0.0 $Variation of curvature Efx with load squared
PEX4 = 0.0404521920031 $Factor in curvature Efx while driving
PKX1 = 6.87360933506 $Longitudinal slip stiffness Kfx/Fz at Fznom
PKX2 = 0.1 $Variation of slip stiffness Kfx/Fz with load

```


PKX3	= 0.1	\$Exponent in slip stiffness Kfx/Fz with load
PHX1	= 0.00249254855608	\$Horizontal shift Shx at Fznom
PHX2	= 0.0	\$Variation of shift Shx with load
PVX1	= -0.000709247115397	\$Vertical shift svx/Fz at Fznom
PVX2	= 0.0	\$Variation of shift svx/Fz with load
PPX1	= 0.0	\$Variation of slip stiffness Kfx/Fz with pressure
PPX2	= 0.0	\$Variation of slip stiffness Kfx/Fz with pressure squared
PPX3	= 0.0	\$Variation of friction Mux with pressure
PPX4	= 0.0	\$Variation of friction Mux with pressure squared
RBX1	= 3.88329883865	\$Slope factor for combined slip Fx reduction
RBX2	= -5.09086496297	\$Variation of slope Fx reduction with kappa
RCX1	= 1.72271864378	\$Shape factor for combined slip Fx reduction
REX1	= 1.06992419743	\$Curvature factor of combined Fx
REX2	= 0.0	\$Curvature factor of combined Fx with load
RHX1	= 3.48696051453e-11	\$Shift factor for combined slip Fx reduction
PTX1	= 0.85683	\$Relaxation length Sigkap0/Fz at Fznom
PTX2	= 0.00011176	\$Variation of Sigkap0/Fz with load
PTX3	= -1.3131	\$Variation of Sigkap0/Fz with exponent of load
PTX4	= 0.0	
-----overturning_coefficients		
[OVERTURNING_COEFFICIENTS]		
QSX1	= 1.14081436608e-07	\$Lateral force induced overturning moment
QSX2	= 0.0	\$Camber induced overturning couple
QSX3	= -0.00475447033788	\$Fy induced overturning couple
QSX4	= 0.683333800093	\$Fz induced overturning couple due to lateral tire deflection
QSX5	= 54.1118246734	\$Fz induced overturning couple due to lateral tire deflection
QSX6	= 0.1	\$Fz induced overturning couple due to lateral tire deflection
QSX7	= 0.0	\$Fz induced overturning couple due to lateral tire deflection by inclination
QSX8	= 0.812670600365	\$Fz induced overturning couple due to lateral tire deflection by lateral force
QSX9	= 0.392206802105	\$Fz induced overturning couple due to lateral tire deflection by lateral force
QSX10	= 0.0	\$Inclination induced overturning couple, load dependency
QSX11	= 0.0	\$Load dependency inclination induced overturning couple
-----lateral_coefficients		
[LATERAL_COEFFICIENTS]		
PCY1	= 2.67737870562	\$Shape factor cfy for lateral forces
PDY1	= -0.661540800099	\$Lateral friction Muy
PDY2	= -0.1	\$Variation of friction Muy with load
PDY3	= 0.0	\$Variation of friction Muy with squared camber
PEY1	= 9.35485341419	\$Lateral curvature Efy at Fznom
PEY2	= -0.1	\$Variation of curvature Efy with load
PEY3	= -0.308444374469	\$Zero order camber dependency of curvature Efy
PEY4	= 0.0	\$Variation of curvature Efy with camber
PKY1	= -128.931115853	\$Maximum value of stiffness Kfy/Fznom
PKY2	= 60.6885736186	\$Load at which Kfy reaches maximum value
PKY3	= 0.0	\$Variation of Kfy/Fznom with camber

PHY1	= -1.6197197732e-05	\$Horizontal shift Shy at Fznom
PHY2	= 0.0	\$Variation of shift Shy with load
PHY3	= 0.0	\$Variation of shift Shy with camber
PVY1	= -4.85912748914e-05	\$Vertical shift in Svy/Fz at Fznom
PVY2	= 0.0	\$Variation of shift Svy/Fz with load
PVY3	= 0.0	\$Variation of shift Svy/Fz with camber
PVY4	= 0.0	\$Variation of shift Svy/Fz with camber and load
PPY1	= 0.0	\$Variation of max. stiffness Kfy/Fznom with pressure
PPY2	= 0.0	\$Variation of load at max. Kfy with pressure
PPY3	= 0.0	\$Variation of friction Muy with pressure
PPY4	= 0.0	\$Variation of friction Muy with pressure squared
RBV1	= 4.07706456691	\$Slope factor for combined Fy reduction
RBV2	= 3.17496551199	\$Variation of slope Fy reduction with alpha
RBV3	= 4.62094201948e-05	\$Shift term for alpha in slope Fy reduction
RCY1	= 1.05600976261	\$Shape factor for combined Fy reduction
REY1	= -0.61692975667	\$Curvature factor of combined Fy
REY2	= 0.0	\$Curvature factor of combined Fy with load
RHY1	= 0.00459460299366	\$Shift factor for combined Fy reduction
RHY2	= 0.0	\$Shift factor for combined Fy reduction with load
RVY1	= -0.000856494072459	\$Kappa induced side force Svyk/Muy*Fz at Fznom
RVY2	= 0.0	\$Variation of Svyk/Muy*Fz with load
RVY3	= 0.0	\$Variation of Svyk/Muy*Fz with camber
RVY4	= 36203.0399129	\$Variation of Svyk/Muy*Fz with alpha
RVY5	= 42.5297244371	\$Variation of Svyk/Muy*Fz with kappa
RVY6	= -1207.72848185	\$Variation of Svyk/Muy*Fz with atan(kappa)
PTY1	= 4.1114	\$Peak value of relaxation length SigAlp0/R0
PTY2	= 6.1149	\$Value of Fz/Fznom where SigAlp0 is extreme
-----rolling_coefficients		
[ROLLING_COEFFICIENTS]		
QSY1	= 0.0	\$Rolling resistance torque coefficient
QSY2	= 0.0	\$Rolling resistance torque depending on Fx
QSY3	= 0.0	\$Rolling resistance torque depending on speed
QSY4	= 0.0	\$Rolling resistance torque depending on speed ^4
-----aligning_coefficients		
[ALIGNING_COEFFICIENTS]		
QBZ1	= 4.3498460205	\$Trail slope factor for trail Bpt at Fznom
QBZ2	= -2.0	\$Variation of slope Bpt with load
QBZ3	= 0.0	\$Variation of slope Bpt with load squared
QBZ4	= 0.0	\$Variation of slope Bpt with camber
QBZ5	= 0.0	\$Variation of slope Bpt with absolute camber
QBZ9	= 0.0	\$Slope factor Br of residual torque Mzr
QBZ10	= 9141.67919451	\$Slope factor Br of residual torque Mzr
QCZ1	= 2.0311332168	\$Shape factor Cpt for pneumatic trail
QDZ1	= 0.165948423247	\$Peak trail Dpt" = Dpt*(Fz/Fznom*R0)
QDZ2	= -0.01	\$Variation of peak Dpt" with load
QDZ3	= 0.0	\$Variation of peak Dpt" with camber
QDZ4	= 0.0	\$Variation of peak Dpt" with camber squared
QDZ6	= 3.403158606e-06	\$Peak residual torque Dmr" = Dmr/(Fz*R0)
QDZ7	= 0.0	\$Variation of peak factor Dmr" with load
QDZ8	= 0.0	\$Variation of peak factor Dmr" with camber
QDZ9	= 0.0	\$Variation of peak factor Dmr" with camber and load
QEZ1	= 8.44970347876	\$Trail curvature Ept at Fznom

QE22	= -5.0	\$Variation of curvature Ept with load
QE23	= 0.0	\$Variation of curvature Ept with load squared
QE24	= 0.00679397519573	\$Variation of curvature Ept with sign of Alpha-t
QE25	= 0.0	\$Variation of Ept with camber and sign Alpha-t
QH21	= 1.31740272935e-05	\$Trail horizontal shift Sht at Fznom
QH22	= 0.0	\$Variation of shift sht with load
QH23	= 0.0	\$Variation of shift sht with camber
QH24	= 0.0	\$Variation of shift sht with camber and load
QPZ1	= 0.0	\$Variation of peak Dpt" with pressure
SSZ1	= 1.20098020217e-06	\$Nominal value of s/R0: effect of Fx on Mz
SSZ2	= -0.317882099654	\$Variation of distance s/R0 with Fy/Fznom
SSZ3	= 0.0	\$Variation of distance s/R0 with camber
SSZ4	= 0.0	\$Variation of distance s/R0 with load and camber
QTZ1	= 0.0	\$Gyration torque constant
MBELT	= 0.0	
\$-----turnslip_coefficients		
[TURNSLIP_COEFFICIENTS]		
PECP1	= 0.7	\$Camber stiffness reduction factor
PECP2	= 0.0	\$Camber stiffness reduction factor with load
PDXP1	= 0.4	\$Peak Fx reduction due to spin
PDXP2	= 0.0	\$Peak Fx reduction due to spin with load
PDXP3	= 0.0	\$Peak Fx reduction due to spin with longitudinal slip
PDYP1	= 0.4	\$Peak Fy reduction due to spin
PDYP2	= 0.0	\$Peak Fy reduction due to spin with load
PDYP3	= 0.0	\$Peak Fy reduction due to spin with lateral slip
PDYP4	= 0.0	\$Peak Fy reduction with square root of spin
PKYP1	= 1.0	\$Cornering stiffness reduction due to spin
PHYP1	= 1.0	\$Fy lateral shift shape factor
PHYP2	= 0.15	\$Maximum Fy lateral shift
PHYP3	= 0.0	\$Maximum Fy lateral shift with load
PHYP4	= -4.0	\$Fy lateral shift curvature factor
QDTP1	= 10.0	\$Pneumatic trail reduction factor
QBRP1	= 0.1	\$Residual torque reduction factor with lateral slip
QCRP1	= 0.2	\$Turning moment at constant turning with zero speed
QCRP2	= 0.1	\$Turning moment at 90 deg lateral slip
QDRP1	= 1.0	\$Maximum turning moment
QDRP2	= -1.5	\$Location of maximum turning moment
\$-----contact_coefficients		
[CONTACT_COEFFICIENTS]		
PA1	= 0.35	\$Half contact length dependency on sqrt(Fz/Fz0)
PA2	= 2.25	\$Half contact length dependency on Fz/Fz0
PB1	= 0.9	\$Half contact width dependency on sqrt(Fz/Fz0)
PB2	= 1.15	\$Half contact width dependency on Fz/Fz0
PB3	= -3.0	\$Half contact width dependency on Fz/Fz0*sqrt(Fz/Fz0)
ROAD_SPACING	= 0.001	\$Spacing of cam sections
MAX_HEIGHT	= 0.1	\$Maximum allowed obstacle height
PAE	= 1.15	\$Half ellipse length/unloaded radius
PBE	= 1.05	\$Half ellipse height/unloaded radius
PCE	= 2.0	\$Ellipse exponent
PLS	= 0.8	\$Shift length / contact length
N_WIDTH	= 6.0	\$Number of cams across tire width
N_LENGTH	= 5.0	\$Number of cams across tire length
\$-----dynamic_coefficients		
[DYNAMIC_COEFFICIENTS]		
MC	= 1.0	\$Contact mass
IC	= 0.05	\$Contact moment of inertia
KX	= 409.0	\$Contact longitudinal damping
KY	= 320.8	\$Contact lateral damping
KP	= 11.9	\$Contact yaw damping
CX	= 435000.0	\$Contact longitudinal stiffness
CY	= 166500.0	\$Contact lateral stiffness
CP	= 20319.0	\$Contact yaw stiffness
EP	= 1.0	
EP12	= 4.0	
BF2	= 0.5	
BP1	= 0.5	
BP2	= 0.67	

APPENDIX E PRELIMINARY LANDING GEAR SIMULATIONS

E.1 Introduction

Having completed and validated the tire model, the integration with the landing gear model has to be accomplished. The first step before starting to work in MSC.ADAMS, was to extract the design files from the CATIA CAD program, in which the landing gear has been designed. Having exported the files, it is straightforward to import them in MSC.ADAMS however without any functionality. To build up a functional model this design was converted to flexible bodies, masses, joints, springs, the wheel and the tire. The bodies were made flexible with the inherent flexible conversion tool in MSC.ADAMS. This conversion divided each body into 8 smaller elements representing beam flexibilities. It has to be mentioned that this is a simplified FEM functionality and is not as realistic as a full FEM model. However a FEM is considered not necessary because the original pro/MECHANICA model uses a similar approach to implement the flexibilities.

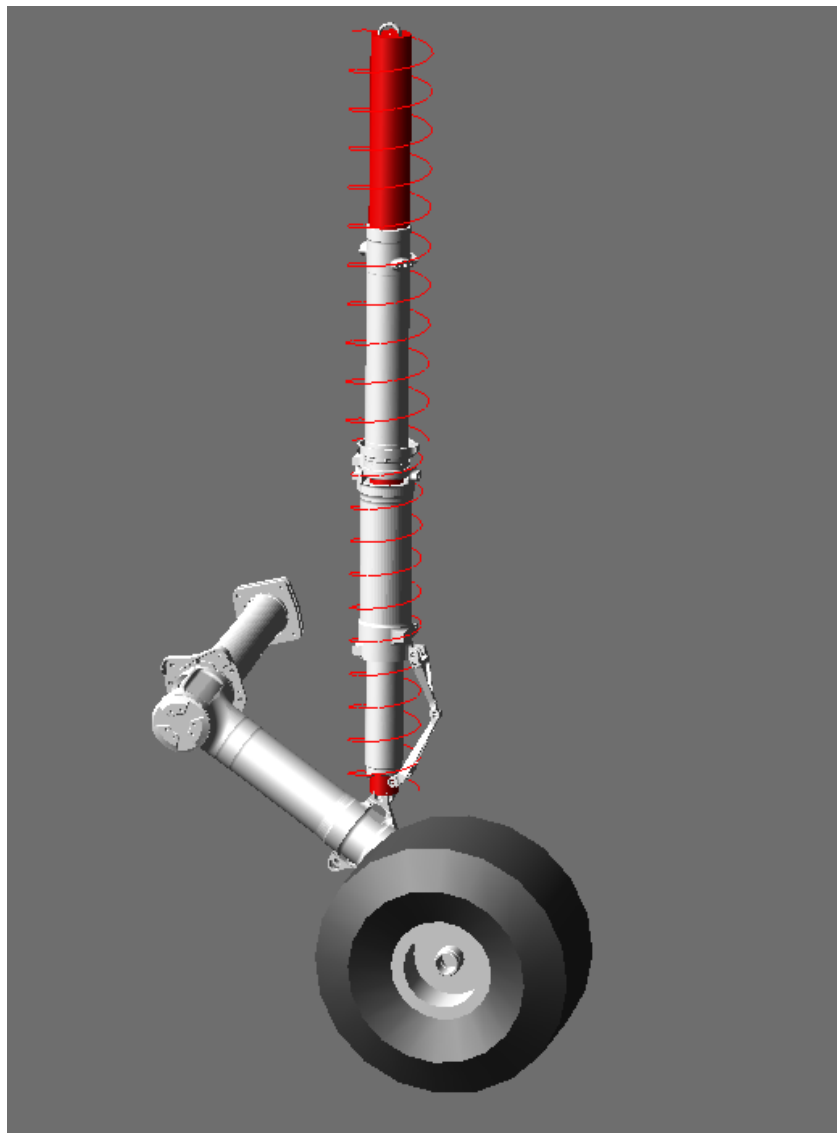


Figure E.1: The landing gear with the BASIC aircraft tire in MSC.ADAMS.

All the connections and joints of the model were taken from [33]. In this reference all the details for the model and their connections were given explicitly. The spring damper coefficients, representing the preliminary shock damper characteristics, were tuned by trial and error because no information about these values is available yet. However a dedicated shock-absorber subroutine will be developed in order to substitute the spring-damper functionality and this is the reason why the simulations presented here are preliminary. The BASIC tire model was implemented due to the better behavior as was described in chapter 3. The parameters were taken for the medium load case, that is 11240 lbs. vertical load. It has to be mentioned that even though the tire models are written in the British unit system, MSC.ADAMS converts everything to the SI system as it was assigned for the Landing Gear Model. The preliminary landing gear model can be seen in the [Figure E.1](#).

E.2 Landing Gear Simulations

In drop test and landing simulations, a number of quantities can be measured. Reference [8] lists the most important quantities that shall be measured and analyzed. In this case, for the purpose of illustration, the Wheel Axle and the Middle Trailing Arm positions are chosen to be presented. In the next figures the time histories of the forces and moments as well as the Tire Deflections and the Strut Actuator are shown which are important for the fatigue and stress analysis. Analogous procedures can be executed to measure forces, moments and deformations at other locations.

This drop test simulation was performed with initial descent velocity of 4 (m/s) and at 0.20 (m) above the ground, and no forward speed. The results can be seen in the figures at the next pages. It can be observed in the simulations that the wheel's axle vibrates a lot during the impact. The measurements from this type of MBD models can be used as input to dedicated FEM programs like MSC.NASTRAN. Exploiting those FEM programs one can determine the internal loads, stresses and deformations. Further analysis can result in conclusions regarding the fatigue- and material strength and failure. However the aforementioned analyses are out of the scope of the present project.

Last but not least, it should be mentioned that the preliminary MLG drop simulations revealed a bug in the tire modelling in MSC.ADAMS. Most of the tire models are dedicated for handling vehicle simulations with specific forward velocity. However because in the drop test there is no forward speed, the tire does not produce the correct amount of forces. This problem can be circumvented by giving the MLG a small forward speed with respect to the ground.

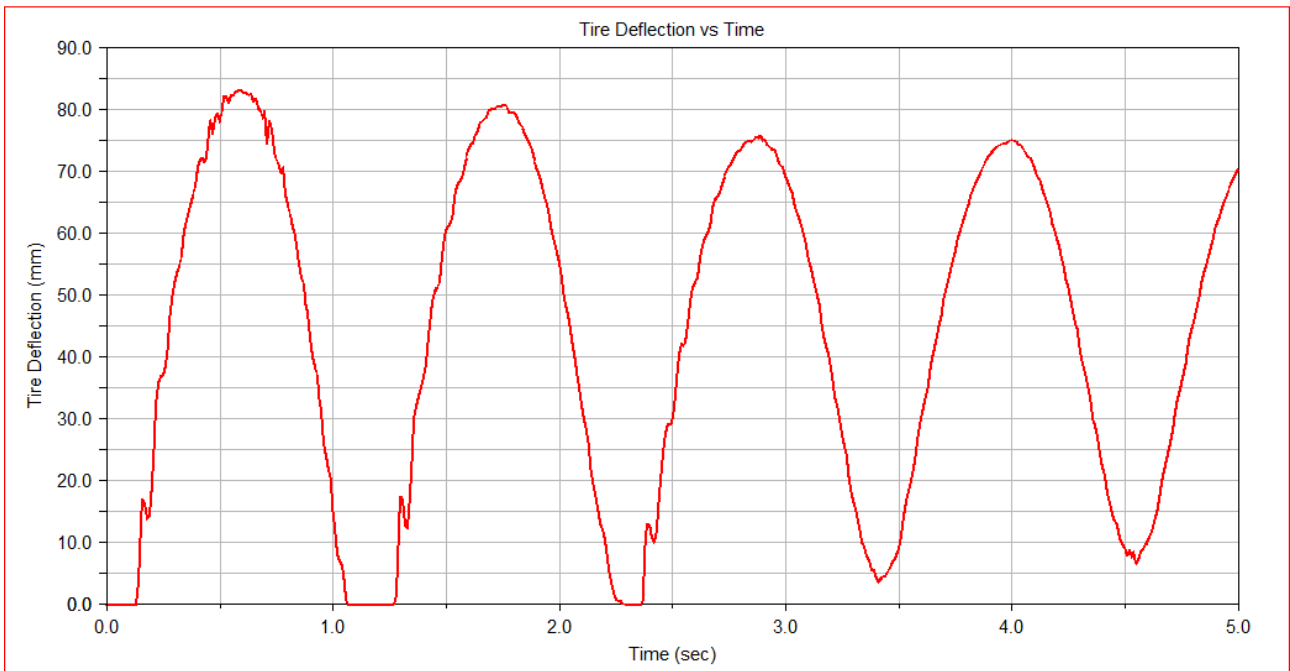


Figure E.2: Tire Deflection during the drop test.

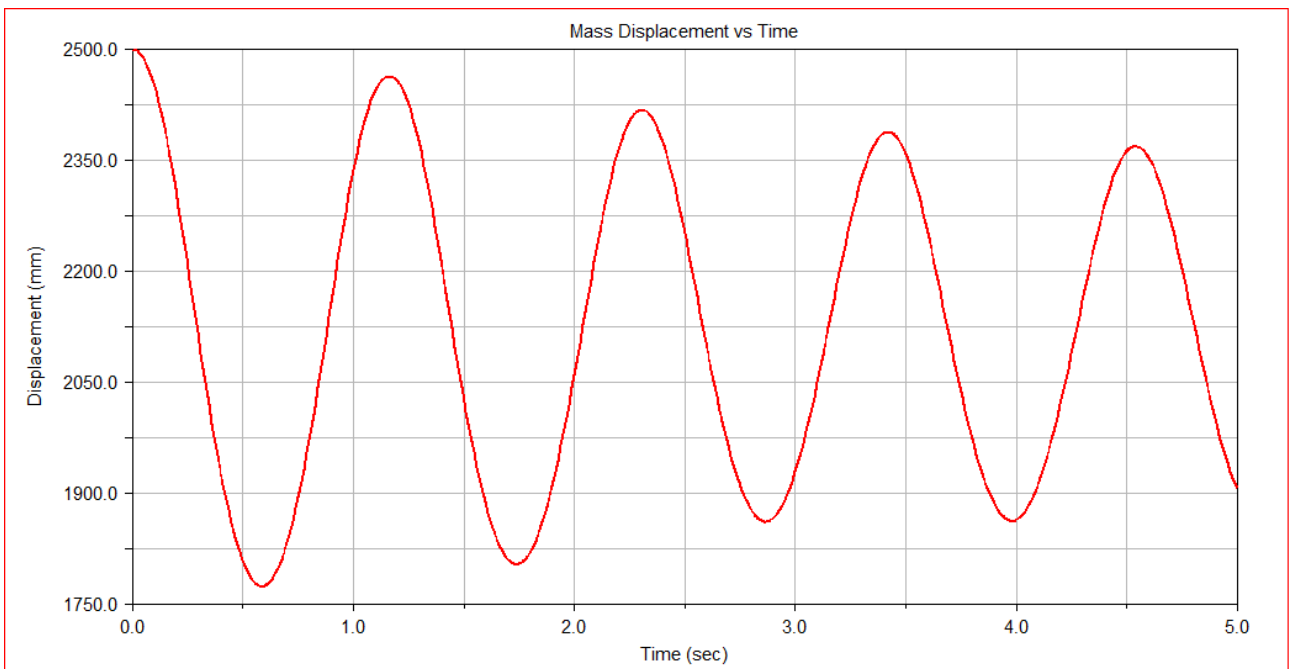


Figure E.3: Displacement of the mass attached to the landing gear during the drop test.

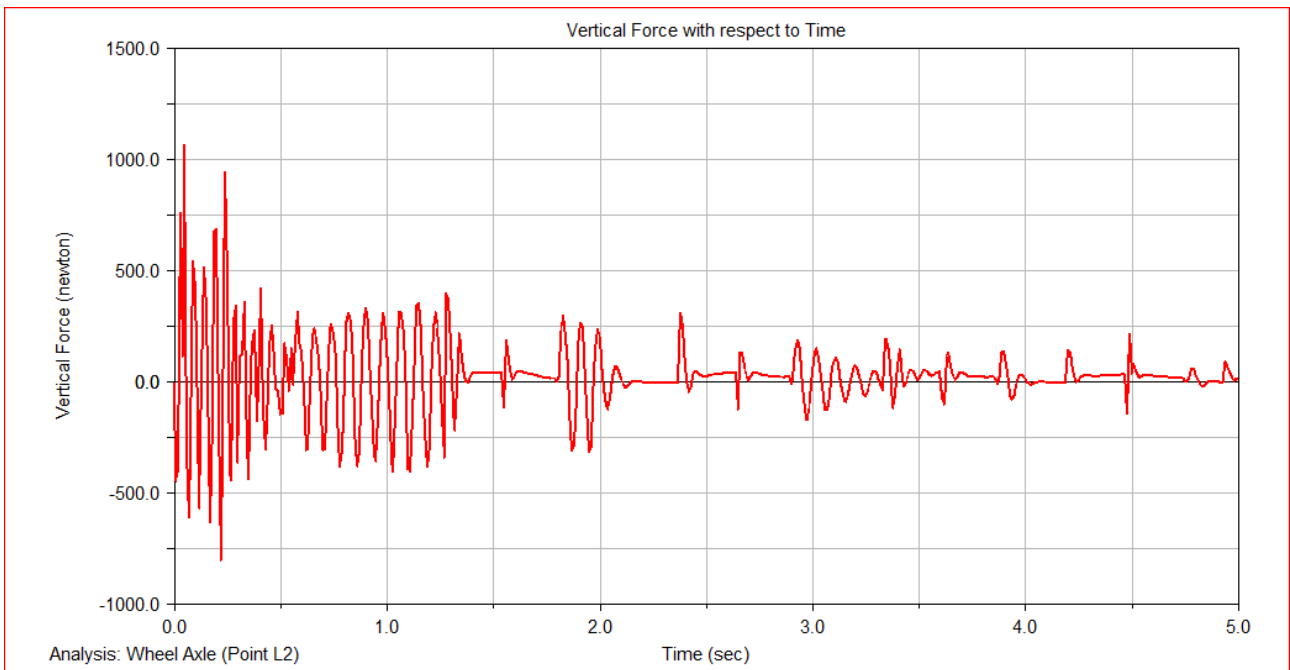


Figure E.4: Vertical Force at the Wheel's Axle during drop test.

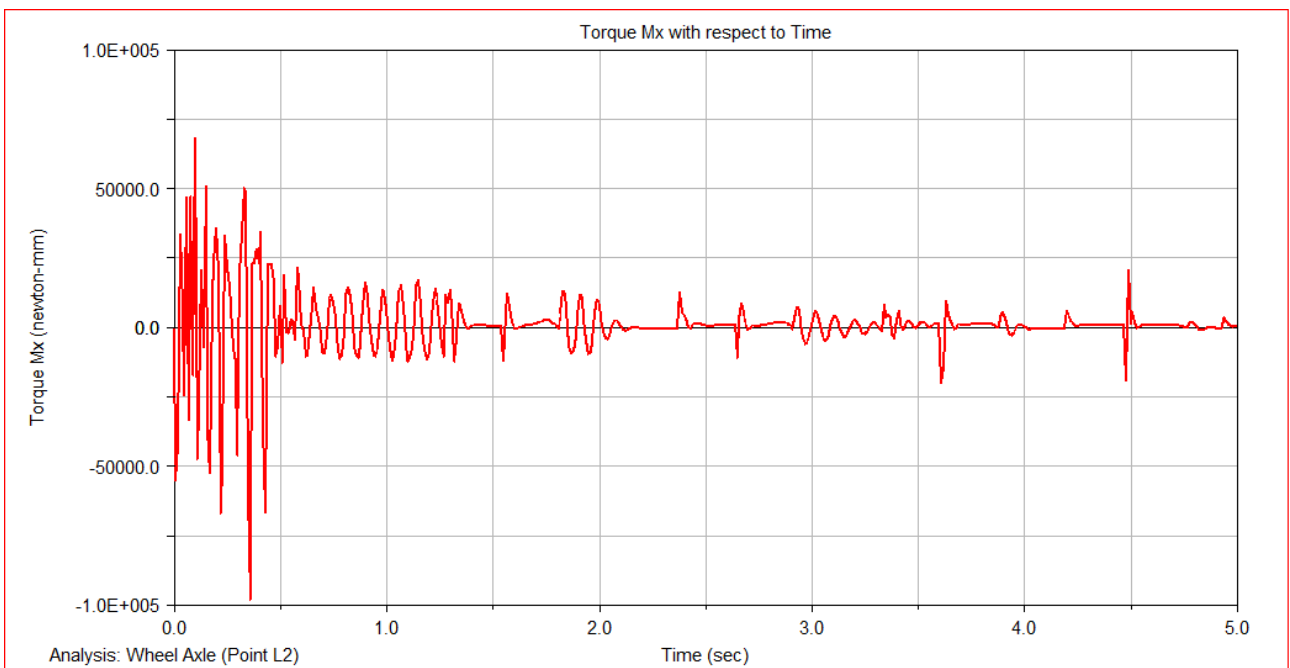


Figure E.5: Moment with respect to x axis at the Wheel's Axle during drop test.

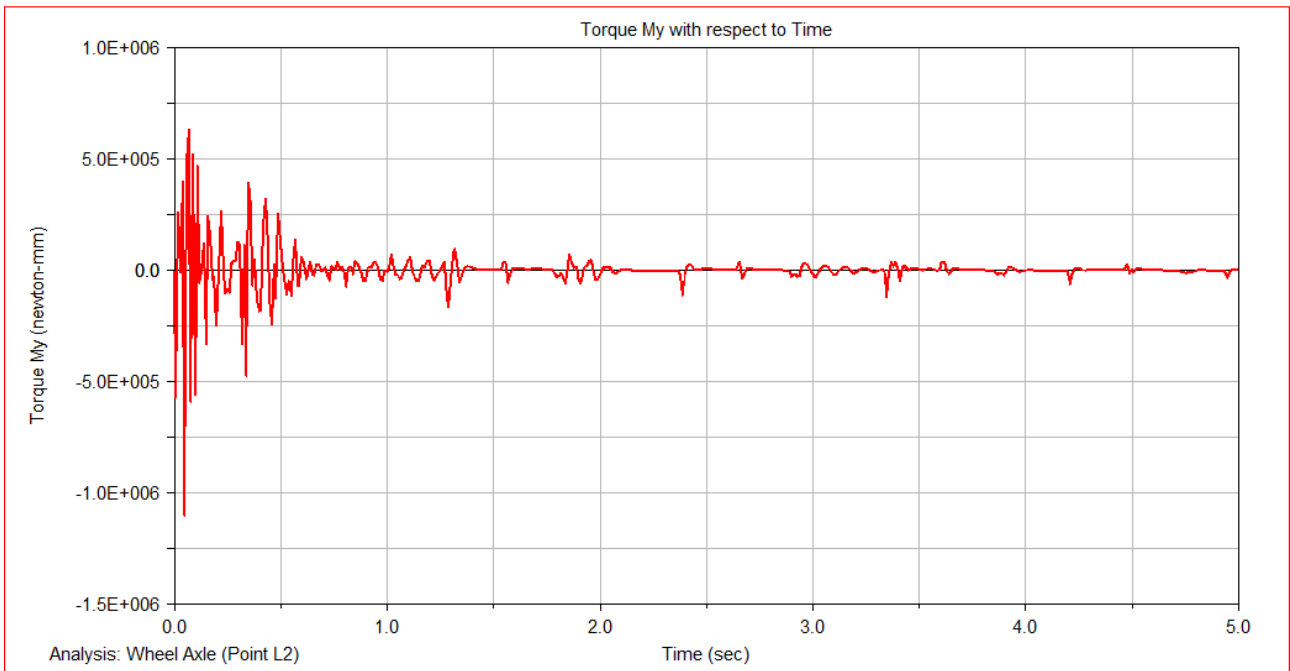


Figure E.6: Moment with respect to y axis to the Wheel's Axle during drop test.

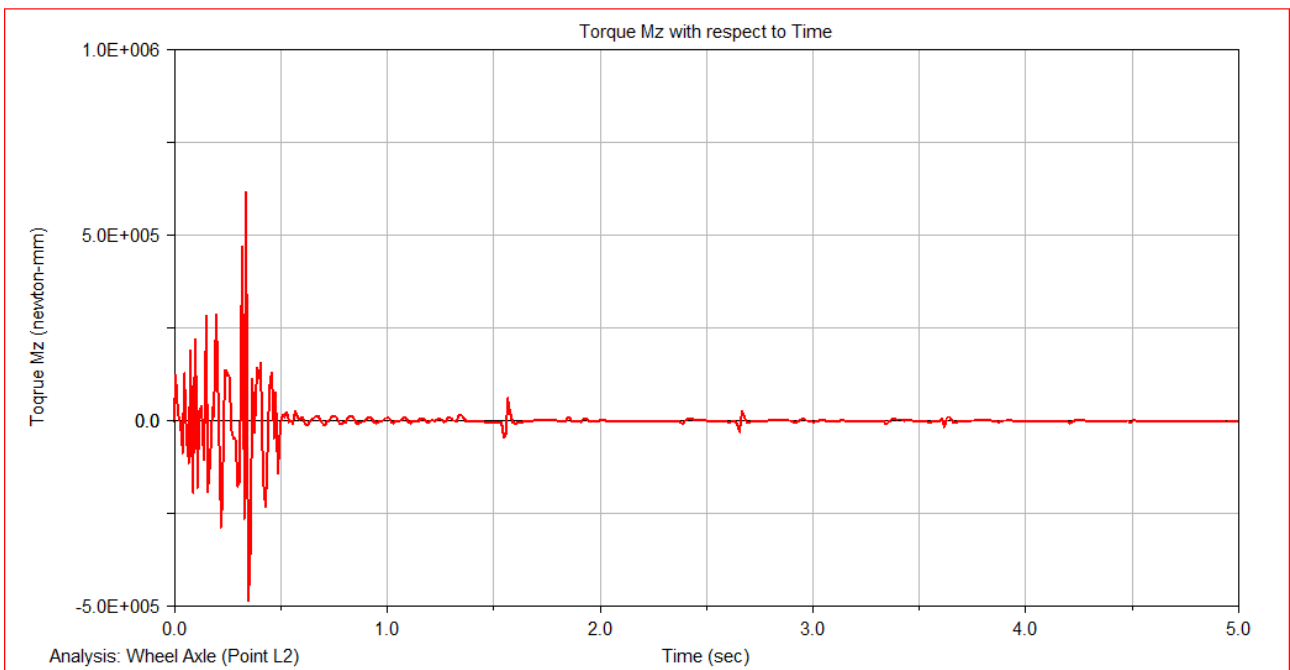


Figure E.7: Moment with respect to z axis at the Wheel's Axle during drop test.

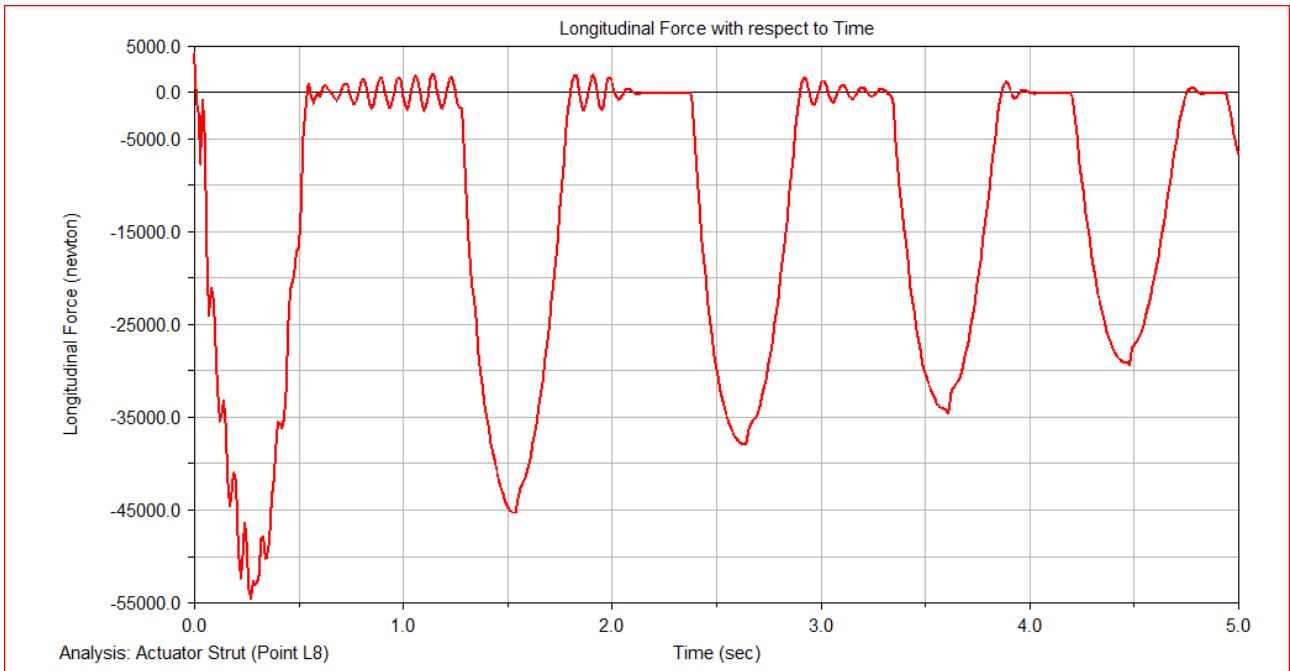


Figure E.8: Longitudinal Force at the Strut Actuator during drop test.

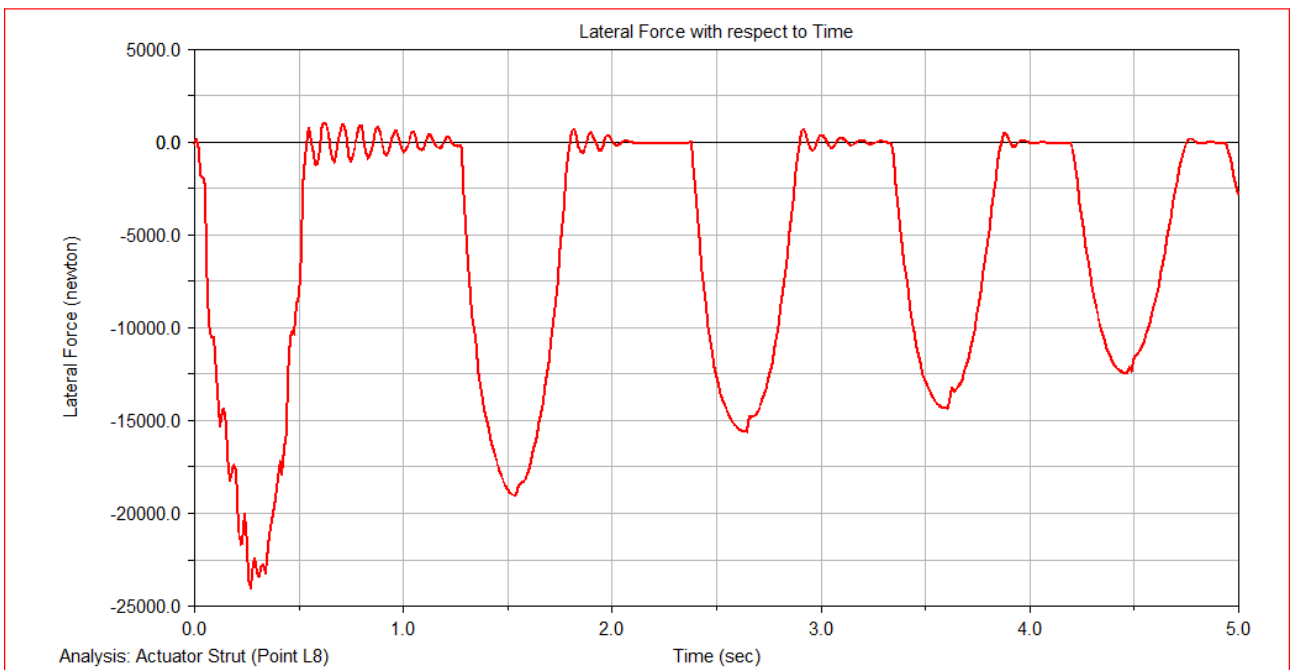


Figure E.9: Lateral Force at the Strut Actuator during drop test.

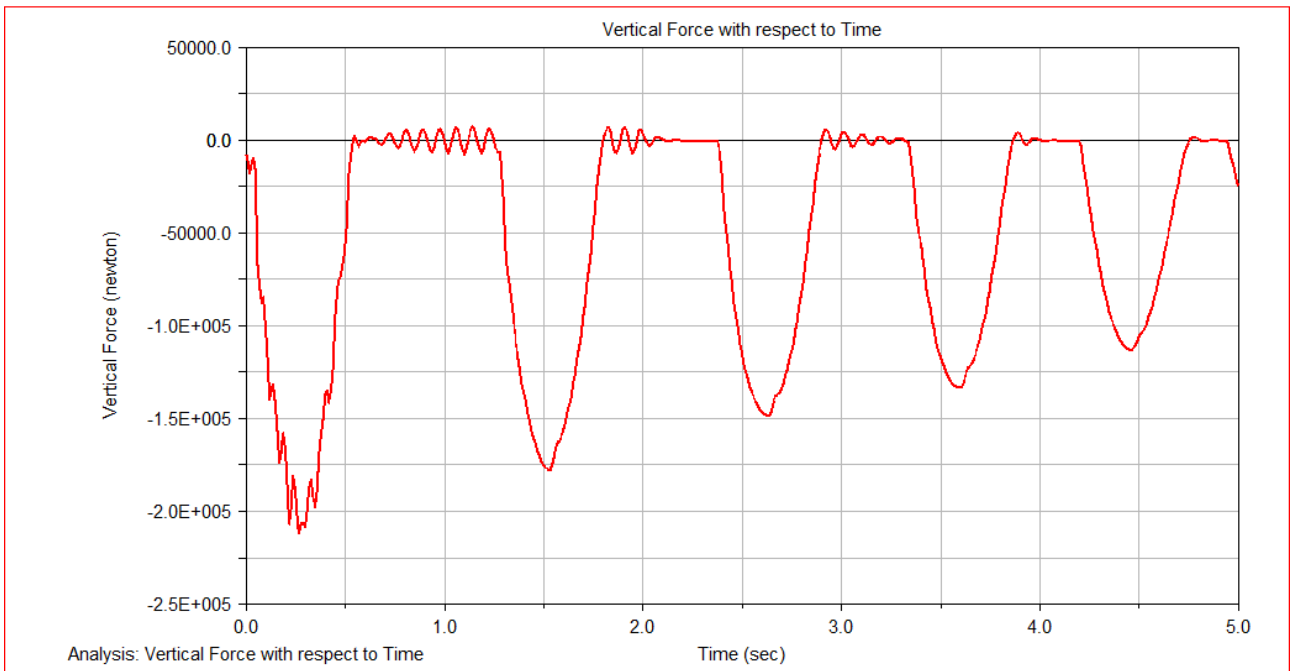


Figure E.10: Vertical Force at the Strut Actuator during drop test.

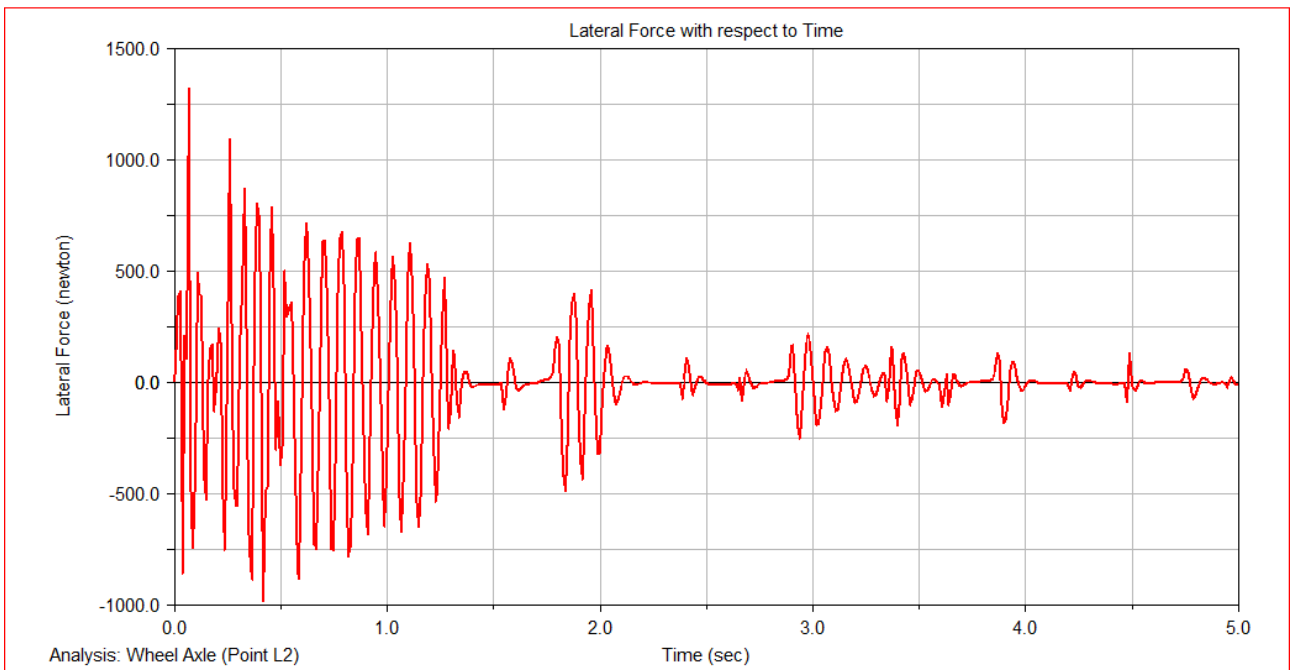


Figure E.11: The Lateral Force at the Wheel's Axle during drop test.

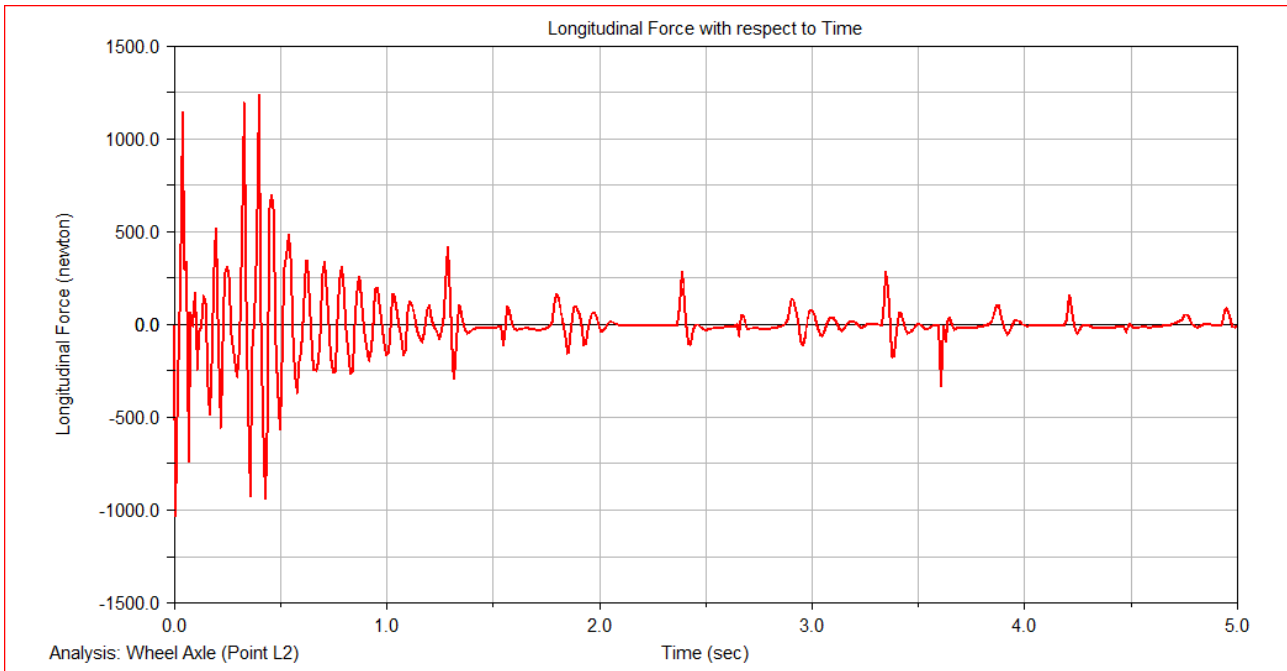


Figure E.12: Longitudinal Force at the Wheel's Axle during drop test.

APPENDIX F STUDENT ASSIGNMENT SCHEDULE

MBD Student Assignment
Tire Simulation Model Development
July 2015

Student Assignment Tire Simulation Model Development

Introduction

Within the NH90 - European Defence Business Line (EDBL) department of Fokker Aerostructures landing simulations of the NH90 Helicopter are performed with the Multi Body Dynamics (MBD) program MSC.ADAMS. For these simulations validated landing gear models are to be defined that comprise of tires, strut assembly, shock absorber and retract actuator as well as (parts of) the helicopter structure.

Tire Modelling and Characteristics

The tire model simulation responses and derived tire characteristics should match those presented by the tire manufacturer and the performed matching tests (operational equivalence). Further the tire responses and characteristics can be compared or fit to theoretical tire model parameters (coefficients) which enable analytical and qualitative comparisons (theoretical equivalence). Both types of equivalences are valuable. While the operational equivalence assures the usage within the scope of the (to be) qualified H/C landing conditions envelope, the theoretical equivalence enables the comprehension of the tire behavior and notion of possible envelope extensions or limitations. In this framework the tire model applications and investigations should be pursued.

Assignment

For the NH90 TTH/NFH MLG new tire models need to be developed within the MSC.ADAMS program.

The following tasks therefore are envisioned to be performed:

- Before the beginning of the assignment the candidate student needs to write a **proposal** that elaborates on his (or her) views and implications on below mentioned tasks and that could serve as a lead during his assignment.
TO-1.
- **Inventory of the tire types** in use for the NH90 TTH/NFH MLG, the tire characteristics and test data as generally available and/or provided by the tire manufacturer (i.e. tire data available for Fokker aircraft).
Finished: **TO+4;**
- **Familiarization with the MSC.ADAMS MBD** program in particular with the standard tire (theoretical) simulation models present in the program.
Finished: **TO+7;**
- While choosing a particular **tire type** decide and elaborate upon the most suitable **theoretical model** that enables the simulation of the particular tire characteristics and test data (theoretical background for the particular tire type).
Report of progress up till present.
Finished: **TO+9;**
- Development of the **MSC.ADAMS tire model** for the particular chosen tire type and theoretical model.
Finished: **TO+10;**
- **Simulation test runs** with the MSC.ADAMS MBD program in order to show/present the tire characteristics as inherited from the simulation model.
Finished: **TO+12;**

MBD Student Assignment
Tire Simulation Model Development
July 2015

- **Comparisons/validation of the tire simulation model** test results with the tire characteristics and test data as generally available and/or provided by the tire manufacturer.
Finished: **TO+14**;
- **Report** all above described steps and merge into a final report.
Finished: **TO+16**;

Accomplishment of all tasks is estimated to span 4 months of time (i.e. **16 weeks**).

Ruud Louw
System Integration Engineer
European Defence Business Line – NH90
Fokker Aerostructures B.V.
Industrieweg 4, 3351 LB Papendrecht
Tel.: +31 (0)78 6419540
Ruud.louw@fokker.com

APPENDIX G FOLDER LOCATION FOR THE ADAMS FILES

Tire models with 130.5 air pressure:

- Basic Aircraft Tire Models

R:\NH90\NH90 Functional\IPO\System Engineering\Landing Gear\LG-Analysis-Multi-Body-Tool (MBD)\Models\Ilias\Adams-Newtire\tire_tests\Tire results\BASIC_NH90

- Enhanced Aircraft Tire Models

R:\NH90\NH90 Functional\IPO\System Engineering\Landing Gear\LG-Analysis-Multi-Body-Tool (MBD)\Models\Ilias\Adams-Newtire\tire_tests\Tire results\ADVANCED_NH90

- TRR64 Aircraft Tire Models

R:\NH90\NH90 Functional\IPO\System Engineering\Landing Gear\LG-Analysis-Multi-Body-Tool (MBD)\Models\Ilias\Adams-Newtire\tire_tests\Tire results\TRR64_NH90

- Pacejka 2002 Tire Model

R:\NH90\NH90 Functional\IPO\System Engineering\Landing Gear\LG-Analysis-Multi-Body-Tool (MBD)\Models\Ilias\Adams-Newtire\tire_tests\Tire results\ Pacejka2002

- DUNLOP calculations

R:\NH90\NH90 Functional\IPO\System Engineering\Landing Gear\LG-Analysis-Multi-Body-Tool (MBD)\Models\Ilias\Adams-Newtire\tire_tests\Tire results\Dunlop

- Test results

R:\NH90\NH90 Functional\IPO\System Engineering\Landing Gear\LG-Analysis-Multi-Body-Tool (MBD)\Models\Ilias\Adams-Newtire\tire_tests\Tire results\Comparisons

Tire models with 143.6 air pressure:

- Basic Aircraft Tire Models

R:\NH90\NH90 Functional\IPO\System Engineering\Landing Gear\LG-Analysis-Multi-Body-Tool (MBD)\Models\Ilias\Adams-Newtire\tire_tests\Tire results Pressure 143.6\BASIC_NH90

- Enhanced Aircraft Tire Models

R:\NH90\NH90 Functional\IPO\System Engineering\Landing Gear\LG-Analysis-Multi-Body-Tool (MBD)\Models\Ilias\Adams-Newtire\tire_tests\Tire results Pressure 143.6\ADVANCED_NH90

- TRR64 Aircraft Tire Models

R:\NH90\NH90 Functional\IPO\System Engineering\Landing Gear\LG-Analysis-Multi-Body-Tool (MBD)\Models\Ilias\Adams-Newtire\tire_tests\Tire results Pressure 143.6\TRR64_NH90

- DUNLOP calculations

R:\NH90\NH90 Functional\IPO\System Engineering\Landing Gear\LG-Analysis-Multi-Body-Tool (MBD)\Models\Ilias\Adams-Newtire\tire_tests\Tire results Pressure 143.6\Dunlop

- Test results

R:\NH90\NH90 Functional\IPO\System Engineering\Landing Gear\LG-Analysis-Multi-Body-Tool (MBD)\Models\Ilias\Adams-Newtire\tire_tests\Tire results Pressure 143.6\TRR64_NH90

Test rig models:

You can select any of the test rig models and put one the aforementioned tires to test it.

- R:\NH90\NH90 Functional\IPO\System Engineering\Landing Gear\LG-Analysis-Multi-Body-Tool (MBD)\Models\Ilias\Adams-Newtire\tire_tests

Main Landing Gear Models:

You can select any of the Main Landing Gear models (Model with Advanced tire model, Model with Basic tire model, Model with Pacejka tire model, Model with TRR64 tire model) and then put one the aforementioned tire models to simulate the model.

- R:\NH90\NH90 Functional\IPO\System Engineering\Landing Gear\LG-Analysis-Multi-Body-Tool (MBD)\Models\Ilias\Adams-Newtire

Road Models:

- R:\NH90\NH90 Functional\IPO\System Engineering\Landing Gear\LG-Analysis-Multi-Body-Tool (MBD)\Models\Ilias\Adams-Newtire\roads.tbl

Default Tire Models provided by MSC.ADAMS:

- R:\NH90\NH90 Functional\IPO\System Engineering\Landing Gear\LG-Analysis-Multi-Body-Tool (MBD)\Models\Ilias\Adams-Newtire\tires.tbl